Bayesian System Identification of Dynamic Structures for Active Vibration Control

A Thesis submitted to the University of Sheffield

for the degree of Doctor of Philosophy in the Faculty of Engineering

by

Nasser Ayidh AlQahtani

Supervisors: Dr. Timothy Rogers and Professor Neil D. Sims

Department of Mechanical Engineering

University of Sheffield

March 10, 2025

To my mother, Huda, for her boundless love, care, and sacrifices.
To the cherished memory of my father, Ayidh, whose wisdom and values continue to inspire me.
To my beloved wife, for her unwavering support, patience, and love.
To my son Omar and daughter Wejdan, for being my source of joy and inspiration.

Acknowledgements

As a scientist and an engineer, I first travelled to Canada and now to the United Kingdom, seeking knowledge that would bring me closer to Allah. All praises are due to Allah for helping me complete this work and for granting me the ability and patience to overcome all the challenges of my graduate studies. O Allah, I ask You for beneficial and valuable knowledge that can be used for the greater good of mankind, and for deeds that will be accepted.

I wish to express my profound gratitude to the many individuals who have supported and inspired me during the course of this thesis. First and foremost, I extend my gratitude to my supervisor, Professor Neil D. Sims, for his unwavering support, motivation, and guidance throughout my doctoral journey. His patience, enthusiasm, and immense knowledge have inspired me to develop a deeper interest in research. I am really grateful that I have been working by his side during this period of intense personal development. The acknowledgments would not be complete without expressing my gratitude and appreciation to my co-supervisor, Dr. Tim Rogers, for welcoming me into the community of Bayesian believers. His supportive attitude and continuous advice have been invaluable throughout this project, particularly in guiding me on how to approach the problem from a machine learning perspective. His supervision style opened my eyes and extended my horizon in the field of system identification.

A big word of appreciation goes to the members of DRG group and special thanks go to my friend Dr. Máté Tóth for not only his academic support, but also for our long discussions on history, religion, and cuisine. Finally, I would also like to extend a special acknowledgement to Qassim University, my sponsor, and my academic advisors at the Saudi Arabian Cultural Bureau in London, for their assistance.

Abstract

Bayesian system identification is a remarkable approach used in either modelling or estimation problems, and especially when addressing uncertainty in structural systems. With the increasing use of flexible structures in aerospace engineering, medicine and robot applications, control techniques are often used to carry out such tasks as unwanted vibration mitigation and damage detection. Therefore, understanding the dynamics of the nonlinear structure from both a design and a control perspective is an important step.

To the author's knowledge, limited cases have been made of the Bayesian approaches either in modelling or control in the context of data driven control for vibration control. This is an area with much potential for offering a new perspective on tackling vibration problems.

This thesis seeks to fill this gap in the literature. In doing so, several Bayesian systems identification methods have been proposed, ranging from incorporating well known identification structures, such as Wiener-Hammerstein model and NARX, with GP models to Bayesian state space model. These are then used to inform the design of a new kind of active vibration control, making use of linear and nonlinear structural systems. This thesis concludes by drawing attention to the feasibility of Bayesian methods in active vibration control.

Publications

Conference Papers

- N. A. AlQahtani, T. J. Rogers and N. D. Sims, 2022. *Feedback control of flexible systems using Bayesian filtering.* The 30th International Conference on Noise and Vibration engineering (ISMA2022), Leuven, Belgium.
- N. A. AlQahtani, T. J. Rogers and N. D. Sims, 2023. *Control of Flexible Structures Using Model Predictive Control and Gaussian Processes.* XII International Conference on Structural Dynamics (EURODYN2023), Delft, Netherlands.
- N. A. AlQahtani, T. J. Rogers and N. D. Sims, 2024. *Towards nonlinear model predictive control of flexible structures using Gaussian process.* XIVth International Conference on Recent Advances in Structural Dynamics (RASD2024), Southampton, UK.
- N. A. AlQahtani, T. J. Rogers and N. D. Sims, 2024. *GP-NARX for Active Control of Nonlinear Flexible Structures.* The 31th International Conference on Noise and Vibration engineering (ISMA2024), Leuven, Belgium.

Late Breaking Results Poster

- N. A. AlQahtani, T. J. Rogers and N. D. Sims, 2024. *Controlling mechanical vibration with Gaussian process based model predictive control.* The 8th IEEE Conference on Control Technology and Applications (CCTA2024), Newcastle, UK.

Acronyms

Acronym	Full Name
MPC	Model Predictive Control
GP	Gaussian Process
NMPC	Nonlinear Model Predictive Control
NOE	Nonlinear Output Error Model
OSA	One Step Ahead
MPO	Model Predicted Output
GP-NARX	Gaussian Process Nonlinear AutoRegressive model with eXogenous input
MBC	Model-Based Control
DDC	Data-Driven Control
PFC	Predictive Functional Control
ANN	Artificial Neural Networks
SHM	Structural Health Monitoring
MESS	Model Error Sensitivity Suppression
LTR	Loop Transfer Recovery
KF	Kalman Filter
UKF	Unscented Kalman Filter
EM	Expectation-Maximization
LQR	Linear Quadratic Regulator
LQG	Linear Quadratic Gaussian

Table of Contents

List of Figures

List of Tables

Chapter 1

Introduction

1.1 Motivation

In recent years, everyone learned that uncertainty is a critical issue, especially once it becomes a part of your daily life. In engineering, this issue has, fortunately, been under the spotlight for decades [1, 2], but there are still challenges. Vibrations are unwelcome guests in many engineering applications and their energy can lead to sophisticated and complex disasters. Vibration occurs as a result of external forces such as wind or earthquakes, or of internal forces such as the result of the excitation of hidden dynamics. This mechanical property must be considered in the design of a system in order to avoid structural fatigue or failure, or the degradation of control performance [3]. Unfortunately, some devastating historical incidents have been caused by vibration. One is the suspension bridge of Tacoma Narrows. Built in 1940, the bridge was at that time the longest suspension bridge; however, the entire bridge was damaged by a phenomenon called an aeroelastic flutter, as shown in Figure (1.1a). More recently, the nuclear accident of the Fukushima Daiichi reactors on March 11, 2011, is a dark example of underestimated external loads. Even though at that time Japan was leading the world in adapting structural control technologies [4], a strong earthquake followed by a tsunami led to a huge disaster at the nuclear power facility. According to the report, a misjudgment of the potential wave height in the design process of the reactor plant was the reason damage could not be avoided during the tsunami, as shown in Figure (1.1b).

(a) The bridge of Tacoma Narrows, New York [1].

(b) Fukushima Daiichi Plants [2].

Figure 1.1: Examples of the effects of vibration and uncertainty.

Maintenance and safety of ageing infrastructures also face uncertainty challenges [5]. Equipment and infrastructure currently used for oil and gas operations, for instance, were often built a few decades ago, based on the designs, materials, and technologies of that time. In some cases, these ageing assets have exceeded the forecasted life expectancy estimated during their design phase. Such ageing equipment is bound to fail and consequently requires continuous monitoring and inspection. In the United Kingdom, there is also an ageing rail network under increasing weather pressure as shown in Figure (1.2). In addition, the growing trend for making major mechanical systems more environmentally friendly has forced engineer designers to utilise lighter and more flexible structures [6, 7]. This comes at great cost, as the mechanical characteristics of the system are more vulnerable to change [8]. With the increasing use of flexible structures in aerospace engineering, medicine, and robot applications, control techniques are often used to carry out such tasks as unwanted vibration mitigation and damage detection [7]. Therefore, understanding the dynamics of the

[1] https://www.britannica.com/technology/bridge-engineering/Tacoma-Narrows
[2] https://www.intechopen.com/chapters/61715

nonlinear structure from both a design and a control perspective is an important first step.

Figure 1.2: The Cambrian Line, UK [3].

In terms of structural dynamics, modelling is a critical stage in any design process and its role has an impact on the outcomes of a system. The modelling process is basically about the translation of real-interest properties into mathematical equations; those equations can be formed into ordinary differential equations or partial differential equations for the purpose of prediction as an example [9]. A successful model is usually combined from three informative elements which are knowledge, data, and assumptions [10, 11]. In other words, a prior knowledge gives interpretations and explanations of the behaviour of the system, whereas data helps in making an estimate of the parameters of the models. Both elements in the modelling stage still require an expert's insight. Data-driven modelling, which is fundamentally a system identification method, has become an alternative approach as a result of the outstanding sensing technology now available, and has become an enabling factor in modern design methods [12]. System identification is an old control problem in which it finds the relation between the input and the output signals mathematically. Even though system identifications provide many useful techniques suiting some industrial problems, missing the physical understanding of these methods degrades their trustworthiness [13].

[3]https://www.networkrailmediacentre.co.uk/resources/cambrian-line-8

There is a growing body of literature that recognises the importance of Bayesian system identification [8]. Bayesian approaches are statistical methods that have been utilised in applied science. Structural dynamics, including Structural Health Monitoring (SHM), are no exemption to this. Bayesian system identification has been used either as a modelling method, such as Gaussian Process (GP), or as a nonlinear estimator, such as Unscented Kalman Filter (UKF). Both methods are reported in the literature [14, 15] with the recommendation and encouragement of exploring this method further in vibration control. The main advantage of Bayesian inference is that it has the ability to quantify uncertainty which helps to define the regions of less certainty. Fortunately, control theory has been addressing the uncertainty issue in feedback control for years and it offers a variety of strategies and techniques, such as robust control [16]. However, despite the advancements in structural dynamics in terms of using nonlinear system identifications, utilising the control strategy or developing a control policy incorporated with Bayesian system identification have been less explored [15]. Hence, the stream of these developments paves the way for adding the controller in order to draw on physical interpretations and close the loop of the systems.

1.2 Research objectives

The overall objective of the thesis aims to introduce and utilise some potentially powerful technologies which, having been developed in the machine learning and control communities, can now bring significant value to structural and mechanical engineering. The work focuses on the application of these methods to active vibration problems. These main objectives are:

O1 To investigate the current literature on system identification and data driven control with a focus of combining these methods to improve the control of structural vibrations.

O2 To model a structural control system based on a Bayesian system identification approach.

O3 To investigate the effect of including the dynamics of the actuator in terms of identifying the structure and how it can be used in control design.

O4 To design a Bayesian state estimator in structural control systems.

1.3 Contribution to knowledge

This thesis investigates active vibration control challenges from a data-driven control perspective, contributing in several key areas.

First, Model Predictive Control (MPC), Gaussian process modelling, and the Wiener-Hammerstein method are combined in order to account for actuator saturation effects in active vibration control. This requires incorporating an inverse GP model of static nonlinearity within the Wiener-Hammerstein model. The modelling starts with designing MPC for a structural system, in which the aim is to identify the optimal control force. Utilising the GP is the second step towards quantifying the uncertainty and limitation of the proof mass actuator by designing an inverse GP for the static nonlinearity. This quantification is then utilised in an MPC controller through a steady-state target optimisation tracking approach, enabling the controller to determine the optimal voltage necessary to mitigate vibrations effectively while operating within the actuator's constraints.

The second contribution considers applying Nonlinear Model Predictive Control (NMPC) to flexible structures by utilising recent developments in models which have been learnt from example data. The GP was identified for use as a black-box model in NMPC; it provides both the prediction of the system output and the associated confidence. In a control context, a GP can be utilised as a discrepancy model for linear or nonlinear flexible dynamic structures within MPC or even as the nonlinear model of the system itself. Nonlinear Output Error model (GP-NOE) is a popular GP structure for dynamic systems that is utilised in predictive control strategies and requires predictions to be propagated to the control horizon. This novel framework was evaluated on a linear and nonlinear system, and the results demonstrate robust control performance in both tracking and regulator tasks. The additional contribution in this work was that clarification of some of the terminologies utilised differently in structural dynamics and control systems.

Numerical models of structural systems are frequently insufficient due to inherent uncertainties. This issue can become more critical when active vibration control is implemented. As a result, the final contribution of this thesis was about addressing the identification of flexible structural dynamics subject to uncertainty by using Bayesian state space models, with the intention of developing a vibration control system. This requires incorporating the identified uncertainty of the structure

into the control strategy. The proposed method comprises a combination of two Bayesian identification techniques, Gaussian filters - namely Kalman Filter (KF) and Expectation-Maximization (EM) algorithms, with Linear Quadratic Regulator (LQR). The key contribution of this work is to demonstrate how the methodology of Bayesian state estimation and LQR control algorithms might work in cases when there is spillover instability from unmodelled modes in the system.

1.4 Thesis outline

The rest of the thesis is organised as follows:

- Chapter 2 provides an overview of data-driven modelling and control methods, focusing on the potential of machine learning models. Since GP and MPC were the main tools used in this thesis, a brief overview is provided for each method.

- Chapter 3 presents a literature review in vibration control with an emphasis on, and navigates through, data-driven methods in three major fields: structural control, structural dynamics modelling, and estimation. Then, recent developments in control algorithms incorporating data-driven models in the wider control engineering field are discussed. In the end, the summary concludes that there is an urgent need to explore the feasibility of these data-driven methods when dealing with nonlinear and hidden dynamics in structural dynamics.

- In order to avoid repetition, Chapter 4 provides the theoretical background for the state space model of a cantilever beam. The cantilever beam serves as a case study in Chapter 5 and Chapter 6, whereas a simply supported beam serves as the case study for a spillover problem in Chapter 8.

- In Chapter 5, the applicability of a data-driven method in an active vibration setting is discussed. The methodology of designing MPC and GP within a Wiener-Hammerstein model is presented. This proposed model is incorporated in a case of addressing a nonlinear saturation problem of an actuator in which the uncertainty is accounted for by a GP. The validity of this idea is explored numerically in the case of a cantilever beam coupled with a proof mass actuator, and the results suggest that the model was able to provide the required control inputs while taking into account the limits of the actuator.

- Chapter 6 addresses the use of a probabilistic black box model for active vibration control systems. The GP-NARX model within MPC is designed, and the methodology of nonlinear system identification using GP is given, emphasising the different terminologies used by structural dynamics and control communities. Then, the design of Predictive Functional Control (PFC) is provided, which explores the concept of coincidence points. The proposed model is evaluated in two linear cases: the linear oscillator and the cantilever beam. Despite the challenges and difficulties in identifying the appropriate GP-NARX model, the results have shown promise in terms of structural system control.

- In Chapter 7, the effectiveness of the GP-NARX model within MPC is evaluated in nonlinear systems. Duffing oscillator systems were used as a case study to validate the probabilistic black box model.

- Chapter 8 introduces the Bayesian filtering approach to solving spillover problems. This chapter presents an alternative data-driven method of considering system uncertainty in which the estimation identifies extra poles in the system and the controller then eliminates spillover effects. The simulation results provide valuable analysis that could lead to data-driven modelling of a spillover problem.

- In Chapter 9, a summary of the thesis, conclusion, overview of the original contribution and future work are presented.

Chapter 2

Background on data driven methods

Highlights:

- The introduction of modern dynamical systems is given and data-driven methods in engineering are presented.
- An introduction to Gaussian process regression from the perspective of system modelling is presented.
- An overview of model predictive control algorithm is presented in a traditional approach.
- The need for employing model predictive control based on probabilistic modelling is motivated.

2.1 Introduction

The dawn of modern control theory began with Kalman's groundbreaking papers on linear quadratic control [17] and the Kalman filter [18], where he introduced innovative methods for handling multivariable systems and noise in dynamic processes.

Following this, the field of dynamical and control systems thrives in terms of theories and applications [19]. The former leads to a new control strategy that begins with optimal control and ends up with adaptive control in the late eighties, going through robust control and H_∞, whereas the latter was found its way into space programs such as Apollo 13. More importantly, all these remarkable control methods come down to not only a simple question but also difficult to answer: What is a model?

Traditionally, the answer to this question is that the model consists of mathematical equations or governing equations that represent real interest physical properties, expressed through ordinary differential equations or partial differential equations for the purpose of prediction. This perspective of a model is the main paradigm in the field of systems and control; in addition, it is commonly known as Model-Based Control (MBC) [20]. This type of model is currently under transition into Data-Driven Control (DDC) due to the powerful tools of machine learning [21].

This thesis constitutes three engineering disciplines: control systems, structural dynamics, and machine learning. Consequently, this chapter introduces theoretical and technical backgrounds and is divided into two parts: Gaussian Processes, and Model Predictive Control. The first part introduces mathematically how the GP works and more importantly how it would be useful in engineering applications, whereas the second part presents the basic components of designing MPC.

2.2 Toward a probabilistic model in engineering

The importance of probabilistic models begins with understanding the regression problem, from classical data modelling to modern machine learning approaches. To explain the basic idea, let us assume there is data from an engineering application consisting of a column vector of observation data, $\mathbf{x}$, and the corresponding output y. The task is to identify the underlying function that maps these observations to the outputs. To fit a model to data, think about using a specific function class, such as first-order polynomials, and minimising the squared error between predicted and observed values, as depicted in Figure (2.1). This conventional approach, often referred to as the best fit model, assumes a fixed relationship between the inputs and outputs. This type of data modelling has been utilised and studied extensively due to its simplicity and flexibility [22], but it suffers from two fundamental issues: how to choose a suitable class of functions to use as a model, and how to represent

uncertainty within the model itself.

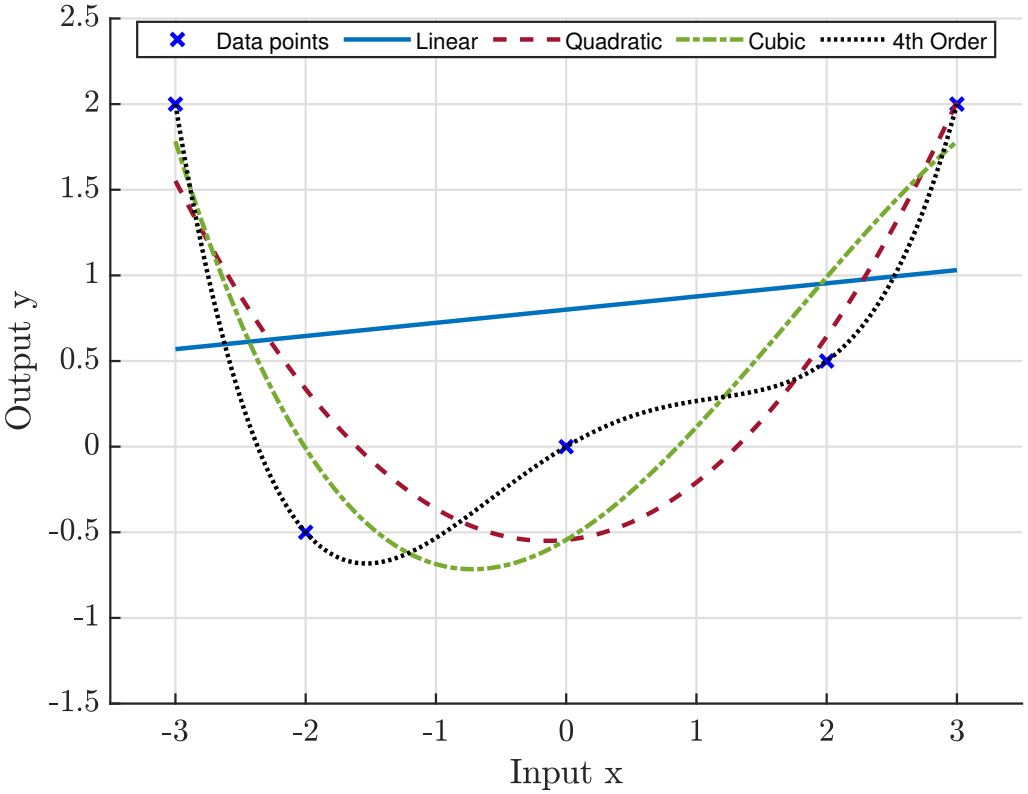

Figure 2.1: Illustration of identifying the underlying function of a system by using polynomial approaches.

To address these challenges, the Bayesian methods in machine learning carry the answer to both of these questions. In the Bayesian sense, the probabilistic distribution is used to represent our knowledge or belief, also known as a prior, over a hidden function value f at a particular input location x. Through the likelihood, we specify how an observed output y at input x is related to the function variable f, encapsulating our current understanding of the unknown variable f in the prior distribution. Using Bayes' rule, we can then update our beliefs about the uncertainty function variable based on new observations. This concept underpins GP, which is discussed in the following section.

2.2.1 Gaussian Process Regression

The Gaussian Process (GP) is a Bayesian approach and it is defined as a collection of random variables which have a joint multivariate Gaussian distribution [23]. Within

the context of regression problems, a GP formulates a prior over the latent function $f(x)$, which is depicted in Equation (2.1).

$$y = f(x) + \epsilon \tag{2.1}$$

Here, x represents a vector of training inputs and X represents a matrix comprised of multivariate input data, and y represents the associated vector of output data obtained for training. The noise component is modelled as a Gaussian-distributed random variable with zero mean and noise variance σ_n^2, $\epsilon \sim \mathcal{N}(0, \sigma_n^2)$. The function f represents a hidden variable that is not directly observable. A GP is comprehensively described by its mean function, denoted by $\mu(\cdot)$, and its covariance function, denoted by $k(\cdot, \cdot)$. These functions encapsulate the prior assumptions about the nature of the underlying latent function. The mean function can be articulated as any linear combination of basis functions dependent on x, with the flexibility to extend to different input spaces. Meanwhile, the covariance function is responsible for quantifying the extent of covariance between any two points within the input space.

$$f(x) \sim \mathcal{GP}(\mu(x), k(x, x_*)) \tag{2.2}$$

As we obtain a training dataset $\{X, y\}_{n=1}^N$, we can update the GP prior based on this dataset to establish a posterior distribution y_* for a new unseen input x_*. Following the methodology outlined in [23], standard Gaussian process equations provide us with an explicit formulation for the posterior distribution of y_*,

$$p(y_*|x_*, X, y, \theta) = \mathcal{N}(\mu[y_*], \Sigma[y_*]), \tag{2.3}$$

where the expected mean value μ and variance Σ are defined as:

$$\mu[y_*] = K(x_*, X)(K(X, X) + \sigma_n^2 I)^{-1} y, \tag{2.4}$$

$$\Sigma[y_*] = K(x_*, x_*) - K(x_*, X)(K(X, X) + \sigma_n^2 I)^{-1} K(X, x_*). \tag{2.5}$$

Defining a covariance function or kernel typically requires selecting several hyperpa-

rameters θ, which can include coefficients for a mean function. These hyperparameters modify the kernel's behaviour and usually have an interpretable meaning. For instance, a common parameter in many kernels is the length scale, which practically determines the required proximity of inputs in the same dimension to affect each other. The Gaussian process framework allows for a systematic approach to estimate these hyperparameters by maximizing the model's marginal likelihood, also known as the model evidence.

2.3 Model Predictive Control

Model predictive control (MPC), also known as model-based predictive control, technically refers to a class of controllers in which there is a direct use of an explicit and separately identifiable model [24]. Control design methods based on the MPC concept have not only become a cornerstone of modern process control, but they are also among the most effective modern advanced control techniques in the industrial landscape [21, 25, 26]. The popularity of this approach stems from a variety of reasons [25]; not all of them are covered here. First, this concept can be applied to both simple and complex process systems. In addition, the MPC strategy can be used in multivariable systems with constraints. Lastly, the MPC technique is an entirely open methodology, which means that the concept can be improved or developed. This flexibility results from the fact that the MPC concept depends on three fundamental principles: prediction, objective functions, and the receding horizon principle. Therefore, this control method has been employed in a wide range of engineering applications, including chemical, robotics, and aerospace engineering.

Historically, the development of predictive control can be traced back to the work of Åström in 1970 [27, 28]; the author proposed a minimum-variance controller in which the predicted output can be driven by solving a simple linear equation for appropriate control action. The first MPC concept in control application was presented by Richalet et al. in [29], where they presented model predictive heuristic control (MPHC). Meanwhile, dynamic matrix control (DMC) was introduced by some engineers at Shell Oil. Following these developments, the control community investigated the MPC algorithm in terms of stability and robustness, leading to the growth of multiple MPC algorithms. Theoretically, the development of the MPC based on optimal control (OMPC) completed in 2000 when dual-mode algorithms

were published by Mayne et al. in [30], demonstrating both optimality and stability. In the research community, this approach has grown in popularity since then [31].

The MPC strategy is depicted in Figure (2.2) and described as follows:

- **Future output**: given the prediction horizon N_P, the future system outputs are calculated for each discrete sample k using the process model. The predicted system output, denoted as $\hat{y}(k+j|k)$ for $j = 1, \ldots, N_P$, depends on known past and current output values $y(k)$, as well as the control scenario in the future, where these control inputs are sent to the system and to be calculated.
- **Future control input**: given the control horizon N_u, the future control input, $u(k+j|k)$ for $j = 1, \ldots, N_u - 1$, is calculated by optimising a determined cost function in order to keep the system output as close as possible to the setpoint or reference trajectory. The optimal control sequence denoted as $\{u^0(k|k), u^0(k+1|k), \ldots, u^0(k+N_u-1|k)\}$.
- **Set point or reference trajectory**: in certain MPC algorithms, the set point $w(k)$ and reference trajectory $\mathbf{r}(k)$ may be the same; in other cases, the reference trajectory, represented as $\mathbf{r}(k+j|k)$ for $j = 1, \ldots, N_P$, is produced from the current output value $y(k)$ to the setpoint $w(k)$.
- **The control signal**: the control signal applied to the process model is the first control element $u^0(k|k)$ of the optimal control sequence, and the rest is rejected. At the next sampling time, the entire procedure is repeated, which is known as the receding-horizon principle.

In order to follow the previous strategy, there is a well known MPC structure. This structure is depicted in Figure (2.3), which consists of optimiser and a process or internal model. The role of this process model is to predict future plant outputs based on previous and present values, as well as the proposed suitable future control actions. The optimiser calculates these actions, taking into consideration both the cost function and the limitations. Mathematically, the nonlinear discrete time system in the form of state space can be expressed as follows:

$$\mathbf{x}(k+1) = \mathbf{f}(\mathbf{x}(k), \mathbf{u}(k), k) \tag{2.6}$$

$$\mathbf{y}(k) = \mathbf{g}(\mathbf{x}(k), \mathbf{u}(k), k) \tag{2.7}$$

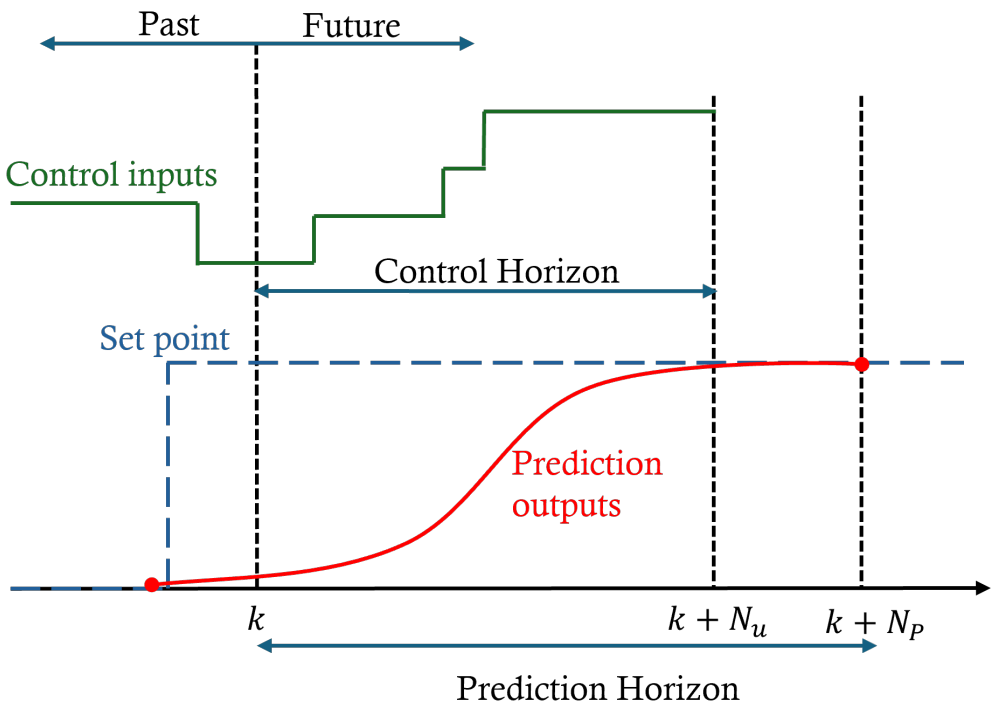

Figure 2.2: The basic MPC strategy.

where:

- $\mathbf{x}(k) \in \mathbb{R}^n$ represents the state vector at time step k,
- $\mathbf{u}(k) \in \mathbb{R}^m$ is the input vector (control actions),
- $\mathbf{y}(k) \in \mathbb{R}^p$ is the output vector,
- $\mathbf{f}$ and $\mathbf{g}$ are nonlinear functions that describe the state dynamics and output equations, respectively.

In general, there are constraints in inputs and states of the system and can be expressed in abstract form as follows:

$$\mathbf{u}(k) \in \mathcal{U} \tag{2.8}$$

$$\mathbf{x}(k) \in \mathcal{X} \tag{2.9}$$

where $\mathcal{U}$ and $\mathcal{X}$ are the sets of input and state constraints, respectively. The non-

linear optimisation problem is defined as:

$$\min_{\mathbf{u}} \ell(\mathbf{x}(k), \mathbf{u}(k), \mathbf{r}(k)) \tag{2.10}$$

The ℓ is the objective function or cost function. In this thesis, choosing the cost function and designing the MPC controller is based on the type of the model, and both MBC and DDC are adopted. The complete nonlinear formalisation of the optimisation problem will be explained in the forthcoming chapters.

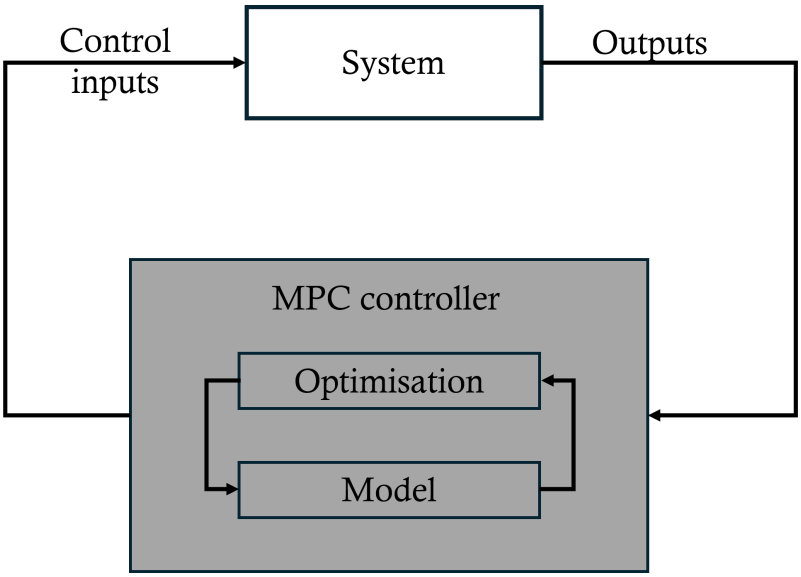

Figure 2.3: The basic MPC structure.

Chapter 3

Literature review

Highlights:

- Vibration suppression is introduced with a brief description of passive and semi-active damping, focusing on active damping in which data-driven methods are feasible to be implemented.
- A brief review of modelling approaches in structural dynamics is presented, especially emphasising the data driven modelling in several fields.
- An overview of control strategies in structural dynamics is presented focusing on improving or solving active vibration problems.
- The summary of the research gap in the literature is provided, highlighting the problem this thesis is addressing.

3.1 Overview

The last chapter introduced data-driven approaches in both modelling, as a probabilistic dynamical model, and control, as MPC based on data. There is no doubt that these methods have contributed to science and research in several fields; however, appropriate application to an engineering problem that requires data-driven meth-

ods is equally important. Consequently, this chapter presents the literature review of structural vibration control, focusing on research problems involving nonlinearity and unknown dynamics.

The literature review is divided into four sections. First, it covers control in structural systems, providing an overview of vibration suppression methods in devices and strategies. Then, an overview of modelling is presented, especially advancements used in SHM in which it can be extended for vibration control settings. Finally, the literature review concludes by providing recent advancements in estimation after discussing several control algorithms in structural dynamics.

3.2 Control in structural dynamics

Modern control theory plays a critical role in structural systems: it arms structural control systems' engineers with tools to alter the behaviour of specific dynamic systems either in mitigating or absorbing unwanted vibrations. Control theory offers numerous different control methods and structures and choosing one of these methods or structures depends on the control problem being tackled. Vibration suppression is one of structural control techniques and it is based on detecting unwanted vibrations, including environmental disturbances, and aiming to keep the effect of vibration within an acceptable range all the time. This method is well established and has been successfully applied to structural control for years [6].

In general, control systems are categorized based on linearity, and time invariance. Linear time-invariant (LTI) systems are systems which obey the superposition properties, and their parameters do not change over time respectively, otherwise they are nonlinear and time varying. The objective of a control system is basically that it is able to understand and manipulate actively the dynamical systems for achieving a certain response [21]. Figure (3.1) shows the basic elements of the feedback block diagram which is one of the strategies of control, in which the ultimate goal of a closed loop system is to find a reliable and appropriate compensator in order to achieve an acceptable performance without affecting the system's stability [3].

The plant contains the dynamic of the system and it is usually described mathematically in the frequency domain by a transfer function or in the time domain by a state space representation. The accuracy of the plant model, sometimes called

the process model when the actuator has its own dynamic representation, depends on the modelling techniques. The controller represents the algorithms that calculate the control input that manipulates and attenuates the behaviour of the system. The controller is mainly responsible for the performance and stability of the system. The feedback control loop requires the information about the output which comes from sensors. However, these sensors may not be always available or too expensive. In this case, estimation can complete the feedback loop and this has its own design process. Because control systems within the structural systems have not been considered during most design approaches, this section will mainly focus on the development of vibration control systems.

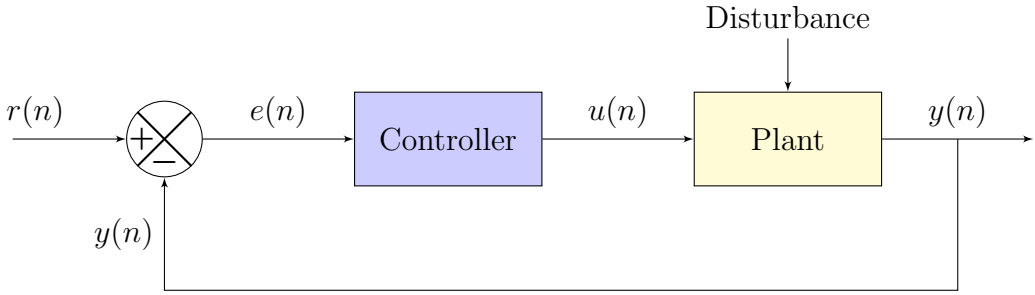

Figure 3.1: Feedback control block diagram.

It is well known that the structural control systems are classified into passive, semi-active, active, and hybrid control systems and the interested reader can find a comprehensive comparison in [32–35]. Damping energy from the system is a key factor in all of these types. The concept of passive control is that it dissipates the external energy by using the motion of the structure to generate the control force without adding external power [35], whereas active control is based on adding sensors to measure the disturbances and an actuator to eliminate or reduce the unwanted vibrations [34]. Semi-active control becomes a solution to the cost inefficiency of the active control, and it combines the concepts of generating the force by the motion of the structure with a small external force. Figure (3.2) presents all control schemes of these systems.

There is growing interest in a smart structure instead of the conventional view of a structure [36]. Basically, structures become dynamic objects capable of interacting with complicated contexts as a result of embedded intelligence. The goal of an intelligent structure is to improve structural performance by recognizing changes in behaviour and loads, adjusting the structure to those changes and recovering previous events to improve future performance [37]. With this in mind, the next

sections briefly provide an overview of these damping techniques.

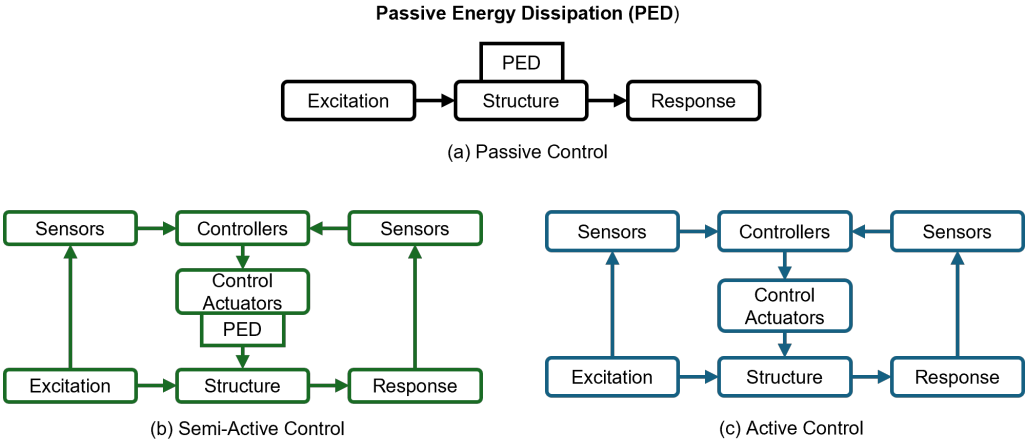

Figure 3.2: Control schemes of structural control systems [33].

3.2.1 Passive control

In practice, vibration suppression through the use of passive devices is frequently preferred because they can be easily integrated into the system without requiring for additional control elements [7]. Tuned Mass Dampers (TMDs) are a type of device that includes a damper, a linear spring, and a mass as shown in Figure (3.3a). TMDs work on the principle that they are tuned to a specific frequency at which the damper's force counteracts structural motion, reducing structural system oscillations. TMDs are ideal for mechanical and civil applications because they are low in cost and require little maintenance.

Since Frahm patented the concept of the TMDs in 1909 [38], TMDs have been studied and implemented numerically and experimentally. Also, they have been applied as a solution for wind and harmonic loads. For instance, the 70-story Park Tower in Chicago, which was completed in 2000, appears to be the first building in the United States that was designed with TMDs incorporated from the very beginning of its design process [39]. In mechanical applications, the TMDs technologies have been installed not only into turbine blades in order to reduce vibration created by turbomachinery blade airfoils [40], but also in cutting tool machines [41]. In terms of research, the majority of research articles about the TMDs system primarily address various aspects of design optimization, including different loading conditions and main structure types, response analysis, and parameter sensitivity analysis [42].

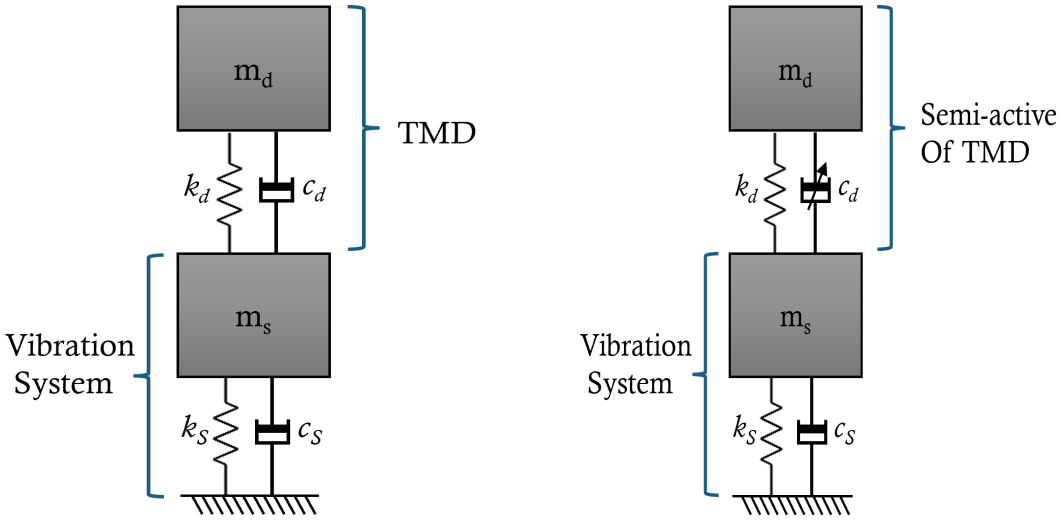

Figure 3.3: (a) A classical Tuned Mass Damper (TMD) consists of three primary components: m, c, and k, representing the mass, damper, and spring, respectively. Also, s represents the structure, and d denotes the passive damper. (b) The semi-active damper variation of TMDs introduces adjustable damping capabilities [33].

Although there are other passive devices, such as an inerter [43], the main drawback of passive damping is that it is incapable of adapting to the changing of the structure or dealing with external excitation [35]. In other words, adding energy to the structure by using a feedback control system is not applicable in passive technology, nor are recent advancements in data-driven control methods. In the next section, these problems were overcome and presented briefly.

3.2.2 Semi-active control

Semi-active control is an alternative control method for dissipating energy from structures through the use of externally powered controllers. This control strategy is basically based on attenuation of structural behaviour by adding a small amount of energy via a control algorithm [44]. A semi-active damping device additionally has properties that can be optimised to reduce system responses [45]. As an example, Active Tune Mass Dampers (ATMDs) are one of the semi active devices which work similarly to TMDs with one exception. ATMDs have the ability to vary the damping in the system as shown in Figure (3.3b). The primary advantage of semi active devices is that they have adapted other damping methods by keeping the inherent reliability of passive control and the capacity of active systems to adapt

without involving substantial external power sources [34]. In this section, some of the semi active devices used in vibration control problems are described.

Fluid dampers are commonly used on semi-active dampers [4]. The Tuned Liquid Column damper (TLCD) is one of these devices which replaces the lumped mass of TMDs with a liquid-filled container, as shown in Figure (3.4a). It reduces structural vibration energy due to fluid head loss as it travels through the orifice. Moreover, it has the ability to tune frequency by adjusting the length of the liquid column. In 1989, the TLCD was introduced by Sakai et al in [46] as a result of improvement of the concept of tuned liquid damper. In terms of applications, TLCD has been employed in tall building such as Hyatt Hotel in Osaka [47] and studied for offshore wind turbines to simulate the structural responses under wave loading excitations [48].

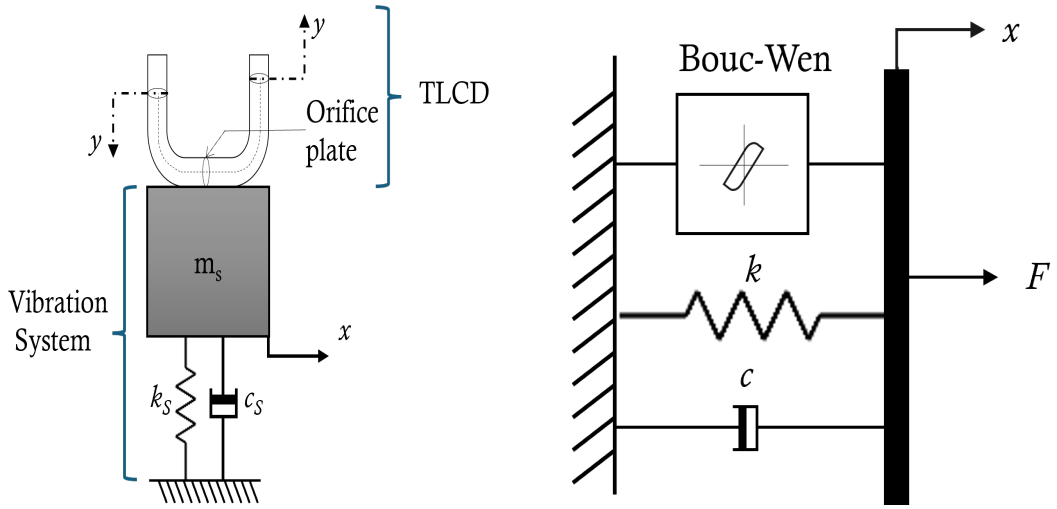

Figure 3.4: (a) A classic semi active device which consists of a vibration system represented by single degree of freedom coupled to TLCD [33]. (b) The Bouc–Wen model of MR damper [4].

However, rheological dampers are more popular and broadly employed in industrial applications [33, 36]. There are two types, which are Magneto-Rheological (MR) and Electro-Rheological (ER). Both dampers operate similarly, but they are different in terms of fluids. Historically, in 1947, Winslow discovered rheological effects by applying an electric field to a colloidal fluid containing microsized particles, which is known as electro-rheological [49]. One year later, Rabinow found a similar phenomena by introducing a magnetic field into a fluid containing magnetisable particles [3, 50]. The utmost advantage of these types of fluid dampers are their ability to

maintain some protections to the structural systems even in the case of no power [51].

ER dampers gained more research interests in terms of civil engineering applications, until the research community found that MR dampers are more effective [51]. MR dampers have the ability to provide more yield stress than ER dampers, and are more robust to changes in the temperature. In terms of cost, MR damper not only requires less power, but also less sensitive to contaminants. As a result, MR dampers have been the subject of comprehensive studies in engineering applications like building and large civil structures [52], railways [53], and vehicle suspension [54].

The MR damper is categorised as a nonlinear semi-active control devices since it exhibits a hysteresis behaviour. In the literature, several modelling methods were proposed to capture this nonlinear behaviour, such as the Bingham model and the Bouc-Wen model. Figure (3.4b) depicts schematically an MR damper where the hysteresis behaviour is represented by the Bouc-Wen model. On the other hand, the lack of a complex and accurate mathematical model for MR dampers has led researchers to utilise more recent data-driven techniques. For instance, Delijani proposed sequential neural network model of parameter identification for MR damper [55], whereas Ahn utilised self tuning fuzzy method [56]. Surprisingly, the probabilistic modelling view in MR damper control setting is still rare [57]. Therefore, there are some probabilistic modelling approaches presented in the literature that could be potential techniques for semi-active methods.

Albeit there is a growing interests into semi active and hybrid control in vibration control in recent years, research on active control still offers a strong foundation in development of smart structures in vibration control [58]. In the following section, the concept of active control will be explored, particularly focusing on issues related to nonlinearity and unknown dynamics.

3.2.3 Active control

Active vibration control has recently received a lot of attention in research and applications because there is a gap between projected and actual performance in practice. This interest motivates the urgent development of intelligent systems for structural control. Furthermore, the active damping device is a part of an active vibration control system, which uses additional actuators to dissipate energy from

the structure. Compared to semi-active control, the popularity of this concept stems from its ability to use a large power source to operate a powerful actuator, such as electrohydraulic or electromechanical actuators, in order to increase structural stiffness or damping [4]. As a result, successful implementation of active damping devices involves fast sensing equipment, a stable control law, and responsive actuator technology [59].

Active control was introduced in the 1970s and first used on a large scale in 1989 [60]. Since then, active damping devices have been used in a variety of applications. In 1993, the Kyobashi Seiwa Building in Tokyo became the first civil engineering project to use active damping control [61]. To avoid the risk of devastating earthquakes, the researchers proposed installing two active devices at the top of a ten-story building, with the first controlling the fundamental mode and the second targeting torsional vibration. In space industry, Okubo et al in [62] addressed the issue of flexible space structure and suggested utilising active control system in order to calculate structural deflections and then apply control forces to restore the desired shape. Similarly, this active concept has been used in vehicles suspension [63] and helicopters [64].

In terms of devices types, ATMDs are an example in which the active control mechanism was considered by an actuator positioned between the vibration system and the TMD system, with a controller, and an accelerometer acting as a sensor. Another example is active tendons, which are prestressed tendons located between the floors of a building structure or at the ends of cables in a cable-stayed bridge. Actuators change the tension in cables, which influences the control force applied to the structure where the actuators are hydraulic.

Spencer in [45] summarised the disadvantages of active vibration control, particularly in civil engineering applications. Among the drawbacks are high capital costs for maintenance, low reliability and robustness, and power consumption. Hence, the main challenge of this concept is that it requires multidisciplinary research because active vibration control systems are comprised of a sensor, a controller, and an actuator, each with its own set of restrictions and limitations. Having said that. a new perspective of a modern dynamical system could be alternative methods of facing these limitations.

As mentioned earlier, consideration of the right engineering problem that requires data-driven methods is important, and the effectiveness of the control system re-

lies on the quality of the model. Moreover, MBC is just one of the possible active vibration control strategies, and it has typically been successfully used in practice when the model is linear. Meanwhile, with the increasing use of flexible structures in aerospace engineering, medicine, and robotic applications, active control techniques are increasingly relevant and offer the possibility of simultaneously addressing damage detection, and other actuation requirements [7]. Therefore, understanding the dynamics of the nonlinear structure from both a design and a control perspective is an important first step. In this thesis, the nonlinearity of the actuators and unmodeled dynamics of the structural system have been considered.

Spillover

The challenge with unmodeled dynamics comes from the fact that flexible structures are characterised as distributed parameter systems, which are theoretically infinite dimensional. The infinite dimensions must be captured in order to model the behaviour of a system, such as a spacecraft. However, numerical models of structural systems remain approximate and frequently insufficient due to inherent uncertainties such as noise and modelling errors, unknown system properties, and the impact of changing operational conditions. This issue can become more critical when active vibration control is implemented. In addition, the inherent low damping of flexible structures and the truncated modes of vibration considered within the controller, can destabilise the control system.

In 1978, Balas introduced Spillover problems [65]. Since then, the spillover phenomenon has been extensively investigated in the literature. Adding extra constraints on the disturbance and damping parameters by utilizing a reduced order model has been suggested; and the placement of sensors and actuators has been proposed in [66], where the control strategy utilized was not optimal. Recently, researchers proposed the idea of utilizing more sophisticated control algorithms such as hybrid control [67], robust minimax optimal controller [68] and adaptive positive position feedback [69]. However, optimal control was still the primary control technique that addressed the spillover issue. Sesak et. al. in [70] suggested investigating the sensitivity in the flexible system by providing three constraints. First, the optimal control and observer gains were required to satisfy the orthogonality condition with suppressed states that spillover effects do not excite. A prescribed degree of stability was the second constraint, which was based on the alpha shift

method introduced by Anderson and Moore in [71]. Third, a low pass filter was used to eliminate high frequencies. This method is called Model Error Sensitivity Suppression (MESS). Loop Transfer Recovery (LTR) provides an interesting situation where process and measurement noises have a direct impact on control performance or, more precisely, on the stability margin [72].

Hence, Bayesian frameworks have become an interesting research topic in structural dynamics, especially where quantifying the uncertainty is concerned. The early work concerning Bayesian active vibration control was done by Dertimanis et al. and Moradi et al. [72, 73], although they have not considered spillover problems in their cases.

Nonlinearity in active damping devices

In most cases, the structural nonlinearities are considered to be the main source of nonlinear dynamics in the control path when active vibration control is applied to a structure [74]. However, the increase demand of employing flexible structures in the industry requires the use of a nonlinear model to precisely predict the actuator's dynamic behaviour if it is subjected to large amplitude signals. In addition, understanding actuators' nonlinear dynamic behaviour and creating efficient control strategies are essential because these actuators can cause damage and destabilise the active vibration control systems.

One of the active devices used to study the effect of nonlinearity in active vibration control systems is a proof mass actuator. The proof mass actuator is a type of inertial actuator that provides a secondary force on a vibrating structure in order to reduce or eliminate the vibrations. The mechanism of the inertial actuator consists of a magnetic proof-mass, a fixed coil and a suspension, which connects the proof-mass with the actuator casing. Its basic method of operation involves using a current to flow through a coil that is subjected to a constant magnetic flux in order to transform electrical power into mechanical power. Moreover, proof mass actuator is widely used in engineering applications such as space structures and satellites [3].

The popularity of inertial actuators stems mostly from their ability to generate a significant inertia force without a ground reference. On the other hand, saturation nonlinearity, often known as stroke saturation, is one of the limitations of proof mass actuators. Technically, the displacement of the proof mass actuator is limited by

the stroke length of the actuator. To control low-frequency vibration, the control system requires a long stroke length caused by a high input voltage, resulting in an impact between the proof mass and the actuator casing against the structure. This large shock might not only damage the structure but also destabilise and limit the performance of the closed loop system. As a result, stroke saturation is a significant nonlinear phenomenon that must be accounted for by using modelling or control methods.

In terms of modelling, Baumann and Elliot in [75] proposed modelling an inertia actuator as a lumped parameter system in which the finite stroke of the actuator proof mass is expressed by a nonlinear stiffness as shown in Figure (3.5). This concept was acceptable in the dynamic research despite the fact that there were two major drawbacks [76]. First, the behaviour of the actuator was assumed to as a linear single degree of freedom system when the input is low and saturation stroke does not occur. Second, it is still uncertain if the nonlinear stiffness accurately reflects the stroke saturation. Alternatively, L Wilmshurst et al in [74] suggested using nonlinear system identification based on measurements where experimental measurements reveal a weakly nonlinear actuator behaviour below saturation threshold, allowing for the use of a linear piecewise model for simulated actuator response.

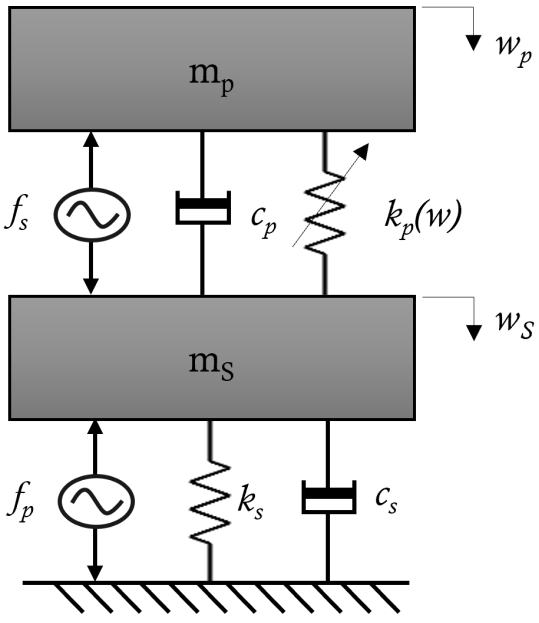

Figure 3.5: A lumped parameter model of the actuator and structure as the authors in [75] proposed. Here, s represents the structure, p denotes the proof mass actuator, and k_p represents the nonlinear stiffness.

From a control perspective, stroke saturation is detrimental to the stability of the

closed loop control system because it reduces the stability margin. This phenomena was encountered by Chase et al in [77]. The authors observed the destabilising effects when the velocity feedback controller is applied to a buckling beam, where the issue was resolved by employing a secondary controller. Furthermore, a number of studies have investigated the stroke limit in an effort to improve control performance and system stability. In early work, Linder et al proposed a local feedback control system by employing two control loops in which the gains were sized so that the hitting the end stroke prevented under commanded motion [78]. Then, they extended their work by utilising nonlinear control laws [79]. Robust techniques then were used in [80]. The University of Southampton's Institute of Sound and Vibration Research has recently conducted extensive theoretical and experimental research on the nonlinearities of inertia actuators, including stroke limits in [81–84]. Despite the fact that the researchers presented excellent and practical results, neither the modelling nor the control have taken into account data-driven approaches based on a probabilistic formulation.

In summary, active vibration control is important for industries, and a number of techniques and approaches have been proposed and utilised in practice in the literature. Generally speaking, the majority of these methods continued to use MBC. In light of this, research on the application of DDC-based control strategies for active vibration settings is still lacking. In the following sections, a number of modelling and control approaches from different engineering domains, including robotics and structural health monitoring, are explored. These approaches are worth investigating with regard to active vibration settings.

3.3 Modelling and estimation in structural dynamics

This section will provide an overview of modelling and estimation in structural dynamics, with a focus on recent advances in both domains and examples of probabilistic models.

3.3.1 Classification of modelling in structural dynamics

Modelling is an essential step in any design process that has significant effects on a system's outcome. Section 2.1 covered the topic of modern dynamical systems; this section will discuss modelling terminology and approaches that are common in many engineering fields, with an emphasis on SHM approaches. To classify modelling methodologies in dynamic systems, new terminology emerged recently [10, 13, 85]. Three types of mathematical models are commonly used to describe the basis of MBC: white box, black box, and grey box models. Various levels of insight regarding the dynamics of the system and data transparency are reflected in each category.

White box

White-box modelling approaches make use of knowledge such as physical and chemical laws or theories to create models that reflect physical behaviors and for years, certain traditional white box modelling techniques have been used [11]. A classic example of a typical physical model is Newton's Law in which deriving the governing equations not only needs a deep understanding of the objective system but also needs to be represented formally by parametric properties. For instance, a lumped mass model is a well-known mechanical system, and it has been described by second order differential equations with mass, spring, and damper parameters as shown in Figure (3.6). The advantage of such a white box model is that there are direct physical meanings attached to the model parameters, and they also give reliability and flexibility for significant changes in system design as well as predicting behaviour over a broad operating range [13].

In the analysis of mechanical vibrations, modal analysis is a procedure used to find

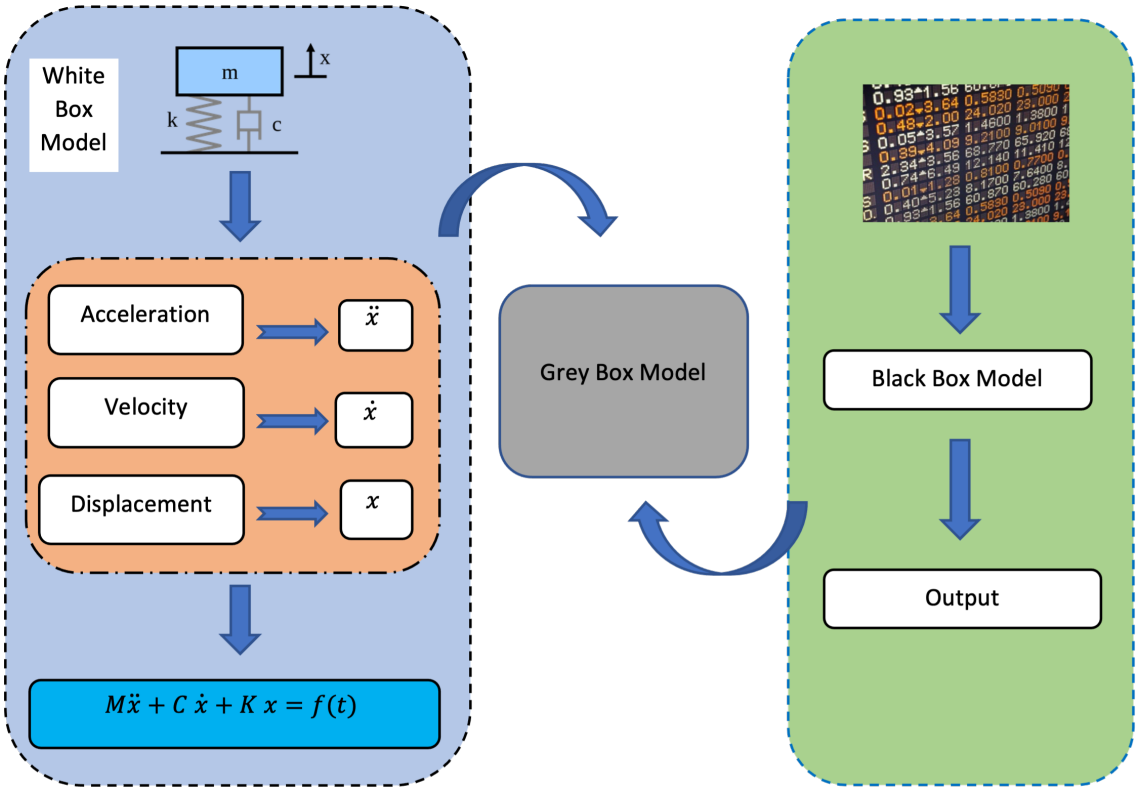

Figure 3.6: White box vs Black box models in dynamic systems.

a response of a mechanical system such as a Hawk T1A aircraft subject to arbitrary force conditions [86]. This procedure helps to identify the modal amplitude and natural frequencies of the system and all of these are useful prior physical knowledge. Even though these physical based models in [44, 87] can be assumed as ideal models, the challenge of avoiding an unhidden dynamic was inevitable for two main reasons. First, white box models were established around a certain range of frequencies in which unknown environmental disturbances can excite the system and lead it to mechanical failures. Secondly, modal analysis is frequently assumed to be linear. While it is acceptable under certain operating conditions, the assumption of linearity is usually incorrect. Nonlinear models are required in this case when a more detailed model for a wider operating range is required.

There are other perspectives which can be used to further classify white box models: static versus dynamic, time varying versus time invariant, deterministic versus stochastic, continuous versus discrete, linear versus nonlinear, and, finally, lumped-parameter versus distributed-parameter models. Most of these properties have been addressed in the literature for example nonlinear vibration control [6] and time varying models [88]. Conversely, the white box is frequently jeopardized by a lack of

accurate knowledge and the necessity to make assumptions that must occasionally be validated. Nevertheless, the extraordinarily complex structure of many system models might make solving them impractical or economically undesirable [89].

Black box

Black-box models are obtained through experimental modelling or identification. Basically, the structure of the mathematical model and the corresponding parameters are identified in this case using the system's input and output data in which the prediction of the model is formed directly from the data as shown in Figure (3.6). In other words, a black-box model can be formed without a prior knowledge or expert's insight and is usually formed from a known class of models, Artificial Neural Network (ANN) for example, with universal approximation property [90, 91]. This model is preferable when the white box fails to understand or capture the internal structure and characteristics of some systems.

Although black box models have gained a lot of attention in recent years especially ANN [92, 93] and fuzzy logic [94], this approach is still used based on its usefulness not trustworthiness [13]. The drawbacks of this data-based black box model can be summarized as follows. To begin with, unlike physical-based modelling, the data-modelling technique only describes the correlation of the data, which means the relationship between the input and output in the black-box model is difficult to interpret [90, 95]. The flaw with this approach is exacerbated when comparing the results of the same model in a different circumstance since there is no physical element to compare [95]. Secondly, misleading conclusions are a serious concern in this approach in effect of either the accuracy limitation in data or missing essential data. Third, since this method of identification can yield fruitful relationships, validations over a broad operational range are required to give a technical background in this identified model.

The advancement in nonlinear system identification has recently been given a lot of attention in deterministic and stochastic models. The former model is uniquely identified by parameters and previous state of the variables with specific initial conditions, otherwise the solution of the model may differ. On the contrary, the stochastic model is identified by probability distribution or stochastic process [10]. Equally important, this perspective can be simplified into parametric and non-parametric models [96]. Although there is no well-known distinction between these categories,

the issue which distinguishes the parametric model is that it presumes a particular functional distribution which may not be viable for all applications. Alternatively, nonparametric density estimation approaches use the range of the set of data to inform the distribution shape. The parameters of these models, in contrast to parametric approaches, are used in order to govern distribution complexity rather than shape [97].

With those categories in mind, research [96] proposed an identification procedure as outlined in Figure (3.7) mainly for parameter estimation methods. This procedure contains three basic stages: detection, characteristics, and parameter estimation. Since then, researchers have followed this procedure and given great attention to the third steps during the last decade as it shows the importance of quantifying the uncertainty [8]. For example, the Bayesian framework has been attributed in the structural community with not only finding the optimum model among possible modal structures [98] but also finding the nonlinear systems in the presence of uncertainty [99]. Moreover, the authors in [96] categorized the nonlinear system identification into seven categories and researchers have also adopted this classification. These categories are linearization, time and frequency domain approaches, time and frequency analysis, modal methods, black box modelling and finally modal updating. Researchers in [100] utilized these nonlinear system identification categories to illustrate all techniques applying to nonlinear damping systems in structural dynamics. It is clear now that parameter estimation methods have been used and improved during the last decade as a consequence of the non-parametric methods seeming to need more attention.

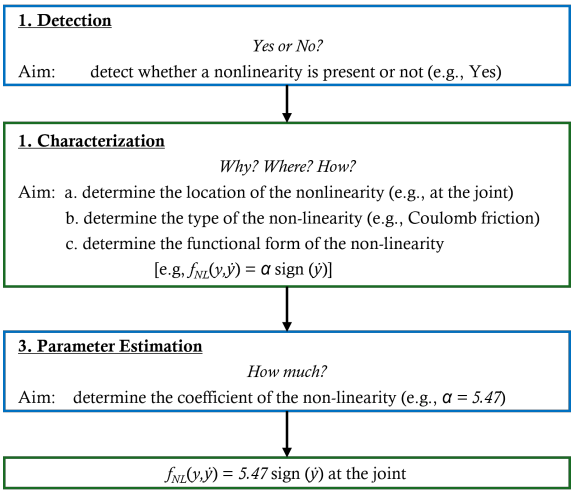

Figure 3.7: Identification process of nonlinear structural dynamics [8, 96].

One of the most powerful black box models in the last three decades is Nolinear Auto-Regressive Moving Average with eXogenous (NARMAX), and it was introduced by Billings in 1984 [101]. The NARX model is a special case of the NARMAX model, and it has been widely used in nonlinear system identification problems [102]. In general, the NARX model is an input-output recursive model whose current output is determined by a nonlinear functional expansion of lagged input and output terms, plus additive noise. One of the challenges in the NARX model is that the nonlinear function $f(.)$ needs to be identified. Several types of nonlinear expansions have been utilized, and one of the earliest methods is a polynomial model class [103, 104]. Although the usefulness of the polynomial expansion comes from its ability to learn the expansion coefficients or parameters by employing the advanced least squares approach, it is a commonly fixed parametric method. As a result, a number of machine learning-based nonparametric NARX model forms have been developed, such as Multi-Layer Perceptron (MLP) and Radial Basis Function (RBF) neural networks [105, 106].

In that category, the GP-NARX model has recently become an alternative non-parameteric method in structural dynamics. The GP-NARX model offers several potential benefits in comparison to the NARX variants in the literature [107, 108]. First, the GP-NARX model not only forms out of a family of feasible functions that may define the relationship between data but also avoids the necessity of fixing the function form. Second, the GP-NARX model also offers uncertainty estimates as confidence intervals. This is especially helpful when the model needs to quantify the uncertainty in its predictions. Lastly, GP-NARX models can provide one prediction for control problems or multi predictions for simulation problems. In terms of applications, SHM utilized the GP-NARX in order to estimate the life time of structures such as offshore structures [108], whereas the author in [109] employed the model for damage detection in composite aircraft structures. More importantly, this model is still rare in control applications, as will be stated in Section 3.4.

Similarly, block oriented models are another nonlinear system identification technique. The models are constructed using two basic building blocks: an LTI block and a static nonlinear block. They can be combined in a variety of ways, including series, parallel, and feedback connections, as illustrated in Figure (3.8). Furthermore, the engineering community considers known structures like Wiener and Hammerstein models to be attractive forms of prior knowledge. Consequently, incorporating GP models in block oriented structures are more suited in which it forms a structural

prior knowledge about the modelled systems [14]. In practice, several works have been reported in [110–112]. To the author's knowledge, incorporating GP models in one of these block oriented structures for vibration control settings has not been explored.

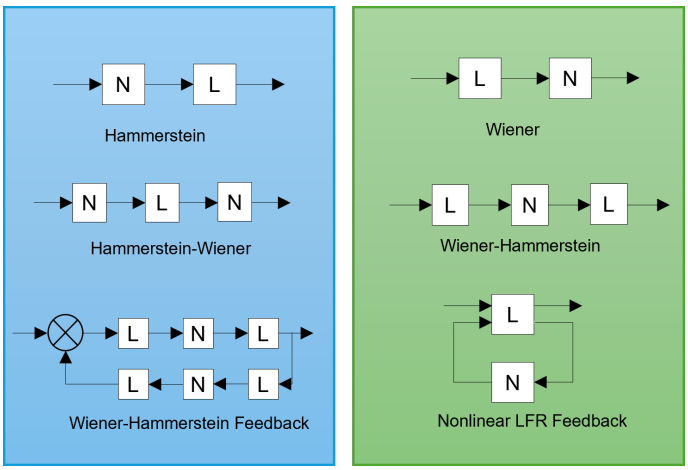

Figure 3.8: Models with a block orientation. To model the nonlinearity, one uses static nonlinear blocks N, whereas the linear blocks L depicts linear dynamics. [12].

Grey box

To avoid white and black boxes flaws, a combination of theoretical and experimental modelling methods is an alternative model especially when the structure is known, partially known, or assumed, and the parameters are optimized [14]. This alternative model is called a grey box model, where the main feature of a grey box is that it incorporates physical insight or a prior knowledge in the model.

In general, a priori knowledge offers information about the system and experimental data that can be integrated more effectively into identification, and which can significantly minimise the requirement for informative experiments, therefore reducing the challenge in carrying out experiments. This is the cornerstone of a grey box design that focuses on efficient ways of integrating prior knowledge into a parametric model. Various ways to incorporate a prior knowledge have been studied. A priori information was handled as a constraint on model parameters and variables in the form of inequality, marginal stability, and other critical process features by the authors in [113, 114]. To illustrate this grey box modelling, Peter Seiler et al implemented two-step approach for identifying the stability and control derivatives [115]. Their technique began with black-box models to find sensitive modes with

considerably different damping ratios and natural frequencies than their original values. This information was then used in grey-box models to selectively update the stability and control derivatives associated with these sensitive modes while leaving the rest of the derivatives at their starting values [115]. Even though this approach has gain attention in SHM [116], it is out of the scope of this work.

3.3.2 Estimation in structural dynamics

The state feedback strategy implicitly assumes that full knowledge of the state variables is available for feedback. This assumption cannot be held in practice, however, either because of the failure of a direct connection to the state variable or because sensor devices are not available or too costly [117]. In either case, designing an estimator is necessary. Without knowledge of the initial condition, the asymptotic state and parameter estimation are the targets given the input and the output [2]. There are a number of ways to address this problem. The Luenberger Observer (LO) is the simplest estimator and is used with a well-defined dynamic model. This method is essentially executed through a feedback mechanism to correct its estimated states or parameters depending on the actual results of the physical systems. The effectiveness of this approach is dependent on the availability of input and output measurements, and the system is considered to be linear and deterministic. In addition, with a reasonable feedback gain, the convergence of estimated states can be guaranteed if the system is observable. For those reasons, this method has proved its worth in control, systems monitoring, detection, and identification in dynamic systems [118]. Observer tuning for linear systems may be carried out using the pole placement approach. The pole placement method enables the determination of observer gain values for system stability and convergence based on the desired eigenvalues. The application determines the best location for the eigenvalues. In general, the faster the convergence rate, the further to the left the complex plane or the more negative the real part of the pole. However, if the poles are placed too far left, noise in the system may increase.

Even though the LO works successfully with state feedback, the noise and model errors are still inevitable issues. Rudolf Kalman addressed the issue of process and measurement noise in his remarkable paper [18] in 1960, late known as the Kalman filter (KF). This approach requires a dynamic system model, known control inputs and, above all, white noise in processes and measurements. Based on these as-

sumptions, the optimal estimation started by predicting the state recursively and then evaluating the uncertainty of the predicted states. Before updating the predicted state, a weighted average of the predicted and measured values needs to be calculated [119]. Technically, KF uses indirect and noisy measurements to provide missing information. As a result, KF is a statistically consistent description of an estimate issue in which it propagates current dynamic system knowledge under the statistical impact of dynamic random disturbances and impacts of all previous observations [120]. The advantages of the KF technique can be summarized in three points [119]. First, in addition to the simplicity of addressing the noise issue in the system, KF is an optimal estimator in which the expected error value between the filter's estimate and true state is zero. Second, compared to LO, the accuracy of KF is higher, but the implementation is more complex. In addition, the KF works as an adaptive low-pass filter and the cut-off frequency is determined by the ratio of system uncertainties to measurement noise, and also the estimate covariance [121]. The limitation of this approach is numerical instability. The cause of this limitation is the covariance matrix, especially when it is symmetric, and the values of the process and measurements' noise are assumed to be small [122].

In real engineering applications, an assumption of the linearity of the model and white noise of the measurements are not always preserved or true. Consequently, a nonlinear filtering problem has been identified in the literature and there are various methods to address it, each with its advantages and drawbacks. Figure (3.9) gives a summary of the most estimators in the literature of Gaussian filter. In civil applications, the Extended Kalman Filter (EKF) has been recently utilized as a standard for nonlinear parameter and state estimation because it is robust, easy to implement, and suitable for real time application [123]. EKF is a nonlinear extension of KF in which it operates around local linear approximations of nonlinear systems by applying Taylor series expansion to state transition and observation matrices [124]. For that reason, the success of this method relies on its validity of the linear approximation or, in other words, how linear the observation and transition models are around the mean [125]. Despite its simplicity and low computational cost, EKF is not optimal when dealing with a highly nonlinear system because of the calculation of the Jacobian matrix. In addition, choosing the initial state estimation is a critical step in EKF algorithms since it effects the convergence performance [119].

Another extension of KF is UKF. UKF does not require a linear approximation of the nonlinear system, but it handles the state random variable as a Gaussian

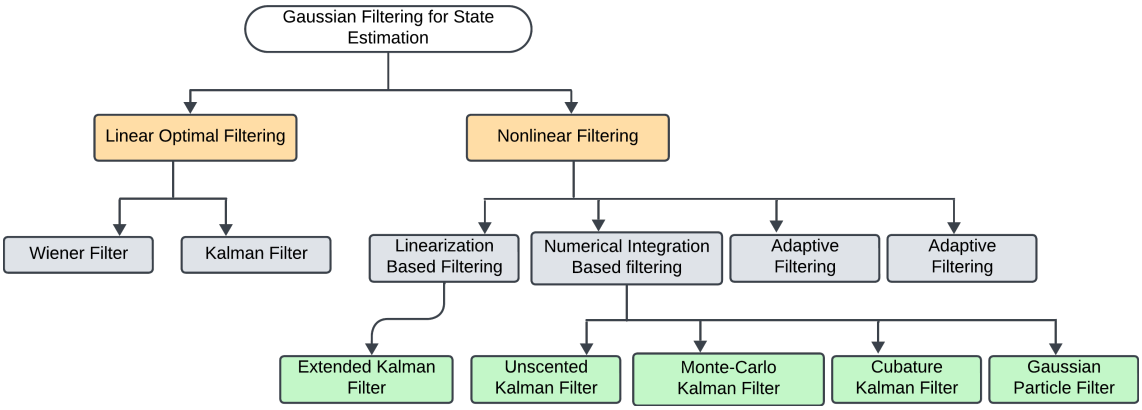

Figure 3.9: A general classification of main Gaussian filters for state estimation [119].

distribution [118]. Basically, it uses the unscented transform as a deterministic sampling approach in which the state is represented by a minimal set of chosen points around the mean [119]. This set of samples are called sigma points which capture the true mean and covariance, and propagate utilizing the prediction and observation function [126]. When those points propagate through real nonlinear systems, UKF can capture the posteriori mean and covariance to the third order for any nonlinearity [124]. Besides computational complexity, UKF also solves issues with both the previous estimation methods. First, as mentioned, it works with nonlinear systems and white noise. Second, UKF is accurate which means it avoids calculating the complex Jacobian matrix; as a result of its simpler computations, it is easier to implement than EKF. Even though there are differences between these approaches, they have the same issues which are sensitivity to initial conditions and assumptions of Gaussian noise.

It is noticeable amongst the methodologies of state estimation that the Bayesian framework has been used for two reasons [127]. First, since it is based on probability, this method can preserve information. Second, state estimation based on the Bayesian framework can be utilized for any probability-based system. To illustrate this point, probability density function (PDF) is a part of the Bayesian framework in which PDF of the model state can be provided based on the availability of the information, so these approaches can be used in control techniques, system identification, and SHM [128]. Also, with the probable density of the state, it is possible to describe the uncertainty in the estimation.

The particle filter (PF) is one of the Bayesian state estimation approaches used

in the literature. Compared to previous methods, PF is more flexible as a result of how this algorithm presents the PDF [128]. Technically, PF utilizes particles which are a set of random samples aiming to estimate the posterior probability of the state sequentially over time [129]. The posterior estimation has to go through those particles where they are placed, weighted, and propagated properly in random space [121]. The feature of this method is that particles are no longer distributed uniformly across the state, but rather are concentrated in high probability regions [129]. Computation complexity is a drawback of this method.

As mentioned in all three state estimation approaches, computation can be an issue in real time applications, especially when it comes to computing the full joint distribution at all time steps. Consequently, Bayesian filtering and smoothing provides three marginal distributions which can be used instead as shown in the Figure (3.10) [130]. First, smoothing makes use of the whole time range of the measurements to refine the estimates even if it is past the time of interest. Filtering uses current and previous measurements, in which the time of interest is included. In contrast, prediction only uses a certain interval of measurements, which is usually prior to the time of interest. Based on the measurements, it predicts the future state of the system [119].

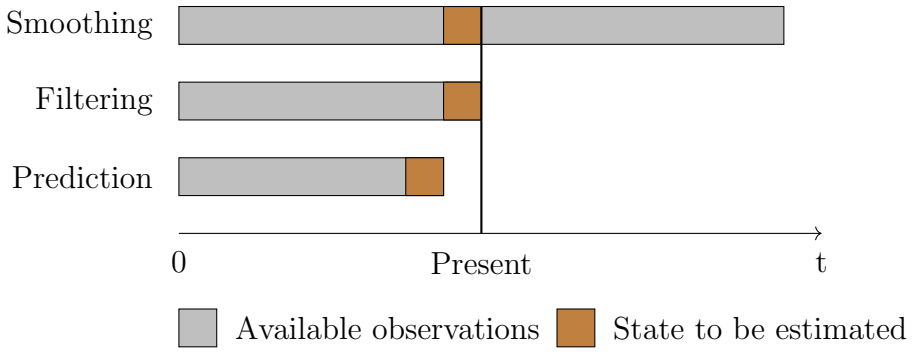

Figure 3.10: Optimal prediction, filtering, and smoothing are state estimation problems depending on the time span of the measurements [130].

Bayesian filtering in structural dynamics

The last section presented elegant algorithms for linear and nonlinear observers aiming to extract values of hidden quantity from indirect, inaccurate, and uncertain measurements. Structural dynamics is one of the fields which has implemented and

utilized these algorithms to gain insights about the internal states of the structure, for example, and to identify damage [119]. However, it is noticeable that there is a huge gap in terms of utilizing the recent advancement of estimation among subfields of structural dynamics such as structural control systems and structural health monitoring. Consequently, this section will present some estimation issues in both fields and highlight the challenges and strategies. To simplify the comparison, the variables of interests for an estimation in structural dynamics could be:

1. State estimation i.e, deformation and acceleration.
2. Input estimation i.e., force input.
3. Parameter estimation i.e., mass and stiffness.
4. State and input estimation.
5. State and parameter estimation.

Generally speaking, control systems and condition monitoring in structural dynamics require a full knowledge of state and parameters. In practice, some existing applications might have difficulties to directly measure these variables. This may be because direct measurements need highly expensive sensors, or because the positioning of the sensor in the structure is unfeasible. The estimation approaches have been used as a solution for some dynamics problems [131]. They may, for example, be utilized for system identification to understand the behaviour of nonlinear structures under dynamic loads, and can also be used in SHM to identify changes in the dynamical characteristics of structural systems during earthquakes. For this project, the capacity to estimate system states in real time may aid in the development of an efficient control strategy for structural control [129].

The traditional technique of estimating states is to measure another variable that is related to the required one and execute a calibration based on the assumption of a continuous relationship [4]. An accelerometer is an example of this method in that it measures the absolute acceleration in which displacement and velocity can be extracted based on integration. Unfortunately, this is not a reliable method since minor changes in the system or other operating circumstances might have a significant impact on the estimations [129]. KF is another popular approach used as a linear estimator to indirectly estimate the states or more precisely the

displacement and velocity of the system in the presence of noise. This approach is used in vibration control in combination with a linear quadratic regulator to develop the proper control forces. For example, Parus et al in [132] addressed a regenerative chatter vibration problem in a flexible milling workspace and they suppressed the vibrations by applying an active control in which they utilized a KF as a linear observer. Also, Song et al in [133] utilized the observer as a new method for non-stationary seismic random excitations in which active control is applied to adjacent tall buildings. In practice, unknown input and parameters in some applications violate the assumptions of the KF in which they are available. Sometimes the response of the system can be measured but the forces that operate on the system cannot be measured. This is an interesting problem in that we know the behaviour of the system but have to try to characterize the forces that cause the behaviour. This is known as the inverse problem because it is the opposite of the forward problem or state estimation. Unfortunately, in comparison to the forward problem, the inverse problem has received less attention [134].

Input estimation or as it's known, the inverse problem, has also been tackled in structural dynamics. For instance, Lin et al in [135] addressed the issue of excitation forces acting on a low reliability of structure such as a cantilever beam. They proposed using KF algorithms and then the recursive least square algorithm method to estimate the input forces. Chih-Kao in [136] utilized the same approach in identifying impulsive loads. This development in input estimation encouraged researchers to utilize the input observer in active controller instead of assuming the input is zero. To illustrate that, Ho et al in [137] used the input estimation method combined with Linear Quadratic Gaussian (Linear Quadratic Gaussian (LQG)) control in which structural vibrations can be suppressed more effectively due to the actions of the proper control forces. Interestingly, dealing with inverse problems is not as straightforward as carrying out state or parameter estimation. For example, calculating differential equations of a system uses a clear analysis approach in state estimation, whereas input estimation solutions are more subject to indeterminacies, such as singularities, which require more analysis than a forward problem [134].

Regarding the parameters, it is obvious that a robust strategy that can account for changing parameters is necessary. Parameter estimation is another method used in the literature where some modifications of KF such as EKF and UKF are used specifically for the nonlinear problem of parameter estimations [138]. To demonstrate this concept, it is not possible to calculate or modify certain structural characteristics

such as mass, damping and stiffness to help the response meet the requirements due to the design restrictions. In mechanical systems, an estimation of external loads on a system is frequently of great importance. This estimation applies to vehicles when the parameters are generally unknown but it is essential for effective control to use the unknown friction coefficient and the vertical displacement of the road [131]. For example, Ray in [139, 140] addressed the effect of the unknown parameters in terms of control perspective by utilizing EKF for estimating the nonlinear behaviour of friction coefficient. While he showed a reasonable result experimentally, he was still relying on the discrepancy model of tire.

Recently, there has been a growing interest in using Bayesian techniques to estimate two variables instead of one, such as the Augmented Kalman filter (AKF), Dual Kalman Filter, and Joint Input State (JIS) methods. In structural control systems, however, similar techniques have received less attention [138]. Furthermore, a research team at ETH Zurich is leading the dynamic community in another approach that can be described as adaptive control in a structural control system. Their novel approach is based on combining one of the Bayesian nonlinear observers with LQR for effective vibration mitigation in dynamic systems subjected to uncertainty as shown in Figure (3.11). This novel approach results in five publications [15, 73, 141–143] which start with linear system and control and end up with nonlinear in both structural system and control. Basically, the implemented method is formed by combining UKF as a nonlinear observer with LQR. The UKF is used to construct an adaptive joint state and parameter estimation problem, recognizing that numerical models of structural systems are frequently insufficient due to inherent uncertainties and the influence of changing operational conditions. The enhanced state-space representation is utilized in the LQR, along with a clipping-based semi-active control method. Since both estimation and control are carried out on the same loop, special attention is paid to the formulation of an adequate LQR approach both for selecting optimal weight matrices and for the tuning of the control parameters in real-time. With nonlinear structure, they used feedback linearization as a nonlinear control method to eliminate the nonlinearity from the system. They then again used the previous control approach. Even though Chatzi and her team produced a remarkable result, there is room not only for improvement, but also for exploring the reliability of this approach. The validity of this method is based on two independent test scenarios. First, to demonstrate the effectiveness of a nonlinear estimator in a real time test, a joint state and parameter estimation of the structure without an actuator was explored in order to avoid the cost of the ac-

tuator's expensive computations. Second, the nonlinear observer was coupled with LQR in order to complete the proposed adaptive control framework. Stability and robustness are still an open research problem.

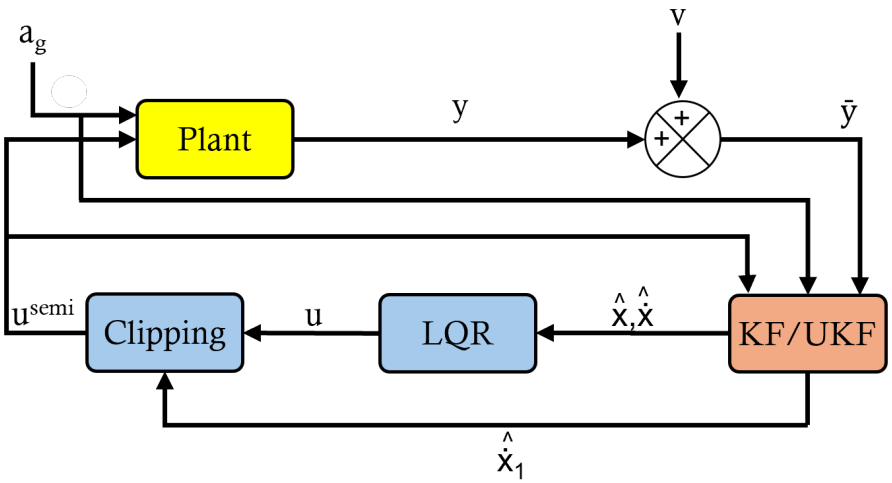

Figure 3.11: The control scheme of semi active control for vibration mitigation with limited sensor information [73].

Now, as stated above, modification of LQR is essential in order to integrate an online method for the calculation of the corresponding state feedback gain matrix in structural dynamics. Chatzi and her team provided three solutions in calculating LQR online. Initial guess is the first and simplest approach in order to solve the discrete time algebraic Riccati equation. The drawback is that it is not optimal, and it does not guarantee safety margin. Second, another option is to solve the LQR problem in each iteration as soon as the UKF's state estimations become available. However, the solution of an eigenvalue issue, which is extremely time-consuming for hard real-time operations, is required for related non-iterative and numerically efficient algorithms. Lastly, the method described in Chowdhary and Lorens in [144] assumes that the structure is subject to small changes between time steps, which in turn leads to slight changes in the best LQR solution. This method creates a recursive formulation of the associated Riccati matrix, which was the one adopted in Chatzi's work. The last point may require more investigation.

In the summary of the modelling and estimation section is that the main advantage of Bayesian framework is that it has the ability to quantify uncertainty which helps to define the regions of less certainty. Fortunately, control theory has been addressing the uncertainty issue in feedback control for years and it offers a variety of strategies and techniques, such as robust control [16]. However, despite the advancements in

structural dynamics in terms of using nonlinear system identifications, utilizing the control strategy or developing a control policy incorporated Bayesian approaches either in modelling or estimation have been less explored [15]. Hence, the stream of these developments paves the way for adding the controller in order to draw on physical interpretations and close the loop of the systems. In the end, it is interesting to note that this thesis involves several fields starting with structural dynamics, control theory, measurements, probability, and machine learning. This crossover leads to an issue of misunderstanding of similar terminology between these fields. As a result, it has become an urgent task within the dynamic community to unify terminologies in a way that helps the reader to distinguish between these terminologies or at least to be able to follow the concepts.

The next section will provide an overview of some control algorithms utilised in vibration control with emphasising in some algorithms that incorporates Bayesian approaches either in modelling or estimation.

3.4 Control algorithms

Control algorithms are responsible for the value of the control input based on minimizing the error between the reference input and the output. MBC is one of the simple control algorithms in structural vibration control and it is mainly designed for disturbance rejection. Pole placement is a technique used for selecting the gains of the control algorithms.

Even though it has been primarily used for vibration reduction, the success of this algorithm is based on the model discrepancy [37]. Reducing the error or the motion of the mechanical systems to the greatest possible extent is the ultimate goal of feedback vibration control. LQR algorithm is the most basic and commonly used methods to solve optimal control problems [58]. This algorithm identifies the feedback gain by minimizing the quadratic performance index i.e. the cost function. This cost function usually does not have a physical impact but is utilised to weight the norm of the output and control energy of the system [32]. The weight of these quantities is calculated based on the constraints and objectives of the system. Even though stability is often not an issue in this method, states of the structure are not always available.

LQG is another optimal control algorithms in which it measures the states indirectly by utilizing KF. As stated in the literature, both algorithms have been utilised and implemented successfully in many structural systems. However, to increase their effectiveness, a modification to the algorithms has been proposed [4]. As example, authors in [145] considered time delay in LQR control for seismic-excited linear structures subject to earthquake. Ho and Ma in [137] considered unmeasurable disturbances or arbitrary external loadings in the calculation of control forces as a result of the conventional LQG do not consider the input forces. Their method was based on combination of LQG and an input estimation approach. Moreover, it is sometimes required or easier to make the calculation of the feedback gain in discrete time, especially when advanced nonlinear estimation methods were used. Therefore, with all benefits of these modified optimal control algorithms, the robustness is still an issue.

In that case, robust and adaptive controls are suitable for tackling the issue of unstructured and parameters uncertainties respectively [146]. Robust control is a type of control that focuses on linear systems and incorporates an a priori knowledge of model uncertainty into the controller design, as well as ensuring system stability and performance for all uncertainties. While the uncertainty definition guarantees stability, robust control approaches may reduce the overall controller performance since the performance target is reduced over all feasible models that fall under the uncertainty specifications [147].

On the other hand, by having a method for adjusting its parameters, an adaptive controller maintains optimal performance under changing conditions [148]. Both methods have their own advantages and drawbacks and can be summarized as follows [16, 146, 148–150]. First, the target of robust control is to maintain a consistent performance in spite of model uncertainties and exogenous disturbances. The idea of adaptive control is, conversely, to adapt to changes of the systems' parameters. That means the robust control is a reasonable option when dealing with hidden dynamics and external forces, while adaptive is preferable on slowly varying systems. Secondly, a prior knowledge of the parameters is essential when drawing the parameter boundaries in robust control, whereas adaptive control can work with little or no prior information of unknown parameters. Third, the uncertainty estimate is not updated throughout the operation in robust control, while adaptive control uses this update to improve its algorithms and performance of the systems. Finally, linearization is a step in adaptive control and sometimes linearized systems are not

applicable. Figure (3.12) shows the architecture of both control systems.

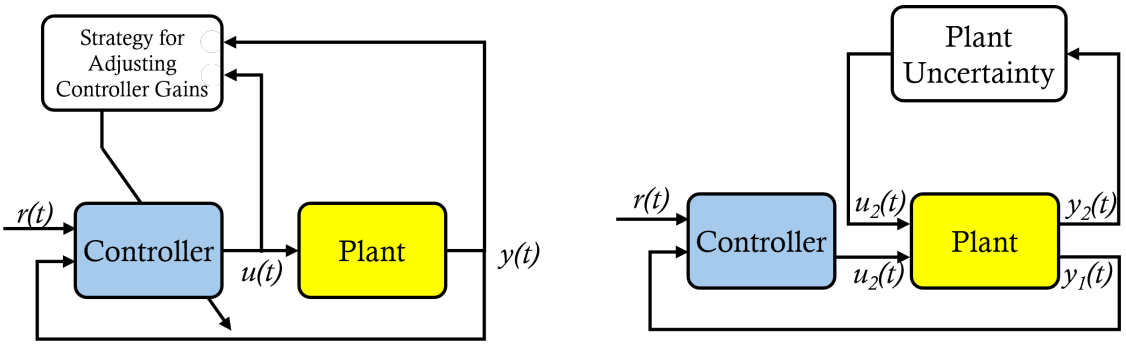

Figure 3.12: Adaptive control scheme (left) and robust control (right) [146].

Before moving to the next point, it is necessary to have a close look into adaptive control for two reasons. First, Bayesian system identification can be used as either modelling or estimation methods in structural dynamics. The former approach coupled with control will be discussed in the next section. When a Bayesian nonlinear observer is coupled with a controller, it forms a practical adaptive control, which this thesis is aiming to investigate. Second, Wagg emphasised that most adaptive control approaches have not been developed with structural control in mind, meaning adaptive control will need appropriate modifications [6, 7]. The idea of the adaptive is that its ability to adjust parameter and incorporating a mechanism to do so. These adjustments contain several steps: the choice of a controller structure and performance criteria, online evaluation with respect to some desired behaviour, and online tuning of the controller gains to reach a closer desired performance [148].

The adaptive control method has been divided into direct and indirect approaches. Model reference adaptive control (MRAC) is a direct method in which the parameters of a controller are directly adjusted based on the difference between the measurements and the desired output. Although the performance criteria of this algorithm are usually met through the model reference, the online tuning makes the systems time varying and nonlinear [32]. Consequently, in terms of structure control, various concerns need to be considered. First, stability is guaranteed in idealised situation such as when no disturbance and no unmodelled dynamics are involved. This scenario is not realistic, and it leads, even with small excitation of unmodelled dynamics, to instability. Second, MRAC does not require persistence of excitation which is important for the convergence of estimated parameters [151]. In structural control, this means that MRAC must be restricted to structures with collocated actuators and sensors. The indirect method is more suitable for structure control

problem [32]. The controller parameters are calculated as the solution of an underlying controller design problem when the parameters of a model for an unknown plant are estimated. While both methods have been reported and demonstrated experimentally in the literature, no specific guidelines on how to choose such design constants are distinguish feature of most adaptive schemes. Alternatively, as mentioned in section 3.3.2, coupling one of Bayesian filtering methods and LQR forms a new way of adaptive control and it can be an analytical method to aforementioned vibration problems.

3.4.1 GP in control systems

The GPs were originally introduced in control systems as alternative nonparameteric models for nonlinear adaptive control in 1999 [152, 153]. Although the interest has expanded over time, GP methods used in control tasks are still mostly unexploited by the wider control community with a few noteworthy exceptions. This section offers a brief review of control algorithms that incorporate GPs, with some detailed mathematical formulations provided in Chapters 5 to 7. For a comprehensive literature review, readers can refer to [14, 154, 155].

The GP has been popular among the scientific community for last two decades for various reasons. The authors in [154] summarized them with a control perspective. GPs firstly provide flexible, probabilistic, and more importantly non-parametric models which means they solve the approximation issue of the parameters used in other classes of model. Secondly, GPs not only work well on small data sets, in which it is useful for learning applications, but also, they provide estimations for uncertainty or confidence in the prediction through the predictive variance. While the predictive mean is often used as the best guess of the output, the full distribution can be used in a meaningful way. For instance, one can estimate a 95 percent confidence bound for the predictions which can be used to measure control performance. Lastly, GPs allow including prior knowledge of the system behaviour by constructing a particular structure of the covariance function. This feature enables incorporating domain knowledge into GP model to improve its accuracy.

The field of learning control or iterative learning was one of earliest control areas utilising GPs starting in [156]. The general idea is that the GPs are used as internal simulations within reinforcement learning (RL) in order to update the control policy

or law before its applied to the real systems. The probabilistic Inference and Leaning for COntrol (PILCO) method was a promising methodology applied in robotic applications such as legged locomotion [157]. The PILCO was based on an iteratively optimised controller and GP model in which the optimal closed loop control law was learnt while taking into account the probabilistic model of the process [158]. However, adaptive control and NMPC were the control algorithms most frequently incorporating a GP.

Model identification adaptive control is one of adaptive control methods coupled with a GP model. Figure (3.13) depicts a block design demonstrating the general idea of model identification adaptive control. As the author in [14] mentioned, there are various paths in which this method can be utilized to quantify the uncertainty of the systems and to design a suitable control strategy of it. Hence, the advantage of the two nonlinear control strategies is that the residual modes are included in the system and the GP will help to determine the uncertainty region in which the controller is able to eliminate the residual effects.

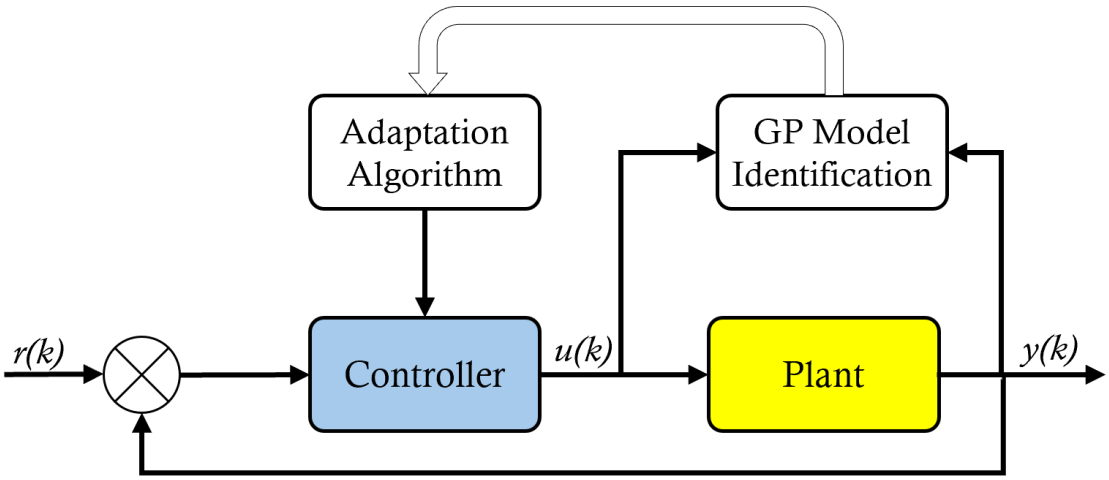

Figure 3.13: General block scheme of the closed-loop system with adaptive controller [14].

MPC was the most suitable method as a result MPC new control laws are computed in each control interval, whilst in classical control theory a single control law, which is computed offline prior to the simulation, is used for the whole duration of the simulation. For that reason, researchers in [159] suggest that with more investigation the GP model could be included within the MPC strategy to form an adaptive controller, with the digital twin directly impacting control performance. If this modification were possible, it would mean that any improvement in control performance could be immediately linked to an action by the digital twin which has

resulted in an improvement in predictive performance. To sum up, utilizing GP as a modelling method coupled with a controller requires further investigation by the dynamics community.

3.5 Summary of the literature review

In this chapter, the literature of active vibration control was reviewed, aiming to provide a new approach to analysing and controlling vibrating systems. Generally, there have been a range of methods developed in recent years aimed at resolving issues of noise and vibration control of structures. These techniques have taken active, passive, and hybrid approaches, and many have been refined over time, with demand nowadays for flexible and lighter structures that offer a lower environmental impact and higher efficiency. These lightweight structures, however, pose new obstacles for vibration control engineers, one of which is how to consistently offer solutions for attenuation effectiveness, especially when operating under the limitations of rising costs and energy consumption. The review highlights that a Bayesian framework, particularly in the context of system modelling and nonlinear state estimation, offers a promising solution to critical issues like spillover and stroke saturation in active vibration control.

As a result, the recent developments in modelling and estimation of structural dynamics were reviewed, emphasizing the Bayesian system identification methods. In the area of modelling, classification of modelling was provided, and special focus given to black box models. Two black box approaches, NARX and block-oriented models, were briefly described, as were how these methods were employed in engineering applications. The GP-NARX model was one of the most promising methods since it provided not only the prediction but also the confidence interval. In the context of Bayesian filtering, the general description of state estimation approaches was provided before emphasizing the importance and applications of Bayesian filtering in structural dynamics. The general remark of this section was that uncertainty in structural control systems is a growing concern due to the growing interest in flexible structures. Advancements in structural dynamics, particularly in SHM, have addressed uncertainty through methods like the GP-NARX model and Bayesian filtering in which structural control systems need to follow suit either to improve control performance or provide an alternative method to the traditional control

techniques.

The literature review concluded with a review of control algorithms. Optimal and adaptive controls were described. However, the Bayesian frameworks, either in modeling or state estimation, provide information about the uncertainty of the prediction or parameters, and using this extra information not only enables a sophisticated control system but also could be useful in calculating a new control input. For that reason, a review of GP models in control systems was provided. Even though several control algorithms incorporating GPs were reported in the literature, these control approaches are still mostly unexploited by the wider engineering fields, and vibration control was no exception.

Based on the current literature review, while several Bayesian approaches have been used in structural dynamics, the design of active vibration control systems using these methods remains unexplored. This research therefore focuses on incorporating Bayesian identification approaches into data-driven control methods subject to active vibration control, which is related to the first objective (O1) of this thesis. The forthcoming chapters elaborate on this objective, detailing the challenges and proposed solutions.

Chapter 4

Dynamics of a cantilever beam

Highlights:

- The modal analysis and dynamics of a cantilever beam are presented.
- A case study of the cantilever beam, in a discrete time formulation, is presented alongside with all necessary equations.
- The numerical values of the case study are presented.

4.1 Overview

The cantilever beam is a fundamental structural system and a standard case study when it comes to employing a new research framework. It can be used as a prototype of a real-world application such as an aeroplane wing. As a result, the cantilever beam has been used as a case study in this thesis as an ideal starting point for modelling and controlling more complex structures.

This chapter begins by introducing the modal analysis and state space approach. These analysis methods are then used in deriving the equation of motion of the cantilever beam. Then, the rest of the chapter is about presenting the numerical values and some responses of the beams.

4.2 Modal analysis

Modal analysis has unquestionably dominated the analysis of vibration in structural dynamics [3]. This analysis method offers a decomposition of the movement of the structures and helps to identify the natural frequencies and mode shapes. The usefulness of modal analysis stems from its wide applicability; modal parameters can explain a system's behaviour for any input type and range. Now, following the notation from [3, 160], consider an unforced and undamped linear system governed by the following equation:

$$m\ddot{q}(t) + kq(t) = 0 \tag{4.1}$$

Here, $q(t)$ represents the displacement vector of the structure, $\ddot{q}(t)$ is the associated acceleration vector, m is the mass matrix, and k is the stiffness matrix of the structure. When the harmonic excitations is assumed, the solution to the differential equation above is,

$$q(t) = \psi e^{i\omega t} \tag{4.2}$$

where ψ is a constant vector. The general Equation (4.1) then simplifies to,

$$-\omega^2 m\psi + k\psi = 0. \tag{4.3}$$

This results in a standard linear eigenvalue problem, and assuming the mass matrix is invertible, which it usually is, leads to

$$m^{-1}k\psi_i - \frac{1}{\omega_i^2}\psi_i = 0 \tag{4.4}$$

where ω_i and ψ_i represent the eigenvalue problem's ith solution. The eigenvalues ω_i of the equation above represent the natural frequencies of the structure under study. The vectors ψ_i are the mode shapes that, as shown in [160], are orthogonal with respect to the mass and stiffness matrix. This means that,

$$\psi_i^\top [m]\psi_j = 0 \quad \text{for} \quad i \neq j \tag{4.5}$$

$$\psi_i^\top [k]\psi_j = 0 \quad \text{for} \quad i \neq j \tag{4.6}$$

This property of the mode shapes enables the decomposition of the equations of motion. In that case of a damped system with forcing, the equation of motion can

be represented by,

$$m\ddot{q}(t) + c\dot{q}(t) + kq(t) = F(t) \tag{4.7}$$

where c is the damping matrix and $\mathbf{F}$ is the external load vector at time t. Substituting the displacement vector q with the calculated modal decomposition given by,

$$[\mathbf{\Psi}]x_s = q \tag{4.8}$$

where x_s is the vector of modal coordinates and $[\mathbf{\Psi}] = [\psi_1, \psi_2, \ldots, \psi_n]$ is the matrix of mass-normalized mode shapes. Once left-multiplying by $[\mathbf{\Psi}]^T$, Equation (4.7) becomes,

$$[\mathbf{\Psi}]^\top[m][\mathbf{\Psi}]\ddot{x}_s(t) + [\mathbf{\Psi}]^\top[c][\mathbf{\Psi}]\dot{x}_s(t) + [\mathbf{\Psi}]^\top[k][\mathbf{\Psi}]x_s(t) = [\mathbf{\Psi}]^\top\mathbf{F}(t) \tag{4.9}$$

The matrices $M = [\mathbf{\Psi}]^\top[m][\mathbf{\Psi}]$ and $K = [\mathbf{\Psi}]^\top[k][\mathbf{\Psi}]$ are diagonal, due to the orthogonality conditions in Equation (4.5). The damping matrix is considered to be a linear combination of the mass and stiffness matrices, such as Rayleigh or proportional damping, then the matrix $C = [\mathbf{\Psi}]^\top[c][\mathbf{\Psi}]$ is also diagonal. Given the aforementioned orthogonality criteria, the equations of motion provide,

$$M\ddot{\mathbf{x}}_s(t) + C\dot{\mathbf{x}}_s(t) + K\mathbf{x}_s(t) = [\mathbf{\Psi}]^\top\mathbf{F}(t) \tag{4.10}$$

In general, Equation (4.10) can be transferred into standard second order differential equations:

$$\ddot{\mathbf{x}}_s(t) + 2\xi\omega_n\dot{\mathbf{x}}_s(t) + \omega_n^2\mathbf{x}_s(t) = f(t) \tag{4.11}$$

where ω_n and ξ define the diagonal matrices of natural frequencies and damping factors, respectively. Also, the external force $f(t)$ is equal to $\mu^{-1}[\mathbf{\Psi}]^\top\mathbf{F}(t)$. Mathematically, the notation of these modal parameters is described below:

$$\xi = \mathbf{diag}(\xi_i) \tag{4.12}$$

$$\omega_n = \mathbf{diag}(\omega_{ni}) \tag{4.13}$$

$$\mu = \mathbf{diag}(\mu_i) \tag{4.14}$$

When dealing with modal analysis, several points must be highlighted. First, the

damper utilised here is classified as classical damping, which is frequently questioned when the damping is significant [3]. Second, the benefit of lightly damped structures is that they are typically simple to model. However, the structures are difficult to regulate since their poles are close to the imaginary axis and they are easily destabilised. Finally, the number of degrees of freedom in a discretised model in Equation (4.7) is usually huge due to the difficulty in effectively reflecting the structure's rigidity. When a band-limited excitation activates a structure, modes with natural frequencies that lie within the excitation's bandwidth dominate the response. As a result, the number of degrees of freedom that contribute to the reaction in modal coordinates is drastically reduced.

4.3 State space model

The modal equation enables decoupling between modal coordinates, and modal control can be accomplished. Second-order differential equations, on the other hand, are not the usual model form in modern control theory. Modal equations can be expressed in the form of state space model, and the state-space model can be normalized to the Jordan standard type for example. The state space approach is based on the state equation and measurement equation, which are described in continuous time domain respectively as follows :

$$\dot{\mathbf{x}}_{\mathbf{s}}(t) = A\mathbf{x}_{\mathbf{s}}(t) + B\mathbf{u}(\mathbf{t}) \tag{4.15}$$

$$y(t) = C_c\mathbf{x}_{\mathbf{s}}(t) + D_c\mathbf{u}(\mathbf{t}) \tag{4.16}$$

Here, $\mathbf{x_s} \in \mathbb{R}^{n\times 1}$ denotes the vector of defined state variables, $\mathbf{u} \in \mathbb{R}^{m\times 1}$ is the input vector, and $y \in \mathbb{R}^{p\times 1}$ represents the output vector. Additionally, $A \in \mathbb{R}^{n\times n}$ is the state transition matrix, $B \in \mathbb{R}^{n\times m}$ is the input matrix, $C_c \in \mathbb{R}^{p\times n}$ is the output matrix, and $D_c \in \mathbb{R}^{p\times m}$ is the feedthrough matrix. While the state and measurement equations are formulated in the continuous domain, control is generally implemented in the discrete domain. The corresponding discrete state-space formulation is:

$$\mathbf{x}_{\mathbf{s}}(k+1) = A_d\mathbf{x}_{\mathbf{s}}(k) + B_d\mathbf{u}(k) \tag{4.17}$$

$$y(k) = C_d\mathbf{x}_{\mathbf{s}}(k) + D_d\mathbf{u}(k) \tag{4.18}$$

where $\mathbf{x_s}(k)$ is the discrete time state vector at the current time k. A_d is the discrete state matrix; B_d is the discrete input matrix; C_d is the discrete output matrix; D_d is the discrete direct transmission matrix. This formulation requires discretisation of Equations (4.15) and (4.16). Even though there are various methods to discretise a system, the method used in this work is zero-order hold (ZOH) as shown below:

$$A_d = e^{A\triangle t} \tag{4.19}$$

$$B_d = (A_d - I)A^{-1}B \tag{4.20}$$

$$C_d = C_c \tag{4.21}$$

$$D_d = D_c \tag{4.22}$$

where $\triangle t$ is the sampling period. Until now, it was assumed that the system was only driven by a deterministic input $\mathbf{u(k)}$. However, in addition to the applied input, there may be other inputs that contribute to the system response in an uncontrollable manner. This unmeasurable influence is referred to as disturbance or noise. As a result, Equations (4.17) and (4.18) must be extended to include stochastic components, yielding the stochastic state space model.

$$\mathbf{x_s}(k+1) = A_d\mathbf{x_s}(k) + B_d\mathbf{u(k)} + w_n(k) \tag{4.23}$$

$$y(k) = C_d\mathbf{x_s}(k) + D_d\mathbf{u(k)} + v_n(k) \tag{4.24}$$

where $w_n(k)$ is the process noise due to disturbance or modelling inaccuracies; $v_n(k)$ is the measurement noise caused by sensor inaccuracy. The assumption here is that they are both independent and identically distributed as shown here:

$$w_n \sim N(0, Q_n) \qquad v_n \sim N(0, R_n) \tag{4.25}$$

where Q_n and R_n are the covariances of the process and measurement noises, respectively.

4.4 Mathematical modelling of a beam

Certain assumptions must be considered before developing a mathematical model of a cantilever beam. First, the beam's material is homogenous and isotropic, and its plane sections are considered to be plain and orthogonal to the neutral axis and the displacement of any point of the beam is driven by the bending moment. Second, the relationship between bending moment and deflection is governed by the Euler-Bernoulli beam theory. Based on these assumptions, the flexural wave equation describing the free vibration of a cantilever beam can be formulated as follows [161],

$$EI_z \frac{\partial^4 w(x,t)}{\partial x^4} + \rho A_b \frac{\partial^2 w(x,t)}{\partial t^2} = 0, \tag{4.26}$$

where $w(x,t)$ is the transversal displacement of a point at any distance x at any time t. E is the Young's modulus of the material, I_z the moment of inertia for the cross-section with respect to the transverse axis, ρ is the material density, and A_b the cross-section area of the beam. The displacement can be expressed as follows using variable separation:

$$w(x,t) = \psi(x)q(t), \tag{4.27}$$

which yields Equation (4.26) into:

$$EI_z \frac{\partial^4 \psi(x)}{\partial x^4} q(t) + \rho A \psi(x) \ddot{q}(t) = 0. \tag{4.28}$$

Equation (4.28) provides an analytical expression for the beam's natural frequencies as follows:

$$\frac{\ddot{q}(t)}{q(t)} = -\frac{EI_z \frac{\partial^4 \psi(x)}{\partial x^4}}{\rho A \psi(x)} = -\omega^2, \tag{4.29}$$

thereby, the flexural wave equation can be divided into two equations: one time-dependent,

$$\ddot{q}(t) + \omega^2 q(t) = 0, \tag{4.30}$$

and one spatial-dependent,

$$\frac{\partial^4 \psi(x)}{\partial x^4} - \beta^4 \psi(x) = 0. \tag{4.31}$$

where

$$\beta^4 = \frac{\rho A_b \omega^2}{EI_z} \tag{4.32}$$

The general solution of Equation (4.30) and Equation (4.31) are expressed as follows, respectively:

$$Q(t) = C_1 cos(\omega t) + C_2 sin(\omega t), \tag{4.33}$$

$$\phi(x) = C_3 \cos(\beta x) + C_4 \sin(\beta x) + C_5 \cosh(\beta x) + C_6 \sinh(\beta x), \tag{4.34}$$

where C_1 to C_6 are unknown constants that can be found by initial conditions and boundary conditions, respectively. Here, it is important to point out that this work contains two types of beams: cantilever and simply supported beams. The former will be used in numerical case of this chapter and Chapter 5 and 6, whereas the latter will be used in spillover problem in Chapter 8.

In case of forced vibration, the forced system of the cantilever beam subject to a primary excitation $F_L(x_L, t)$ is shown in Figure (4.1) and can be written as,

$$EI_z \frac{\partial^4 w(x,t)}{\partial x^4} + \rho A_b \frac{\partial^2 w(x,t)}{\partial t^2} = F_L(x_L, t). \tag{4.35}$$

The general solution of Equation (4.35) can be expressed as a linear superposition of the natural modes in addition of assuming harmonic excitation:

$$w(x_L, t) = \sum_{n=1}^{\infty} \psi_n(x_L) q_n(t) \tag{4.36}$$

With respect to the motion resulting from the n-th mode, the forced wave Equation (4.35) becomes,

$$EI_z \psi_n(x)'''' q_n(t) + \rho A_b \psi_n(x) \ddot{q}_n(t) = F_L(x_L, t) \tag{4.37}$$

After integrating along the beam's length and multiplying Equation (4.37) by the

m-th mode, the result is:

$$EI_z \int_0^L \psi_n(x)''''\psi_m(x)q_n(t)\,dx + \rho A_b \int_0^L \psi_n(x)\psi_m(x)\ddot{q}_n(t)\,dx = \int_0^L \psi_m(x)F_L(x_L,t)\,dx; \tag{4.38}$$

Using orthogonality and normalisation conditions of Equations (4.5) and (4.6), the following equation is obtained for $n = m$,

$$\ddot{q}_n(t) + \frac{K_n}{M_n}q_n(t) = \frac{1}{M_n}\int_0^L \psi_n(x)F_L(x_L,t)\,dx; \tag{4.39}$$

where,

$$M_n = \rho A \int_0^L \psi_n(x)^2\,dx = \rho A_b L = m_{\text{beam}}; \tag{4.40}$$

is the modal mass, which is the total mass of the beam, and

$$K_n = EI_z \int_0^L \psi_n(x)''''\psi_n(x)\,dx = EI_z\beta_n L; \tag{4.41}$$

is the modal stiffness. Since the excitation is a point force, it follows that,

$$\int_0^L \psi_n(x)F_L(x_L,t)\,dx = \psi_n(x_L)F_L(t); \tag{4.42}$$

hence, Equation (4.39) can be rewritten as,

$$\ddot{q}_n(t) + \omega_n^2 q_n(t) = \frac{1}{M_n}\psi_n(x_L)F_L(t); \tag{4.43}$$

This equation results, essentially, the same as the equation of motion of vibrating system as Equation (4.11) without the damping part. Consequently, the rest of this thesis follows the notation of Equation (4.11) of a structural system.

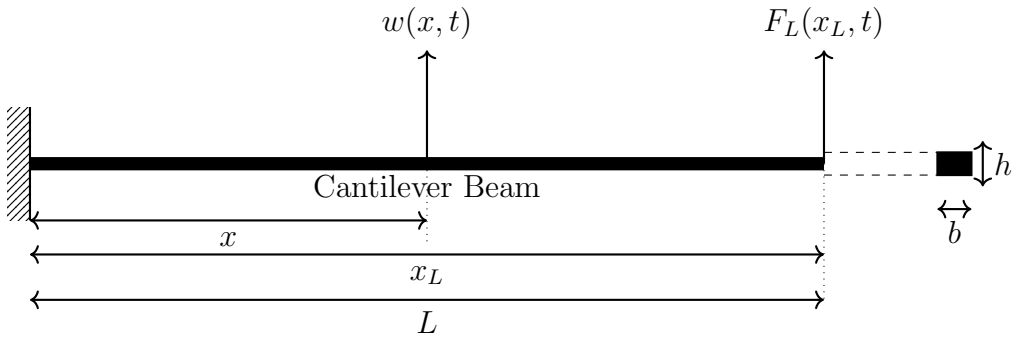

Figure 4.1: A schematic representation of a cantilever beam. The displacement $w(x,t)$ is shown at a specific distance x from the fixed support. The total length of the beam is L. The cross-sectional area is shown with height h and width b.

4.5 Numerical values

This section considers the dynamics of a cantilever beam. In order to form a collocated system, this system typically consists of a uniform beam with a point force actuator and a displacement sensor at the tip. For convenience of use, Table (4.1) shows all of the beam's essential parameters.

Table 4.1: Essential parameters of the cantilever beam.

Element (Symbols)	**Value (Units)**
Height (h)	25 mm
Width (b)	1 mm
Moment of Inertia ($I = \frac{bh^3}{12}$)	$1.3021{*}10^3$ mm^4
Length (L)	350 mm
Modulus of Elasticity (E)	210 GPa
Density of steel (ρ)	7850 kg/m^3
Damping ratio (ζ)	1%

Following Blevin's formula [162], the formula of natural frequency and mode shapes of a Clamped-Free beam are shown below:

$$f_i = \frac{{\lambda_i}^2}{2\pi L^2}\sqrt{\frac{EI}{m}} \tag{4.44}$$

$$\begin{aligned}&\cosh\left(\frac{\lambda_i x}{L}\right)-\cos\left(\frac{\lambda_i x}{L}\right)-\sigma_i\left(\sinh\left(\frac{\lambda_i x}{L}\right)-\sin\left(\frac{\lambda_i x}{L}\right)\right)\\&\approx 2.1\left[1-\cos\left(\frac{\pi x}{2L}\right)\right],\quad i=1\end{aligned}\tag{4.45}$$

where λ_i and σ_i are dimensionless natural frequency and nondimensional parameters, respectively. The values of these parameters are shown in Table (4.2):

Table 4.2: Values of λ_i and σ_i for a Clamped-Free beam.

i	λ_i	σ_i
1	1.87510407	0.73408505
2	4.69409113	1.01846507
3	7.85475744	0.99919997
4	10.99554073	1.00000000
5	14.13716839	1.00000000
$n>5$	$\lambda_i=\frac{(2n-1)\pi}{2}$	$\sigma_i=1$

When considering all these parameters values, the first five natural frequencies ω_n are $[15.3399, 96.1337, 269.1770, 527.4796, 871.9615]$ in rad/sec. In addition, Figure (4.2) depicts the corresponding mode shapes of those five natural frequencies.

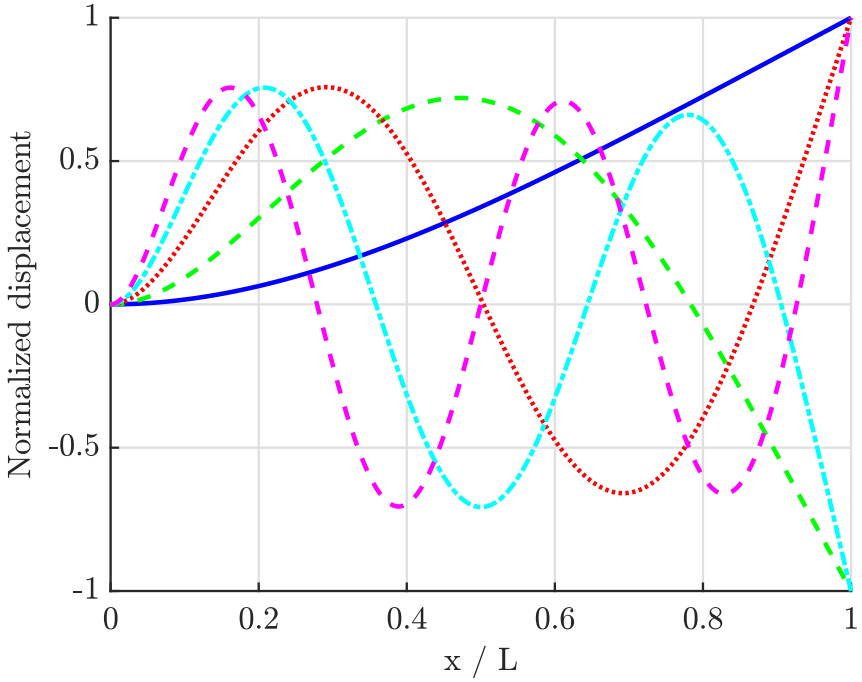

Figure 4.2: The corresponding mode shape of Clamped free beam.

To obtain an open dynamic system for data purposes, the cantilever beam needs to be expressed using Equations (4.15) and (4.16). The state and measurement matrix generally takes the following form:

$$A = \begin{bmatrix} O & I \\ -{\omega_i}^2 & -2\omega_i\xi_i \end{bmatrix} \quad B = \begin{bmatrix} 0 \\ B_i \end{bmatrix} \quad C_c = \begin{bmatrix} C_{c_i} & 0 \end{bmatrix} \tag{4.46}$$

where i represents the ith mode. The values of these matrices for the first three modes in the time domain are:

$$A = 10^4 \times \begin{bmatrix} 0 & 0 & 0 & 0.0001 & 0 & 0 \\ 0 & 0 & 0 & 0 & 0.0001 & 0 \\ 0 & 0 & 0 & 0 & 0 & 0.0001 \\ -0.0235 & 0 & 0 & -0.0000 & 0 & 0 \\ 0 & -0.9242 & 0 & 0 & -0.0002 & 0 \\ 0 & 0 & -7.2456 & 0 & 0 & -0.0005 \end{bmatrix}$$

$$B = \begin{bmatrix} 0 \\ 0 \\ 0 \\ 17.4207 \\ -17.4207 \\ 17.4207 \end{bmatrix}$$

$$C_c = \begin{bmatrix} 2.0000 & -2.0000 & 2.0000 & 0 & 0 & 0 \end{bmatrix}$$

$$D_c = 0$$

With these values, obtaining an open response from the cantilever beam is straightforward, and each case will be discussed in the chapters that follow. Finally, the majority of the methods proposed in this thesis operate in discrete domains, which means that all previous matrices' values must be converted to discrete domains. Appendix A.1 presents these values. Furthermore, Appendix A.2 presented the validation approach for the validity of cantilever beam data.

Chapter 5

Nonlinear model predictive control for flexible structures: Wiener-Hammerstein model

Highlights:

- A novel approach is presented to address the limitation of an actuator in active vibration settings.
- The Wiener-Hammerstein model's integration with traditional MPC is explored and discussed.
- The design and difficulties of traditional MPC, as well as the feedforward MPC tracking control problem, are discussed.
- The cantilever beam is used as a numerical example.

5.1 Overview

There is still an ongoing effort to investigate the limitations and effects of actuators, particularly inertia actuators, in active vibration control systems [83]. This

emphasises the importance of investigating the efficacy of data-driven modelling combined with MPC for addressing actuator limitations in active vibration control. The purpose of this chapter is to design an NMPC controller that uses the Wiener-Hammerstein model to determine the mechanical nonlinearity of an inertia actuator using one of the machine learning algorithms. The cantilever beam model, presented in Chapter 4, is used as a case study. The GP-NMPC design process is divided into two stages:

- Data-driven identification of the system model using GP and MPC within the Wiener-Hammerstein model.
- A closed feedback loop of the NMPC of Wiener-Hammerstein model with GP.

The first task is included in this thesis, whereas the second task requires advanced control theory background and is beyond the scope of this work.

5.2 Wiener-Hammerstein model in structural systems

The Wiener-Hammerstein model is one of the block oriented approaches used to identify a complex system based on data. The general idea of designing an active control by using GP-MPC for vibration purposes is depicted in Figure (5.1). The efficacy of this approach is that within the MPC, the model of the system is represented by the Wiener-Hammerstein model. This approach is constructed from three distinct blocks: two MPC models of LTI dynamic blocks, and one nonlinear block. They are all coupled in series with the nonlinear block being placed between the linear blocks as shown in the orange box. The nonlinear block in the model is considered as a static nonlinearity and it has been represented by a GP. The benefits of this proposed model are as follows. First, the Wiener-Hammerstein model helps to accurately represent various complex dynamic systems, including nonlinear systems [12], which can be useful for control systems. Second, the GP can incorporate uncertainty which can be insightful for active vibration control. Finally, these previous aspects could be helpful in terms of the limitations of the actuator when implementing active vibration control. Moreover, to author's knowledge, the integration of the Wiener-Hammerstein model with GP for structural systems has not

been previously explored.

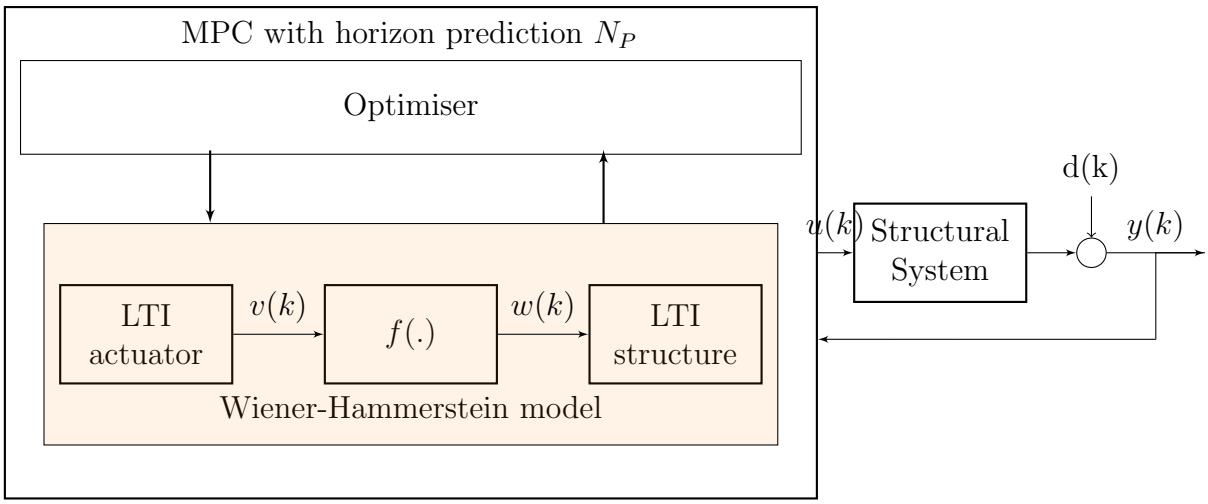

Figure 5.1: Overview of the proposed control system.

5.3 Problem statement

Consider a single-input, single-output discrete-time non-linear structural system described by the Wiener-Hammerstein model in Figure (5.2). Mathematically, the model can be represented as a series of time-discretised systems as follows:

$$\begin{cases} x_p(k+1) = A_p x_p(k) + B_p u_p(k) \\ v(k) = C_p x_p(k) + D_p u_p(k) \end{cases} \quad \text{First linear system (actuator)} \tag{5.1}$$

$$\Big\{ w(k) = f(v(k)) \quad \text{Nonlinear function} \tag{5.2}$$

$$\begin{cases} x_s(k+1) = A_s x_s(k) + B_s w(k) \\ y_s(k) = C_s x_s(k) \end{cases} \quad \text{Second linear system (structure)} \tag{5.3}$$

The first linear state space system (with subscript p) represents a proof mass actuator with state vector x_p, input vector u_p , and output vectors v. The second linear system is a model of the structure being controlled, in this case a cantilever beam, that can be represented by subscript s. More importantly, the nonlinear function f

represents the static nonlinearity of the saturation of the proof mass actuator in an active vibration setting. The static nonlinearity $w(k)$ is modelled using input-output data and a GP as represented in Equation (5.4).

$$w(k) \sim \mathcal{GP}(\mu(x), k(x, x_*)) \tag{5.4}$$

In order to quantify the uncertainty or end stroke of the proof mass actuator, the proposed model has to go through three design stages as shown in Figure (5.2):

1. To design a constrained Linear Quadratic Model Predictive Control (LQ-MPC) for the regulator case. This step helps the model to identify the minimum required force $w(k)$.

2. To design the inverse GP model, which maps the minimum required force $w(k)$ to the actual force $v(k)$ through the static nonlinearity GP model.

3. The final stage is to design a constrained LQ-MPC using a steady-state target optimisation tracking approach. This step highlights the ability of the proof mass actuator to follow the required force input taking into account the static nonlinearity of the saturation of the actuator.

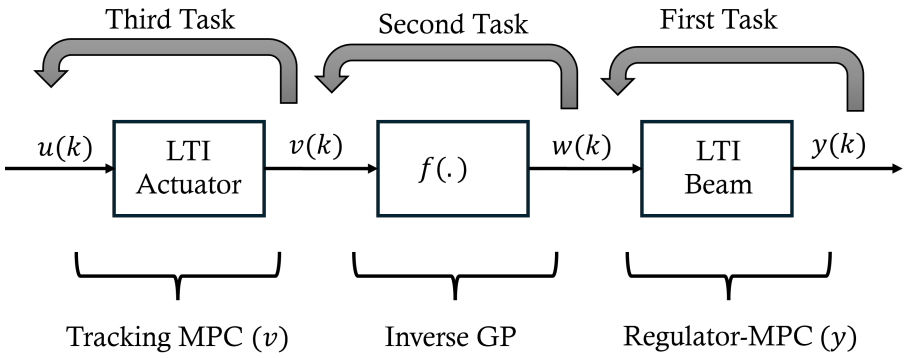

Figure 5.2: General overview of designing the Wiener-Hammerstein model.

In the following sections, the background theory of classical regulator and tracking MPC approaches will be examined. To understand the proposed model, a brief description of LQ-MPC is provided. The first section will be devoted to the regulator case, followed by a discussion of the tracking case. The reader is encouraged to review all of the constrained LQ-MPC information in these resources [163–165].

5.4 Basic components of MPC

MPC is widely recognised as a control strategy rather than a control algorithm. Therefore, there are some basic ingredients that must be used to create the MPC algorithm. This section describes the fundamental elements of developing a regulator and tracking constrained MPC.

5.4.1 System models

There are many system models that can be used in model predicted control; the prediction model can mainly be developed in either a transfer function model or a state space model. The state space model is used in this work because, in addition to being appropriate for the proposed approach, it can handle multi-variable systems more easily than a transfer function model [163]. There are three main types of state space models used in the prediction model: nominal, closed loop, and steady state models. Nominal or closed-loop models are mainly for regulator control tasks, whereas steady-state models are generally for disturbance rejection and tracking control problems. In this thesis, the nominal and steady state models were chosen for predictions. Mathematically, the nominal model represents a linear discrete state space model, and it has been described in Equations (4.17) and (4.18). Here, the feedthrough part of the measurement equations and noise were not included in this model, so the model is represented as follows:

$$x_s(k+1) = A_d x_s(k) + B_d u(k) \tag{5.5}$$

$$y(k) = C_d x_s(k) \tag{5.6}$$

Alternatively, steady state model, sometimes it is called nominal disturbance free model, consider the case where there are disturbances in state and measurement equations. The model begins with the plant dynamic represented as follows:

$$x_s(k+1) = A_d x_s(k) + B_d u(k) + B_{dd} d(k) \tag{5.7}$$

$$y(k) = C_d x_s(k) + D_d d(k) \tag{5.8}$$

where d is the disturbance vector. B_{dd} is the disturbance matrix in the input whereas

B_{dd} is the disturbance matrix in the output. Then, the plant dynamic in equilibrium satisfies when the expected state in the future can be defined as follows.

$$x_{ss} = A_d x_{ss} + B_d u_{ss} + B_{dd} d \tag{5.9}$$

$$y_{ss} = C_d x_{ss} + D_d d = r \tag{5.10}$$

Where x_{ss}, u_{ss}, r, y_{ss} are the state, input, reference, and output steady-state values, respectively. Also, the steady-state equilibrium equation can be expressed in compact form as follows:

$$\underbrace{\begin{bmatrix} I - A_d & -B_d \\ C_d & 0 \end{bmatrix}}_{A_{\text{eq}}} \underbrace{\begin{bmatrix} x_{\text{ss}} \\ u_{\text{ss}} \end{bmatrix}}_{x_{\text{eq}}} = \underbrace{\begin{bmatrix} B_{dd} d \\ r - D_d \end{bmatrix} d}_{b_{\text{eq}}} \tag{5.11}$$

Later, in the tracking case, the aim of the control system is to regulate the system, which means taking the state from current state $x_s(k)$ to the steady state x_{ss}. As a result, it is preferable to define deviation variables which are presented as

$$z = x_s(k) - x_{ss}; \quad v_c = u(k) - u_{ss}; \quad \hat{y} = y(k) - y_{ss} \tag{5.12}$$

In this equation, z, v_c, and $\hat{y}$ are deviation variables in state, input, and output, respectively. Although these models are described using the symbols of the structural system, the steady-state model will be used with a proof mass actuator for the tracking control problem.

5.4.2 Prediction

Making predictions is a key component of MPC, as it provides the state prediction associated with a sequence of future control input based on the starting state. Obtaining predictions begins with the model's form selection. The prediction in this case is based on the open loop state space model as shown in Equation (5.5). This prediction model is obtained by applying the model recursively in a number of steps ahead starting from the starting state $x_s(k)$, and then collecting the state prediction and input sequence in a stacked variable vector. In particular, the i-step ahead state prediction is:

$$x_s(k+i|k) = A_d^i x_s(k) + A_d^{i-1} B_d u(k|k) + A_d^{i-2} B_d u(k+1|k) + \cdots + B_d u(k+i-1|k) \quad (5.13)$$

which can be written as:

$$x_s(k+i|k) = A_d^i x_s(k) + \begin{bmatrix} A_d^{i-1}B_d & A_d^{i-2}B_d & \dots & B_d \end{bmatrix} \begin{bmatrix} u(k|k) \\ u(k+1|k) \\ \vdots \\ u(k+i-1|k) \end{bmatrix} \quad (5.14)$$

Collecting predictions over all steps $i = 1, \dots, N_P$ ahead from k, we obtain the prediction equation:

$$\underbrace{\begin{bmatrix} x_s(k+1|k) \\ x_s(k+2|k) \\ \vdots \\ x_s(k+N_P|k) \end{bmatrix}}_{\mathbf{x_s}(k)} = \underbrace{\begin{bmatrix} A_d \\ A_d^2 \\ \vdots \\ A_d^{N_P} \end{bmatrix}}_{F} x_s(k) + \underbrace{\begin{bmatrix} B_d & 0 & \dots & 0 \\ A_d B_d & B_d & \dots & 0 \\ \vdots & \vdots & \ddots & \vdots \\ A_d^{N_P-1}B_d & A_d^{N_P-2}B_d & \dots & B_d \end{bmatrix}}_{G} \underbrace{\begin{bmatrix} u(k|k) \\ u(k+1|k) \\ \vdots \\ u(k+N_P-1|k) \end{bmatrix}}_{\mathbf{u}(k)} \quad (5.15)$$

Finally, the compact form is written as:

$$\mathbf{x_s}(k) = F x_s(k) + G\mathbf{u}(k) \quad (5.16)$$

The stacked vectors of state predictions and future inputs are represented by the boldface variables $\mathbf{x}_s(k)$ and $\mathbf{u}(k)$, respectively; the initial state from which the predictions originate is represented by the normalface variable $x_s(k)$. The matrices A_d and B_d combine to generate the larger matrices F and G. As a function of the initial state $x_s(k)$, the prediction equation provides the state predictions associated with a sequence of future control inputs. It is clear that, given a current state $x(k)$, different choices of $\mathbf{u}(k)$ will lead to different predicted state trajectories $\mathbf{x_s}(k)$. Therefore, the goal of MPC is to select $\mathbf{u}(k)$ as optimally as possible in order to get the best $\mathbf{x_s}(k)$.

5.4.3 Cost functions or performance index

Obtaining an appropriate performance index is critical in developing a control law. Despite the existence of various performance indices in the literature [166], the linear quadratic cost function is an appropriate choice in terms of penalising the state and input within the constraints imposed by the state and input. In general, the unconstrained finite-horizon linear quadratic (FH-LQ) regulator optimal control problem is given by:

$$J(x_s, u) = \min_{x_s, u} \sum_{k=0}^{N_P-1} \ell(x_s(k)), u(k)) \tag{5.17}$$

where the stage cost $\ell(x_s(k)), u(k))$ is defined as:

$$\ell(x_s(k), u(k)) = x_s(k)^\top Q x_s(k) + u(k)^\top R u(k). \tag{5.18}$$

In this equation, Q and R are the weighting matrices for state and input, respectively, with N_P denoting the finite horizon value. Additionally, the stage cost function is modified to include a terminal cost for stability reasons, as given by:

$$\ell(x_s(k), u(k)) = x_s(k)^\top Q x_s(k) + u(k)^\top R u(k) + x_s(N_P)^\top P x_s(N_P). \tag{5.19}$$

In this formulation. $x_s(N_P)$ represents the state at the terminal time step N_P and P is the terminal cost matrix, which is positive semi-definite.

5.4.4 Inequality constrains

The ability of MPC to handle constraints is its most useful and important feature. The constraints can be either hard such as actuator saturation or soft constraints such as performance specification, but imposing constrains generally for performance and economic reasons. In practice, most constraints are mathematically represented as limits, commonly referred to as box constraints [165]. Equations (5.20) and (5.21) illustrate the state and input constraints, respectively.

$$x_{\min} \leq x_s(k) \leq x_{\max} \tag{5.20}$$

$$u_{\min} \leq u(k) \leq u_{\max}, \tag{5.21}$$

where *min* and *max* here represent the lower and upper limits of each constrains. Technically, with a number of future predictions, these box constraints need to be transformed into liner inequality constraints. Equation (5.22) and (5.23) represent the general linear inequality constraints on the state and inputs of the model:

$$\underbrace{\begin{bmatrix} I \\ -I \end{bmatrix}}_{P_x} \begin{bmatrix} x_s(k|k) \\ x_s(k+1|k) \\ \vdots \\ x_s(k+N_P-1|k) \end{bmatrix} \leq \underbrace{\begin{bmatrix} +x_{\max,1} \\ +x_{\max,2} \\ \vdots \\ -x_{\min,1} \\ -x_{\min,2} \\ \vdots \end{bmatrix}}_{q_x} \tag{5.22}$$

$$\underbrace{\begin{bmatrix} I \\ -I \end{bmatrix}}_{P_u} \begin{bmatrix} u(k|k) \\ u(k+1|k) \\ \vdots \\ u(k+N_P-1|k) \end{bmatrix} \leq \underbrace{\begin{bmatrix} +u_{\max,1} \\ +u_{\max,2} \\ \vdots \\ -u_{\min,1} \\ -u_{\min,2} \\ \vdots \end{bmatrix}}_{q_u} \tag{5.23}$$

In these equations, P_x and P_u represent the state and input constraints matrices, respectively, while q_x and q_u denote the corresponding limit vectors. Additionally, constraints on the terminal state of the system are illustrated as follows:

$$P_{x_{N_P}}(x(k+N_P|k)) \leq \widetilde{q}_{x_{N_P}} \tag{5.24}$$

where Px_{N_P}, and $\widetilde{q}_{x_{N_P}}$ are constraints and its limit of terminal state of the system. Additional mathematical details are provided in Appendix B, when the cost function needs to be transformed into a Quadratic Programming (QP) form with these constraints imposed, leading to the formulation of the following linear inequality equations:

$$P_c\mathbf{u}(k) \leq q_c + S_c x(k) \tag{5.25}$$

5.5 Control law of the constrained LQ-MPC regulator problem

The first task of the Wiener-Hammerstein model incorporating with MPC requires a control law for LQ-MPC regulator applied to a LTI system. In that case, the general LQ-MPC problem is formulated as follows:

$$\begin{aligned}
\mathbf{P_{N_P}}(x_s(k)) = \min_{u(k)} & \sum_{i=0}^{N_P-1} \left[x_s(k+i|k)^\top Q x_s(k+i|k) + u(k+i|k)^\top R u(k+i|k)\right] \\
& + \underbrace{x_s(k+N_P|k)^T P x_s(k+N_P|k)}_{\text{terminal cost}} \\
\text{subject to} \quad & x_s(k+i+1|k) = A x_s(k+i|k) + B u(k+i|k), \\
& x_s(k|k) = x_s(k) \\
& P_x x_s(k+i|k) \leq q_x, \\
& P_u u(k+i|k) \leq q_u, \\
& P_{x_{N_P}} x_s(k+N_P|k) \leq \tilde{q}_{x_{N_P}}
\end{aligned} \tag{5.26}$$

This optimisation problem is categorised as the FH-LQ optimisation problem where it is denoted as $\mathbf{P_{N_P}}(x(k))$. To define the control law, certain assumptions need to be made. First, the control parameters is assumed to be that Q and P are positive semi-definite whereas R is positive definite. Also, the properties of the choosing system model in MPC is stabilizable, meaning all uncontrollable modes are stable, and delectable $(Q^{1/2}, A)$. Second, the full measurements of structural state x_s is available at current time k. Given these conditions, for any initial condition $x_s(k)$, there exists a unique optimal solution that converges. Moreover, the solution of Equation (5.26) can be efficiently solved using standard Quadratic Programming (QP) algorithms in vectorised forms [167], represented as follows.

$$\begin{aligned}
\min_{u(k)} \quad & 0.5\mathbf{u}^\top(k) H \mathbf{u}(k) + x^\top(k) L^\top \mathbf{u}(k) + x^\top(k) M x(k) \\
\text{subject to} \quad & \\
& P_c \mathbf{u}(k) \leq q_x + S_c x(k)
\end{aligned} \tag{5.27}$$

where,

$$H = 2G^{\top}\widetilde{Q}G + \widetilde{R}, \qquad L = 2G^{\top}\widetilde{Q}F, \qquad M = F^{\top}\widetilde{Q}F + Q$$

and,

$$\widetilde{Q} = \begin{bmatrix} Q & 0 & \dots & 0 & \\ 0 & Q & 0 & \dots & 0 \\ \vdots & \vdots & \vdots & Q & 0 \\ 0 & 0 & 0 & \dots & p \end{bmatrix}, \qquad \widetilde{R} = \begin{bmatrix} R & 0 & \dots & 0 & \\ 0 & R & 0 & \dots & 0 \\ \vdots & \vdots & \vdots & R & 0 \\ 0 & 0 & 0 & \dots & R \end{bmatrix}$$

In this formulation, H, L, and M are the cost matrices that are derived from the given weight matrices from Q and R. These are also based on the prediction matrices in Equation (5.16). Once the solution to this optimization problem is found, the control law can be formed based on receding horizon principle. It is basically the system is only applied to the first control in the optimised sequence, and the optimization problem is re-solved. This repeated action of applying the first optimised control in the sequence $\{u^0(k|k), u^0(k+1|k), \dots, u^0(k+N_P-1|k)\}$ defines a feedback control law.

$$u(k) = u^0(k|k) = \kappa_N(x_s) \tag{5.28}$$

where κ_N is nonlinear feedback control gain. The remaining task here is to identify the terminal cost penalty P. Several methods are reported in the literature [163], but dual-mode MPC has been efficient in terms of stability. The main feature of dual mode MPC is that under previous conditions and P satisfies Lyapunov equation for some stabilising control gain K_∞, the feedback control law in Equation (5.28) is globally asymptotically stabilising. Mathematically, the terminal cost matrix P can be computed numerically by solving Lyapunov equation as:

$$P = (A - BK_\infty)^T P(A - BK_\infty) + K_\infty^T R K_\infty + Q \tag{5.29}$$

The control gain K_∞, on the other hand, can be calculated by using deadbeat control methods or by solving Discrete Algebraic Riccati Equation (DARE). The optimal control gain for terminal cost is then given by:

$$K_\infty = -(R + B^T P B)^{-1} B^T P A \tag{5.30}$$

Finally, the general control algorithm of this FH-LQ control problem is depicted in Appendix B.2.

5.6 MPC tracking control problem formulation

It was shown in the previous section that the MPC algorithm consists of a variety of control theories and some basic MPC elements. The tracking problem is more challenging. The last task of developing the Wiener-Hammerstein model requires to design a MPC tracking control problem with a changeable reference. The challenge with this task is that even in the control community, the MPC tracking problems have often been considered as regulating problems around a steady-state operating point rather than full tracking problems [168]. As a result, MPC tracking problems with a changeable target are still ongoing research problems [31]. Furthermore, until recently, that assumption is still acceptable in the control community. In that case, the general overview of the tracking control strategy is depicted in Figure (5.3). This approach involves two optimisation problems. The first one is the feedforward steady state target optimisation (SSTO), and the second is the standard LQ-MPC control problem. In the coming sections, those optimisation problems will be described with all necessary changes of MPC basic components from the regulator problem. In addition, it is important to note that the notation of the state will be now x_p because this second part is about designing MPC for actuator.

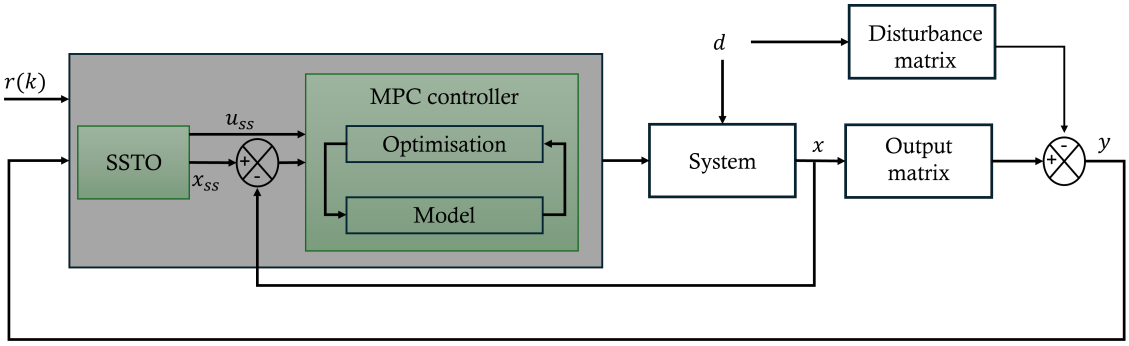

Figure 5.3: The block diagram of LQ-MPC using a steady-state target optimization tracking approach.

5.6.1 Feedforward steady state target optimization

The tracking control problem aims to steer the current state $x_p(k|k)$ to a desired state, or in our case, steady state x_{ss}. In the case of disruptions and changeable references, an offset-free MPC algorithm needs to determine the equilibrium target

that ensures accurate tracking of the control variable. The feedforward tracking with SSTO is the method used in this thesis. The optimal steady state, denoted (x_{ss}, u_{ss}) , is the solution to the following optimization problem:

$$\begin{aligned} &\min_{x_{ss},u_{ss}} \|y_{ss} - r\| + \rho\|u_{ss}\| \\ &\text{subject to} \\ &\qquad A_{eq}x_{eq} = b_{eq}d. \end{aligned} \tag{5.31}$$

In this equation, ρ is a penalty constant and r is the reference signal. More importantly, y_{ss} is steady state of the system output and it is calculated based on the steady state model described in Equation (5.9) and Equation (5.10). With this method, the LQ-MPC of tracking problem can be formulated based on the deviation state as stated in Equation (5.12).

5.6.2 Control law of the constrained LQ-MPC tracking problem

The control law of LQ-MPC tracking case requires to formalize the problem with deviation variable as follows:

$$\begin{aligned} \mathbf{P_{N_P}}(z(k)) = \min_{u(k)} & \sum_{i=0}^{N_P-1} \left[z(k+i|k)^\top Q z(k+i|k) + v(k+i|k)^\top R v(k+i|k)\right] \\ & + \underbrace{z(k+N_P|k)^\top P z(k+N_P|k)}_{\text{Terminal Cost}} \\ \text{subject to} \quad & z(k+i+1|k) = Az(k+i|k) + Bv(k+i|k), \\ & z(k|k) = z(k) \\ & P_x(z(k+i|k) + x_{ss}) \leq q_x, \\ & P_u(v(k+i|k) + u_{ss}) \leq q_u, \\ & P_{x_{N_P}}(z(k+N_P|k)) \leq \tilde{q}_{x_{N_P}} \end{aligned} \tag{5.32}$$

The solution of optimisation problem provides the control sequences in which it can be formed as the feedback control law as demonstrated above. However, the control

law of tracking is coupled with the input in steady state:

$$v(k) = u_{ss} + v^*(k|k) \tag{5.33}$$

Two points need to be considered. First, $y_{ss} = r$ is a critical condition to ensure offset free tracking with constraint satisfaction. Second, there are extra changes into linear inequality constraints. The dual mode that ensures stability and convergence in the system requires a different linear inequality equation in which it adopts a proper deadbeat mode and values of steady state of the input and state itself. As a result, the inequality constraints of tracking problem with steady state values are illustrated in these following equations:

$$\begin{aligned} \underbrace{\begin{bmatrix} C \\ -C \end{bmatrix}}_{P_x} z(k+j|k) &\leq \underbrace{\begin{bmatrix} x_{max} \\ -x_{min} \end{bmatrix}}_{q_x} - \underbrace{\begin{bmatrix} C \\ -C \end{bmatrix}}_{P_x} x_{ss} \\ \underbrace{\begin{bmatrix} I \\ -I \end{bmatrix}}_{P_u} v(k+j|k) &\leq \underbrace{\begin{bmatrix} u_{max} \\ -u_{min} \end{bmatrix}}_{q_u} - \underbrace{\begin{bmatrix} I \\ -I \end{bmatrix}}_{P_u} u_{ss} \end{aligned} \tag{5.34}$$

$$\underbrace{\mathbf{I_{nxn}} \otimes \begin{bmatrix} P_x \\ P_u K_\infty \end{bmatrix} \begin{bmatrix} (A+BK_\infty)^0 \\ \vdots \\ (A+BK_\infty)^{N-1} \end{bmatrix}}_{P_{x_N}} z(k+N_P|k) \leq \underbrace{\mathbf{I_n} \otimes \begin{bmatrix} q_x - P_x x_{ss} \\ q_u - P_u u_{ss} \end{bmatrix}}_{\widetilde{q}_{x_N}} \tag{5.35}$$

Appendix B.3 represents the control algorithm of LQ-MPC tracking with SSTO.

5.7 Transfer function of a proof mass actuator

The proof mass actuator that was taken into consideration in this work is based on the ADD-45 inertia actuator from Micromega Dynamic, whose dynamic is described in terms of a transfer function as stated in Equation (5.36) [169]. The proposed model operates in a discrete domain in which the dynamics were discretized using the zero hold method at a sampling rate of 0.001. The values of the dynamic

parameters based on state space model are shown in Table (5.1).

$$\frac{f_{act}(s)}{v_{in}(s)} = \frac{5s^2}{s^2 + 15.843s + 2785.6} \tag{5.36}$$

Table 5.1: Discrete-time control parameters for proof mass actuator.

Variable	**Values**
A_p	$\begin{bmatrix} 0.9986 & 0.0010 \\ -2.7624 & 0.9829 \end{bmatrix}$
B_p	$1.0 \times 10^{-3} \times \begin{bmatrix} 0.0005 \\ 0.9917 \end{bmatrix}$
C_p	$\begin{bmatrix} 1 & 0 \end{bmatrix}$
D_p	$\begin{bmatrix} 5 \end{bmatrix}$
B_d	$\begin{bmatrix} -0.0050 \\ 0.0020 \end{bmatrix}$
A_{eq}	$\begin{bmatrix} 0.0014 & -0.0010 & -0.0000 \\ 2.7624 & 0.0171 & -0.0010 \\ 1.0000 & 0.0000 & 5.0000 \end{bmatrix}$
b_{eq}	$\begin{bmatrix} 0 \\ 0 \\ -0.0015 \end{bmatrix}$
K_p	$\begin{bmatrix} 0.0438 & -0.0313 \end{bmatrix}$
P_p	$1.0 \times 10^{5} \times \begin{bmatrix} 8.7910 & 0.0000 \\ 0.0000 & 0.0032 \end{bmatrix}$
Q_p	$\begin{bmatrix} 10 & 0 \\ 0 & 10 \end{bmatrix}$
R_p	$\begin{bmatrix} 10 \end{bmatrix}$

5.8 Numerical results

This section presents a case study of implementing the proposed method of using a data-driven identification model of a structural system, which consists of a cantilever beam coupled with an ADD-45 inertia actuator. Chapter 4 discussed the dynamics of the cantilever beam, and the remainder of the section focusses on the outcomes of each stage of the Wiener-Hammerstein model.

5.8.1 LQ-MPC for cantilever beam

The first step in designing LQ-MPC for a cantilever beam is to verify all necessary assumptions, which ensures that the system is controllable and observable. The main point in this stage of the Wiener-Hammerstein model is that the MPC was designed to direct the controller to the control input limit. To achieve this, the MPC controller, as shown in Table (5.2), was penalising the state more heavily than the control input. Normally, the best weighted matrix for state in LQ-MPC is the transpose of the output matrix times the output matrix (C^TC). Figure (5.4) depicts the control input response, while Figure (5.5) demonstrates the structural system response, which requires the highest force to eliminate vibration. Therefore, this control input can be used to train the GP model and identify the limitation of mechanical nonlinearity of the actuator.

Table 5.2: Summary of control parameters with prediction horizon $N_P = 7$.

Parameter	**Values**
Q	$\begin{bmatrix} 100 & 0 & 0 & 0 & 0 & 0 \\ 0 & 100 & 0 & 0 & 0 & 0 \\ 0 & 0 & 100 & 0 & 0 & 0 \\ 0 & 0 & 0 & 100 & 0 & 0 \\ 0 & 0 & 0 & 0 & 100 & 0 \\ 0 & 0 & 0 & 0 & 0 & 100 \end{bmatrix}$
R	10
K	$\begin{bmatrix} 8.8275 & 95.5708 & 269.4689 & -2.7572 & 2.5922 & -2.3119 \end{bmatrix}$
P	$10^8 \times \begin{bmatrix} 0.0199 & 0.0040 & -0.0024 & 0.0000 & 0.0000 & -0.0000 \\ 0.0040 & 0.8580 & -0.0438 & -0.0009 & -0.0000 & 0.0001 \\ -0.0024 & -0.0438 & 5.5455 & 0.0008 & -0.0009 & 0.0000 \\ 0.0000 & -0.0009 & 0.0008 & 0.0000 & 0.0000 & -0.0000 \\ 0.0000 & -0.0000 & -0.0009 & 0.0000 & 0.0000 & 0.0000 \\ -0.0000 & 0.0001 & 0.0000 & -0.0000 & 0.0000 & 0.0000 \end{bmatrix}$
N	7

5.8.2 GP model for nonlinear function

The structural control input was acquired and provided to the GP. Based on the actuator's saturation, the GP was trained using data obtained from the optimal

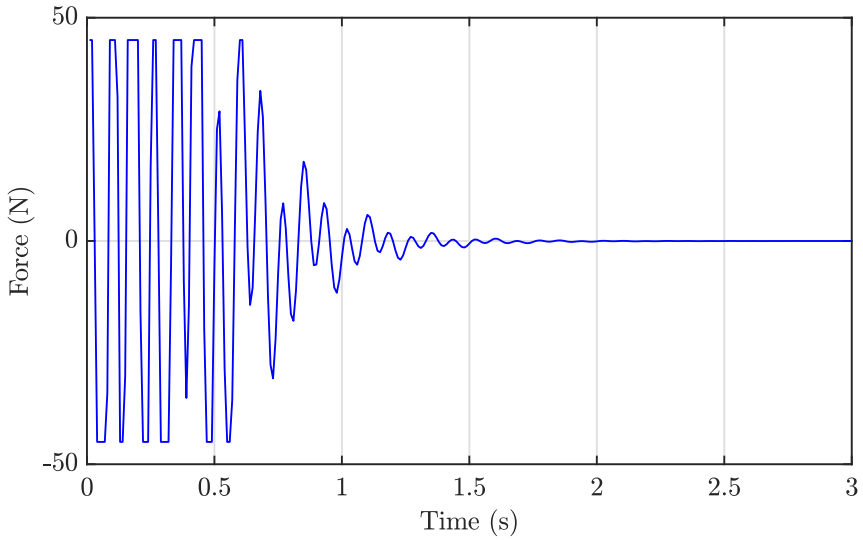

Figure 5.4: Control input of the cantilever beam.

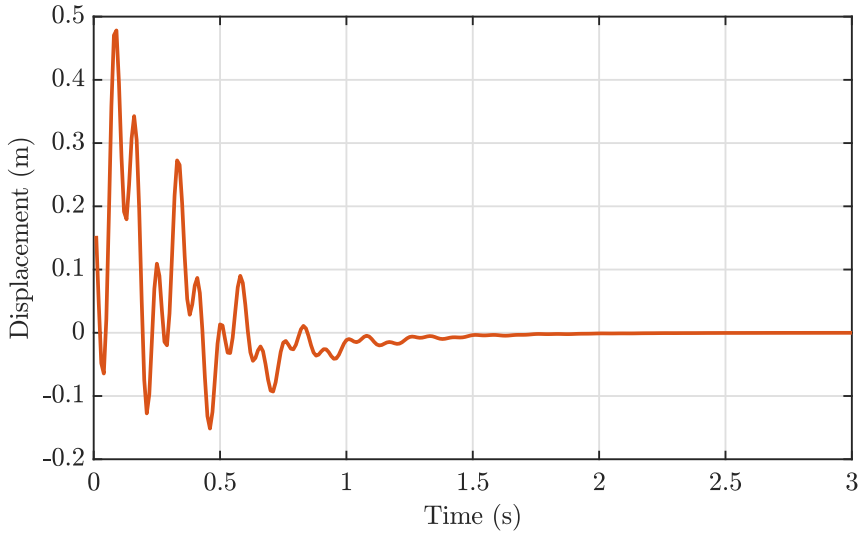

Figure 5.5: Response of the cantilever beam.

control force in the previous section. The task of choosing the hyperparameters is not challenging since the mapping task simply involves identifying the underlying function that relates training inputs to training targets. A Squared Exponential covariance function is used for this task to ensure smooth and reliable predictions. Figure (5.6) illustrates the GP training process, where the model learns the inverse of static nonlinearity to define the force space and the region of uncertainty. Figure (5.7) shows the GP prediction of the minimum force, highlighting the uncertainty region. Due to a lack of information, the GP predicts a higher force than the sat-

uration limits. Additionally, when the data varies rapidly, this GP model struggles to capture the relationship between inputs and outputs accurately.

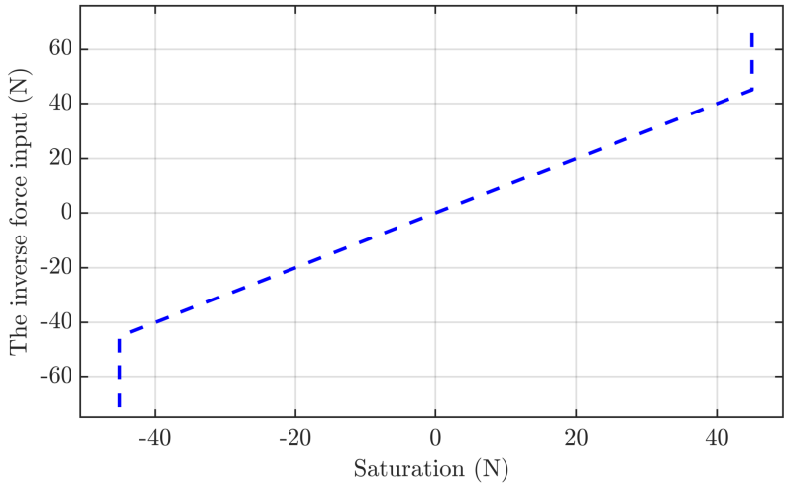

Figure 5.6: The model of GP considered the static nonlinearity of the system.

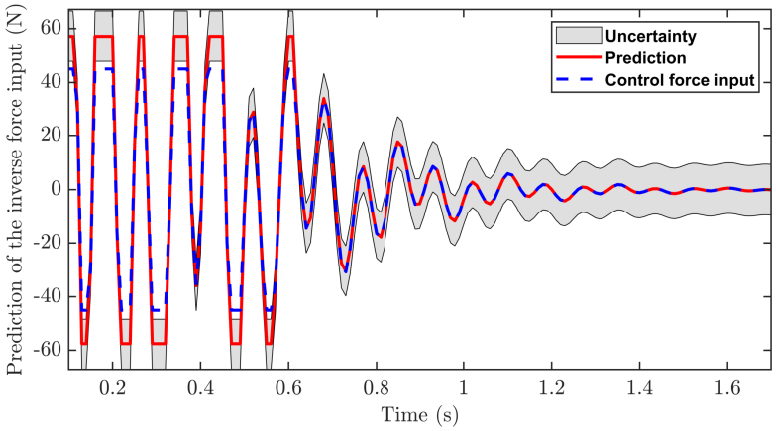

Figure 5.7: The prediction of the Gaussian process with the region of uncertainty.

5.8.3 MPC for proof mass actuator

After obtaining the inverse GP, LQ-MPC with steady-state optimiser tracking is established, with the mean of the GP at each sample serving as the reference. In the literature, this issue is known as MPC tracking with changing target [31]. Figure (5.8) demonstrates how the MPC controller was able to provide the required voltage

for the actuator to deliver the optimum force to the structure. Figure (5.9) compares the LQ-MPC regulator's control force with the actuator's output based on LQ-MPC tracking. It is obvious that an MPC controller for an actuator system faces feasibility problems due to the rapid change of the control signal. Based on the GP prediction of this problem, the controller was guided to either maximum or minimum control input. Both previous figures demonstrated that the proposed model was able to provide the control input into the structural system with static nonlinearity in the system taken into account.

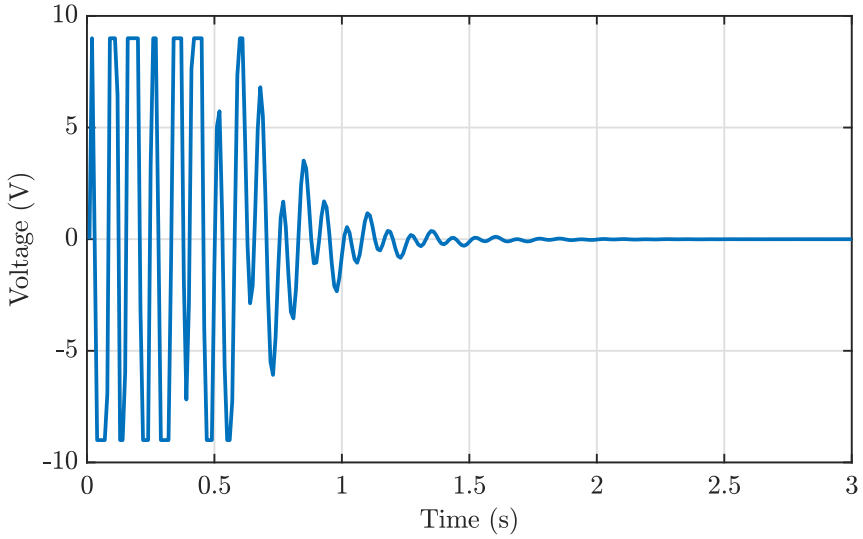

Figure 5.8: Optimum required voltage input to the actuator.

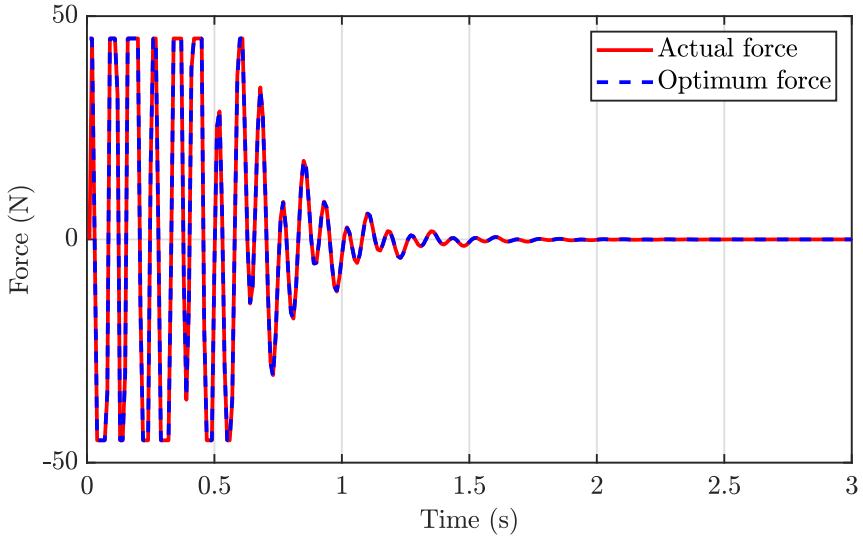

Figure 5.9: Comparison between reference force input and actual force input.

5.9 Discussion

The numerical simulation of data-driven identification with GP within the Wiener-Hammerstein model has shown that the conceptual framework was able to provide the required voltage input to the proof mass actuator, which delivers the optimal control force for the structural system taking into account the nonlinear saturation. This resulted in a demonstration of the feasibility of data-driven methods in an active vibration control setting, as related to O2 and O3 in this thesis.

In both MPC controllers, the control design was still based on MBC methods, even though the target reference trajectories were generated based on a data-driven approach. For the MPC regulator, the control design processes were established around the idea of pushing the MPC controller to its limits, such as control inputs, which were between $\pm 50\,\mathrm{N}$. In that way, the time series of the optimum force inputs can be used as training data input for the GP. In other words, the main objective in this stage of the model is not finding the best control response based on the traditional control measures. Consequently, most of the control parameters, starting from the weighting matrix to the control gain K and ending in the prediction horizon, play a criteria role in obtaining a sufficient control response of the cantilever beam. The most outstanding feature of the LQ-MPC controller is that obtaining all necessary assumptions of controllability and observability of the cantilever beam is sufficient to ensure feasibility and convergence of the control system, without requiring an extensive comparison of control parameters.

That is difficult to quantify when it comes to LQ-MPC tracking using a steady-state target optimisation tracking method. All necessary control assumptions have been obtained and supported, indicating that there is a reasonable and converged solution to the constrained control optimisation problem; however, the changeable target reference trajectory remains a research topic. Excluding the mathematical difficulty of LQ-MPC tracking, the controller provided the actuator with the minimum required voltage input to provide the required control force while taking mechanical saturation into account. Following to the MPC regulator, control performance could be improved by taking into account different control parameters and employing more insightful control measures.

The GP model was trained using static maps from the input and target data. Despite its simplicity, the GP model prediction provided an insightful modelling perspective,

especially in the end stork region as shown in Figure (5.7). This additional information was incorporated into the design of LQ-MPC tracking. More importantly, these results encourage the use of GP models in more complex vibration control conditions.

5.10 Summary

This chapter addressed the first step in designing active vibration control based on the recent development of data-driven methods. The introduced novel framework integrated MPC and GP into the Wiener-Hammerstein model, with the objective of quantifying the uncertainty or end stroke of the proof mass actuator. The proposed model needs to go through three design phases. Designing a constrained Linear Quadratic Model Predictive Control (LQ-MPC) for the regulator case is the first step, which facilitates the model in determining the minimal force needed. The second step is to create the inverse GP model, which helps in mapping the minimal force necessary to force space using the GP model of static nonlinearity. Designing a constrained LQ-MPC utilising a steady-state target optimisation tracking approach is the last step. This step demonstrates the proof mass actuator's capacity to track the required force input while accounting for the saturation of the actuator's static nonlinearity. The cantilever beam coupled with a proof mass actuator was used numerically as a case study.

In summary, it can be stated that the proposed model was able to provide the optimal control force for the structural system, taking into account the nonlinear saturation. This intuitive conclusion has been published in the XIIth International Conference on Structural Dynamics (EURODYN2023), Delft, Netherlands. Having said that, the conceptual model was still complex as a result of designing the MPC controllers based on MBC methods. Dealing with this complexity requires an advanced control theory in case of completing the feedback loop of the control system. In the next chapter, designing the MPC controller based on DDC methods will be proposed in which it will overcome the issue of modelling complexity.

Chapter 6

Nonlinear model predictive control for linear flexible structures: Gaussian process model

Highlights:

- A novel approach of controlling flexible structure by using recent developments in modelling and control is presented.
- Nonlinear system identifications using GP and their role in the design of control of dynamic systems is explored and discussed.
- Designing GP-NARX within NMPC for flexible structure is challenging especially without identifying a suitable reference trajectory and cost function.
- A combination and clarification of terminologies in control and structural systems are identified and discussed.

6.1 Overview

The aim of this chapter is to demonstrate an alternative method of controlling a flexible structure employing one of the DDC approaches. This novel approach applies NMPC to flexible structures using machine learning-derived models. GP function as black-box models in NMPC, providing system output predictions and confidence levels. In NMPC, GP can be utilised as the nonlinear model of the system itself to allow optimisation of the control inputs. To keep things simple, this chapter begins with a brief overview of GP-NMPC, followed by a two-part presentation of this novel approach. The first section describes learning GP for flexible structures, followed by a demonstration of the NMPC control algorithm. This chapter concludes with two case studies designed to evaluate the proposed idea.

6.2 Towards GP-NMPC of structural systems

Over the past two decades, data-driven modelling has gained popularity in structural dynamic applications; nevertheless, there has not been significant research conducted regarding data-driven modelling and control in active vibration fields [170]. One reason for the lack of implementation of recent approaches is the difficulty in developing a reliable dynamic model of linear or nonlinear dynamic systems, especially when applied in control systems [171]. The previous chapter was an excellent example of the difficulty in developing an appropriate model for control purposes in a complex system. As a consequence, it is critical to investigate whether data-driven control, particularly GP and NMPC approaches, can improve the control performance of an active vibration system.

The GP is a probabilistic nonparametric modelling approach, and its popularity in dynamic system identification stems from its ability to predict the output value of the system along with the measure of its confidence. More importantly, the GP can be used in a time series model to highlight parts of the input space where there is insufficient data and model systems that exhibit nonlinearity [172]. Furthermore, the popularity of system identification using GPs has sparked interest in NMPC, particularly given the efficacy of data-driven modelling in control engineering. One of the main advantages of NMPC is its ability to deal with practical constraints, such as input energy or state limits. As a result, GPs have been integrated into

NMPC to benefit from its prediction uncertainty, with control input adjusted to take the region of uncertainty into account. This control strategy was originally used in a first-order process system as a theoretical approach in [173] and later in a chemical system in [174]. Although the use of a GP model in a control system is not new in control applications such as car racing [171] and unmanned quadrotor [175], including a fully offline GP model into an NMPC has been rare [176].

Despite several GP structures being suggested, the Gaussian Process Nonlinear AutoRegressive model with eXogenous input (GP-NARX) has been extensively employed in SHM applications such as wind turbines [177] and bridges [107]. In the SHM context, GP-NARX can be formed into One Step Ahead (OSA) and Model Predicted Output (MPO) predictions [178]. From a control systems perspective, these GP structures use different terminology and serve distinct objectives, as discussed in forthcoming sections. Consequently, the contribution of this work is implementing and comparing GP structures as a black box model trained and fixed offline in which it gives the prediction of the output while optimising inside NMPC.

The general idea considers applying NMPC to flexible structures by utilising one of GP structures such as GP-NARX. The GP model is identified offline for use as a black-box model in NMPC; it provides both the prediction of the system output and the associated confidence. In a control context, a GP can be utilised as a discrepancy model for linear or nonlinear flexible dynamic structures within MPC or even as the nonlinear model of the system itself. The common GP structures for dynamic data are GP-NARX and the Nonlinear Output Error model (GP-NOE). One difference between these models is the number of predictions ahead that are used within the predictive control strategy and the requirement to propagate predictions to the control horizon. GP-NARX is most easily utilised for one prediction ahead, whereas GP-NOE is more suited to addressing simulation problems that require multiple steps ahead. The ultimate objective is to explore the possibilities of utilising both these models in an active vibration control setting, making use of the framework of improved control design in NMPC. The success of this idea relies on developing an adequate offline model, and the process of achieving that is presented in the next section.

6.3 Learning GP for nonlinear control of flexible structures

To attain a reliable GP model, the identification process typically contains five stages. These stages, as summarized from [14, 23, 172], are illustrated in Figure (6.1) and include the following:

- defining the purpose of the model
- selection the set of model
- design the experiment
- training the model
- validating the model

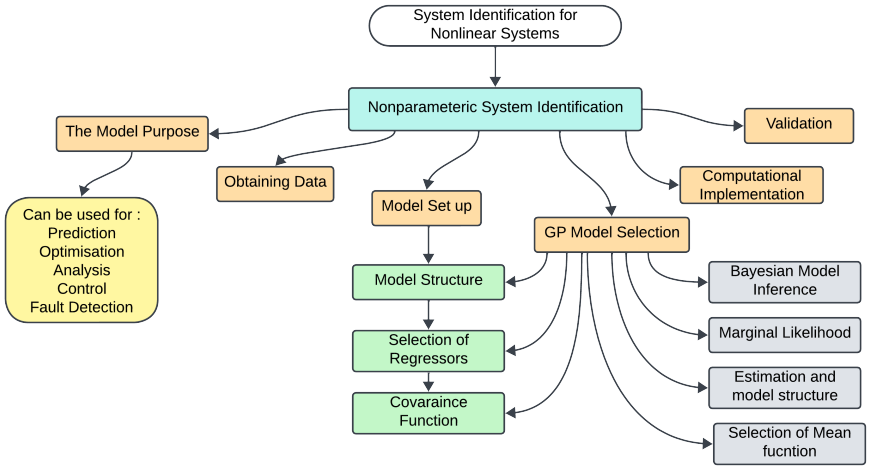

Figure 6.1: This diagram outlines the majority of the steps that must be taken into account when identifying a dynamic system using GP.

System identification with GPs is quite challenging, especially when the relationship between the input and target data is nonlinear. This implies that identifying the model is a continuous process, with the possibility to return to a previous step at any point during the identification process, which is sometimes necessary. In modelling,

identifying the model's purpose in the first stage is crucial because it determines the model's level of detail and intended use. Fortunately, the purpose of this work is control, which implies two points. First, the form of the model relies on the control design method, which implies that the model should contain the behaviour of closed-loop system performance and not only the process model. Second, designing a GP model based on a reasonable amount of data along with validation criteria should be sufficient to avoid unnecessary computational costs.

To simplify the identification process of the GP model, the following subsections cover all design phases and discuss the components required for this work. For more information, readers can refer to these comprehensive resources [14, 23, 172].

6.3.1 GP model setup

From Figure (6.1), the key components of the GP model are the model structure, regressor or lag selection, and covariance function. Here is a brief overview of each of these components.

Model structure

At this point in the thesis, the GP models presented until now are essentially static maps between input and output training data. However, identifying a dynamic system requires a learning framework, and an autoregressive model based on GP is one method for capturing and learning nonlinear relationships [107]. The GP-NARX model is a more general type of autoregressive model in which the model's prediction is based on lagged versions of the inputs and outputs. Mathematically, the GP-NARX is given as:

$$\hat{y}(k) = f(y(k-1), \ldots, y(k-L_y), u(k-1), \ldots, u(k-L_u)) + \epsilon \tag{6.1}$$

In this equation, the exogenous inputs are defined as a vector $u(k-i)$ at each time step k, and the autoregressive is defined as $y(k-i)$. The numbers of lags in the exogenous term and in the autoregressive term are denoted by L_u and L_y, respectively. The noise term ϵ is assumed to be Gaussian, $\epsilon \sim N(0, \sigma_n^2)$, with the noise variance σ_n^2. This form allows the GP prior to be assumed over functions of $f(.)$. SHM supports two types of GP-NARX predictions: OSA and MPO. In the

OSA prediction, a model makes a single-step prediction into the future based on the current and past control of both input values $u(k-i)$ and measured output values $y(k-i)$. In contrast, the MPO prediction involves a model making multiple-step predictions into the future, which is based on using the model predictions from previous steps as input to compute the next step.

From control perspective, GP-NARX model is just one prediction ahead and it is sometimes refered to as prediction method [178]. More importantly, the simulation model of predicting multiple steps ahead in the future without additional observations of the true output value is termed as GP-NOE. Even though these terminologies are different among structural and control fields, these models operate in the same principle and this work adopted the control field terminologies. The mathematical representation of GP-NOE is given as follows:

$$\hat{y}(k) = f(\hat{y}(k-1), \ldots, \hat{y}(k-L_y), u(k-1), \ldots, u(k-L_u)) + \epsilon \tag{6.2}$$

The GP-NOE model is further divided into different types of dynamic system simulations. Naive simulation is based only on including the predicted model's mean values, whereas approximation simulation considers both the mean and the uncertainty of future predictions. The naive simulation is more computationally efficient, while the approximation type is more realistic. In general. Figure (6.2) illustrates the general concepts and terminology of the GP structure in dynamic systems.

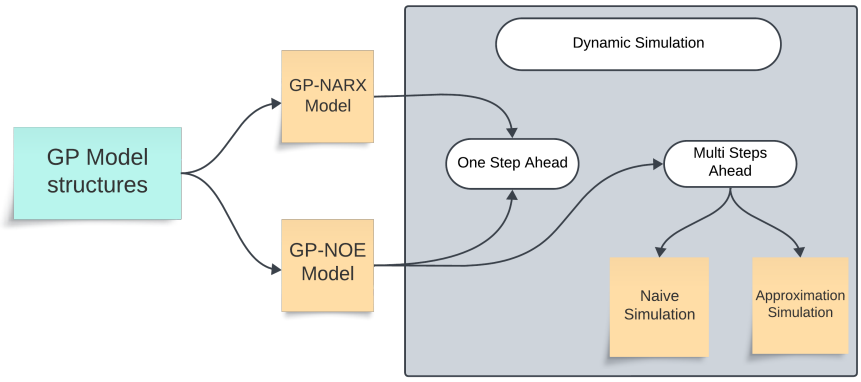

Figure 6.2: Conceptual framework illustrating the structure and process of GP models in dynamic simulation. Simulation is mainly about multi steps ahead where this figure presents the terminology that suits both GP research community in structural and control fields.

Covariance Function

The choices of covariance function $k(x, x_*)$ is a fundamental importance for successful modelling with GP. Selecting the appropriate covariance function not only reflects the correlation between different training data observation, but also determines the number of hyperparameters to be trained and optimised. Some common functions are listed in [23], but in practice there is a common function used with a control intent. When the modelled function assumed to be continuous and not smooth and non-differential, the exponential covariance function is more suitable and it is in the form:

$$k(x, x_*) = \sigma_f^2 \exp\left(-\frac{r}{l}\right) \tag{6.3}$$

where σ_f^2 and l are the scaling factor of the possible variations in vertical and horizontal of the function, respectively. The variable r is the input distance measure and is defined as $|x - x_*|$. The Matérn covariance function is another popular function when the assumptions of the function are less stringent regarding the smoothness and differentiability:

$$k_{\text{Matérn}}(x, x_*) = \sigma_f^2 \left(1 + \frac{\sqrt{3}r}{l}\right) \exp\left(-\frac{\sqrt{3}r}{l}\right) \tag{6.4}$$

However, squared exponential with automatic relevance determination (SE-ARD) is the most commonly used covariance function in predictive control with GP [173, 174], especially when the model is fixed and trained offline. The SE-ARD is:

$$k_{SE-ARD}(x, x_*) = \sigma_f^2 \exp\left(-\frac{1}{2}\sum_{d=1}^{D} w_d (x_{d_i} - x_{d_j})^2\right) + v_0 \tag{6.5}$$

where $[w_1, \ldots, w_D, \sigma_f^2, v_0]^T$ represents a hyperparameter vector θ. While D represents the length of the lags vector x, and w_i represents the relative importance of each component x_d of the lags vector. v_0 denotes the white noise variance. The importance of this function is that the length scale is optimised for each lag of the delayed output and input values. Finally, it is worth noting that comparing between these choices based on validation criteria is required when the modelling process is

complex and there is no prior knowledge.

Selection of lags

The selection of the lags, sometimes called the model order, is a critical element in the model setup. Unfortunately, this topic has not been thoroughly covered in the literature even though some research attempts have been reported [178, 179]. Since the proposed idea is for control purpose, the selection of lags is based on criteria of the model prediction performance.

6.3.2 The model training

Once the model setup is identified, the hyperparameter vector θ must be optimised. Learning hyperparameters is extensively discussed in GP literature [23, 172]. However, three important points must be addressed. First, the hyperparameter vector identified based on the training data and evaluated on a validation data set in which these hyperparameter be utilised in offline black box within a control algorithm. Second, the concept of maximum marginal likelihood is applied, which is optimised using a conjugate gradient method. Finally, to avoid getting stuck at the local minimum, we repeat the training process using different initial hyperparameter values.

6.3.3 Model prediction performance

In order to assess the reliability of GP models, the following metrics are commonly used [14, 23]. In the dynamic system, mean-squared error is the general approach to quantifying the performance of a model. Standardised mean-squared error (SMSE) is a common measure that normalises the mean-squared error between the predicted output of the model and the measured output of the system by the variance of the output values of the validation dataset and it is defined as:

$$\text{SMSE} = \frac{1}{N\sigma_y^2}\sum_{i=1}^{N}(y_i - \mathbb{E}[\hat{y}_i])^2 \tag{6.6}$$

where σ_y^2 is the variance of the output values of the validation dataset. A lower SMSE value indicates better model performance and a more accurate match between the model's predictions and the actual system outputs. In terms of incorporating uncertainty, log predictive density error (LPD) is a performance metric that considers both the mean of the model prediction and the entire predicted distribution, and is expressed as:

$$\text{LPD} = \frac{1}{2}\ln(2\pi) + \frac{1}{2N}\sum_{i=1}^{N}\left[\ln(\sigma_i^2) + \frac{(y_i - \mathbb{E}[\hat{y}_i])^2}{\sigma_i^2}\right] \tag{6.7}$$

In this metric, higher values of LPD suggest better model performance by putting greater weights on the output error when the output variance σ^2 is small. Alternatively, the mean standardised log loss (MSLL) is another important measure for a probabilistic model. This metrics is presented mathematically as:

$$\text{MSLL} = \frac{1}{2N}\sum_{i=1}^{N}\left[\ln(\sigma_i^2) + \frac{(y_i - \mathbb{E}[\hat{y}_i])^2}{\sigma_i^2}\right] - \frac{1}{2N}\sum_{i=1}^{N}\left[\ln(\sigma_y^2) + \frac{(y_i - \mathbb{E}[y])^2}{\sigma_y^2}\right] \tag{6.8}$$

MSLL is calculated by including the mean and variance of the measured output, subtracting from the model LPD, and taking the means of the obtained results. Negative values of this performance measure indicate a better model fit, or approximately zero for a simple model.

With these metric performances, the overview of nonlinear system identification with GP is completed. The next section is devoted to the second part of the proposed method, which is the control design.

6.4 Nonlinear model predictive control

Following the advancements in machine learning and data-driven control, nonlinear predictive control has grown in popularity with researchers. In practical applications, non-linear predictive control is less common than linear predictive control [14]. Although there have been notable efforts in the NMPC field, the majority of the work is focused on research or experimentation [28, 180]. One of the primary reasons for the relatively slow adoption of NMPC is the difficulty of building a non-linear model consistently and reliably from available data. NMPC with GP as a model addresses this issue by providing information about the model's confidence. This

additional information can be used to evaluate control performance and constrain the behaviour of a closed-loop system within the model's trusted region.

Despite these GP-NMPC features, the optimisation problem, from selecting an objective function to constructing constraints, remains difficult. The most significant hurdle is the computational burden. This problem has been addressed, and there are numerous approaches to overcoming it [181]. Alternatively, the computation costs can be reduced by minimising the complexity of the cost function and the MPC algorithm. In light of this, Predictive Functional Control (PFC) was chosen in this study to demonstrate predictive control based on GP. The next section describes the PFC, followed by the control design.

6.4.1 Predictive functional control

In 1987, PFC was introduced by Richalet in [182], and it has since been identified as simple MPC algorithms with trivial coding, straightforward implementation, and simple handling that does not require advanced knowledge [183]. In principle, PFC still follows the MPC strategy as explained in Chapter 2, it places a different emphasis on some of the MPC features, particularly the use of control input and the concept of coincidence points.

The distinctive feature of PFC is the parametrisation of the future input trajectory. In other words, the future control input is constructed as a linear combination of a few simple basis functions; in practice, the future control is assumed to be a polynomial function, so it can be assumed as step or ramp functions. Then, the form of future input is assumed as follows:

$$u(k+i) = u_o(k) + u_1(k)i + u_2(k)i^2 + \ldots + u_c(k)i^c, \quad i = 1, 2, \ldots N_u \tag{6.9}$$

In this equation, the predicted input trajectory is parameterised by $c+1$ coefficients, such as $u_o(k)$ for constant input. The popularity of PFC stems from the fact that it constructs the input trajectory with a low value of c, allowing for optimisation of only two or three parameters in the SISO system. This can provide an advantage when controlling nonlinear systems [25].

Furthermore, the concept of coincidence points is that there are points where the closed loop response and the reference trajectory should concide as shown in Figure

(6.3). In light of this concept, the reference trajectory is different from set point, and its role plays a critical part of getting a smooth control signal, especially in nonlinear systems. Figure (6.4) depicts an update of the MPC strategy which is different from the one presented in Figure (2.2). In literature, the response of first order system is adopted. Now, the moving horizon minimisation problem is simpler and contains only a few points over which the cost function is minimised. In following sections, PFC is utilised and presented mathematically.

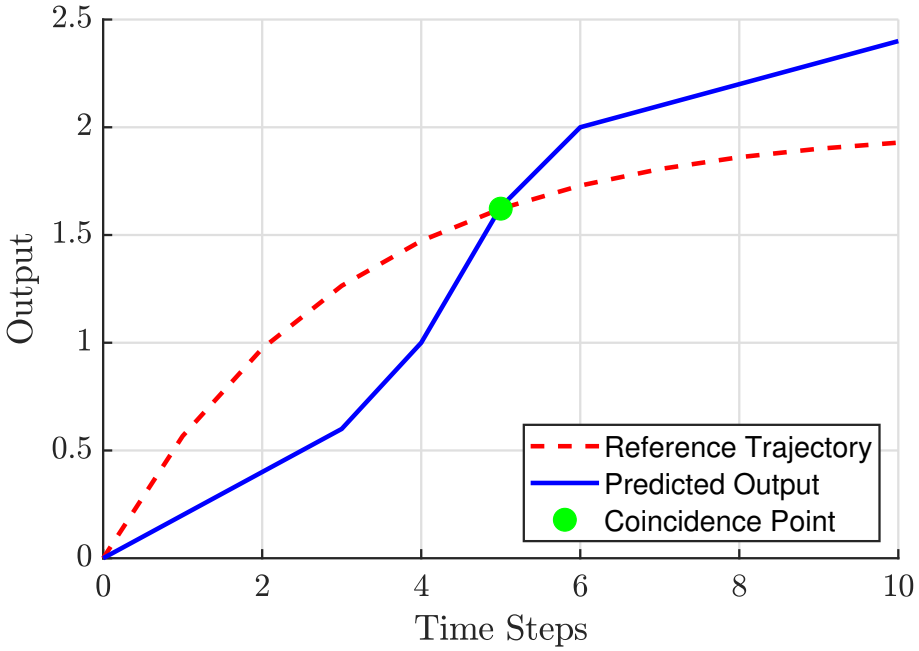

Figure 6.3: The concept of PFC control by matching prediction to reference trajectory at a single point is illustrated [163].

6.4.2 Controller design

As explained in Section 2.3, the formalisation of nonlinear optimisation problem consists of a cost function and constraints, while using the process model to provide the prediction model. Here, the process model is the GP-NOE model for multiple step ahead. In addition, the key factor of this GP model is being trained and fixed offline, meaning the performance of NMPC is relying on prior knowledge of the system dynamics and the model's hyperparameters. Consequently, the general unconstrained moving horizon minimisation problem is defined:

$$\min_{u} \ell(u, \hat{y}(k), r(k), u(k-1)) \tag{6.10}$$

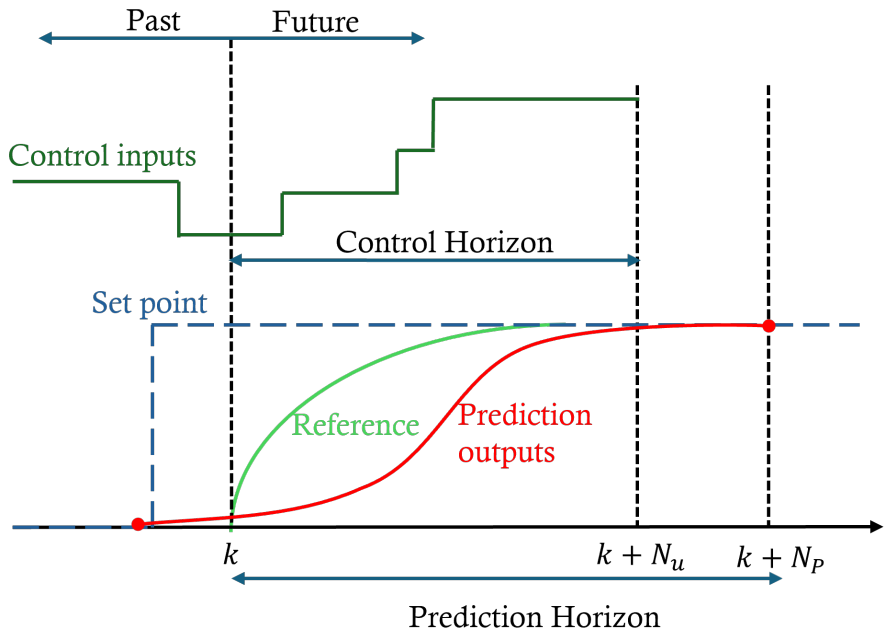

Figure 6.4: Illustration of MPC strategy modification with the adoption of PFC, showing the differences between the set point and reference trajectory.

Now, the selection of appropriate cost function is a critical step in designing an GP-NMPC controller. In order to simplify this optimisation problem, the concept of the coincidence point in PFC has been utilised for two reasons [184]. First, the reference trajectory significantly impacts the required performance, so tuning the cost function weights is unnecessary. Second, the future control signals, based on polynomial structure, provide the optimiser with a few degrees of freedom, leading to smooth input trajectories. While these modifications do not affect the generality of the solution, they do impact the numerical solution. Hence, the cost function in the case of a single coincidence point is presented as:

$$\ell(u, \hat{y}(k), r(k), u(k-1)) = [r(k+P) - E(\hat{y}(k+P))]^2. \tag{6.11}$$

This cost function requires that the value of the reference trajectory at the coincidence point P matches to the estimated output value of the system. Selecting the appropriate coincidence point remains challenging; the designer plays a critical role in this task. The control sequence is obtained by finding the optimal solution of Equation (6.10):

$$u_o = [u_o(k), u_o(k+1), \ldots, u_o(k+P-1)]. \tag{6.12}$$

Once this optimisation problem is solved, the control law can be formed based on the receding horizon principle. This repeated action of applying the first optimised control in the sequence defines a feedback control law:

$$\kappa_N(x) = u_o(k). \tag{6.13}$$

Equation (6.11) is an appropriate first option; however, the control action still does not include the level of confidence of GP in the control optimisation. When the prediction uncertainty $var(\hat{y}(k+P))$ exists in the MPC problem, the constrained moving horizon minimization problem can be used as an alternative. To reduce computational costs, it is appropriate to make the MPC problem unconstrained and include uncertainty as part of the cost function, as expressed below:

$$\ell(u, \hat{y}(k), r(k), u(k-1)) = [r(k+P) - E(\hat{y}(k+P))]^2 + var(\hat{y}(k+P)). \tag{6.14}$$

6.4.3 Design of a reference trajectory

The remaining control design is now generating the NMPC controller's reference trajectory. The goal of developing the reference trajectory is not only to determine the trajectory that the plant should take to return to the set-point trajectory, but it is also crucial in determining the controlled plant's closed loop behaviour. Determining the reference trajectory is firstly set by identifying the current error $e(k)$ between the set point trajectory $w(k)$ and the current output measurement value $y(k)$:

$$e(k) = w(k) - y(k), \tag{6.15}$$

Since it is assumed that the reference trajectory is considered to approach the set point exponentially from the current measurement output value, the next step is to calculate the error at the number of steps (i):

$$e(k+i) = e^{-iT_s/T_{\text{ref}}} e(k), \tag{6.16}$$

where T_s is the sampling time and T_{ref} is the time constant of the exponential defining the speed of the response. Then, the reference trajectory is completely defined by:

$$r(k+i) = w(k+i) - e(k+i) = w(k+i) - e^{-iT_s/T_{\text{ref}}} e(k). \tag{6.17}$$

Finally, the general algorithm is used within NMPC as shown in Figure (6.5).

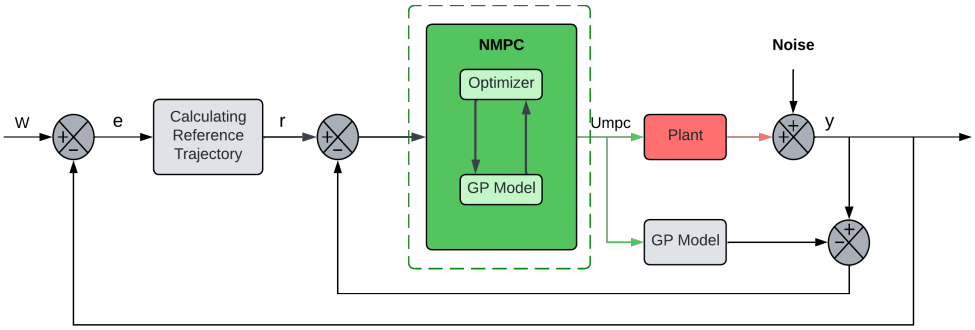

Figure 6.5: General block diagram of the GP-NMPC method, highlighting the core algorithm within the NMPC block.

6.5 Case study: discrete and continuous flexible systems

This section presents two fundamental simulation cases in active vibration control. Technically, the control task in vibration control is a regulator; however, demonstrating the effectiveness of the proposed idea requires the control tasks in both cases to be tracking. To avoid repetition, a detailed analysis of nonlinear system identification and control performance will be provided in the cantilever beam case, while the linear oscillator study presents a simple proof of concept. In both numerical cases, there are three subsections. Creating dynamic data is the first step towards establishing a relationship between the system's input and output. Next, the model identification describes the procedure for choosing the GP model. The control performance section concludes with a description of the control design and how it is used.

6.5.1 Linear oscillator system

The equation of a linear oscillator is given by :

$$\ddot{x}(t) + 2\xi\omega_n\dot{x}(t) + \omega_n^2 x(t) = f \tag{6.18}$$

where ω_n and ξ define the natural frequencies and damping factors. Now, the objective of this investigation is to excite this dynamic system in which its data could be used in developing an adequate offline GP model. This goal requires Equation (6.18) to be transformed into state space model as:

$$\begin{bmatrix} \dot{x}_1 \\ \dot{x}_2 \end{bmatrix} = \begin{bmatrix} 0 & 1 \\ -\omega_n^2 & -2\omega_n\xi \end{bmatrix} \begin{bmatrix} x_1 \\ x_2 \end{bmatrix} + \begin{bmatrix} 0 \\ 1 \end{bmatrix} u \tag{6.19}$$

$$y = \begin{bmatrix} 1 & 0 \end{bmatrix} \begin{bmatrix} x_1 \\ x_2 \end{bmatrix} + v \tag{6.20}$$

where $\dot{x}_1$ and $\dot{x}_2$ are the vector of defined state variables, u is the input vector, y the output vector. The state and observation equations are expressed in the continuous domain but typically control is implemented in the discrete domain. Even though there are various methods to discretize a system, the method used in this work is zero-order hold (ZOH) as stated in Chapter 4. In this stage, the most challenging part in the identification process is the discretization. We assume that the natural frequency of the system is 5.5 rad/sec and damping ratio is 0.1. As a result, the sampling frequency used, and also according to Nyquist's theorem, is 11 times the natural frequency. The sampling time is therefore:

$$T_s = \frac{2\pi}{11 * \omega_n} = \frac{2\pi}{60.5} = 0.1s \tag{6.21}$$

This sampling time is sufficient for converting the system to a discrete domain. Later in control design, the sampling time in MPC should be the same or greater than the sampling time in the discretisation process, which can sometimes lead to costly computations. In that case, the sampling time in generating data and MPC controller is the same across the cases studies in thesis.

Obtaining data

Two separate sets of dynamic data were obtained as a result the GP model intended to be used in control system. The first set was collected by exciting the linear oscillator using a random input generator. The input magnitude ranged from -7 to 7 N, with a total of 350 training points. The validation data was obtained using the same method but over extended periods of time. The input signals were longer with 450 points for validation. To obtain a full experimental design, white noise with a variance of 0.5 and a mean of zero was applied to both the identification and validation sets of data. Figure (6.6) displays the linear oscillator responses and input signals for both data sets. It is worth noting that the number of training points affected the dimension of the covariance matrix. The drawback of obtaining a high number of sample points is leading to longer computation time. Consequently, rule of thumb is to choose a number of training points that capture the system dynamics sufficiently. Moreover, Figure (6.7) shows the relationship between the data and it is clear that the data represents a linear system.

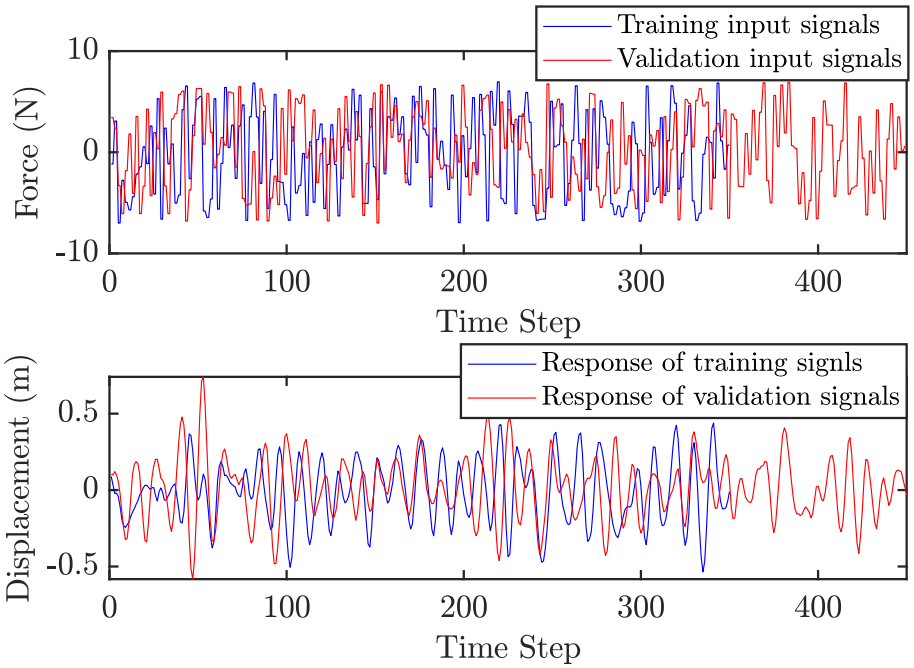

Figure 6.6: Comparison of training and validation input signals (top) and their corresponding displacement responses (bottom) over time.

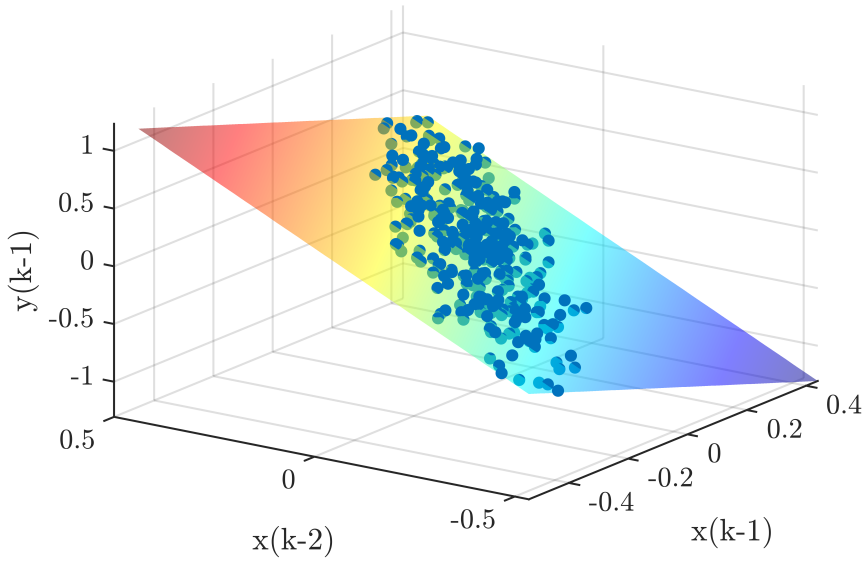

Figure 6.7: Visualization of the space between the input and target data. The 3D scatter plot shows the relationship between the input and target,illustrating that the data represents a linear system.

Model identification

After acquiring dynamic data, the process of selecting an appropriate GP model began by determining the system's order. Intuitively, the number of lags is more than the order of the physical system. Since the linear oscillator here is second order, the number of lags in the GP model is expected to be two or three. In addition,the SE-ARD covariance function was then used, providing a specified scale for each lag. Table (6.1) compares several higher-order models based on some validation features. The values of the model performance criteria indicate that having a higher number of lags leads to better performance as expressed in all three performance measures. Having said that, overfitting is a problem that needs to be considered. In that case, order 2 is more suitable since we have prior knowledge of the dynamic system.

Table 6.1: Values of model performance based on training and validation data sets.

Order	**Identification Data**			**Validation Data**		
	SMSE	**LDP**	**MSLL**	**SMSE**	**LDP**	**MSLL**
3	1.30E-03	-3.4893	-3.3195	1.34E-03	-3.4911	-3.3068
2	3.12E-03	-3.0552	-2.8841	2.62E-03	-3.1441	-2.9590
1	2.33E-01	-0.8980	-0.7262	0.21929	-0.9410	-0.75539

The hyperparameter vector θ of order 2 is presented as [0.1535, 0.1287, 0.0111, 0.0107, 42.625], and these values express two points. First, the small values of individual lags in either input or prediction indicate less flexibility, meaning the model may not capture rapid changes in the system dynamic. Second, the value of the length scale suggests that the model has a smooth response. Figure (6.8) shows the GP model for the training data, and it is clear that it fits the system response quite well. The final step in this modal identification is to validate the GP model setting with different dynamic data sets. Even though the validation signal was longer than the training signal, Figure (6.9) shows that the selecting GP model setting was also suitable for validation data. Having said that, the GP model is now suitable for NMPC as an offline and fixed GP model.

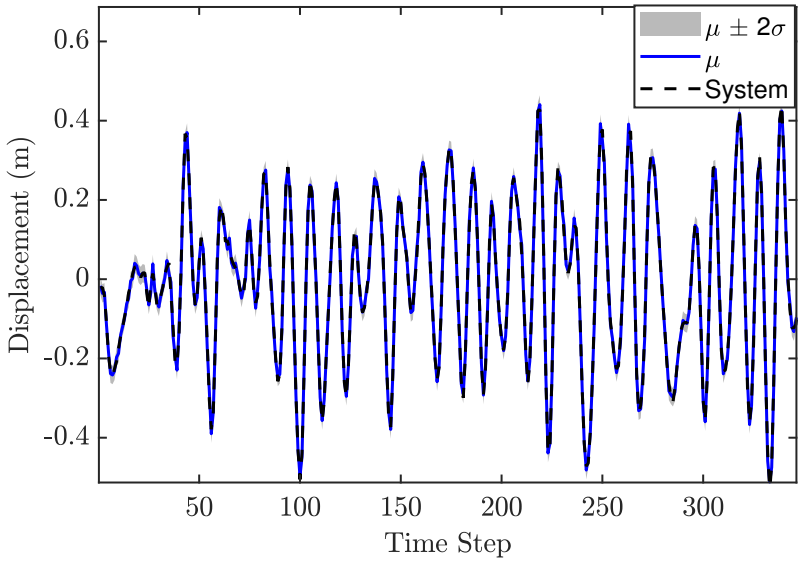

Figure 6.8: The plot shows the trained GP model of displacement over time, with the GP prediction (solid blue line) compared to the actual system (dashed black line). In this and the following figures, $\mu \pm 2\sigma$ represents the uncertainty in the prediction, indicating the confidence interval. μ represents the mean of the prediction. The system data corresponds to the training data that the GP model aims to capture.

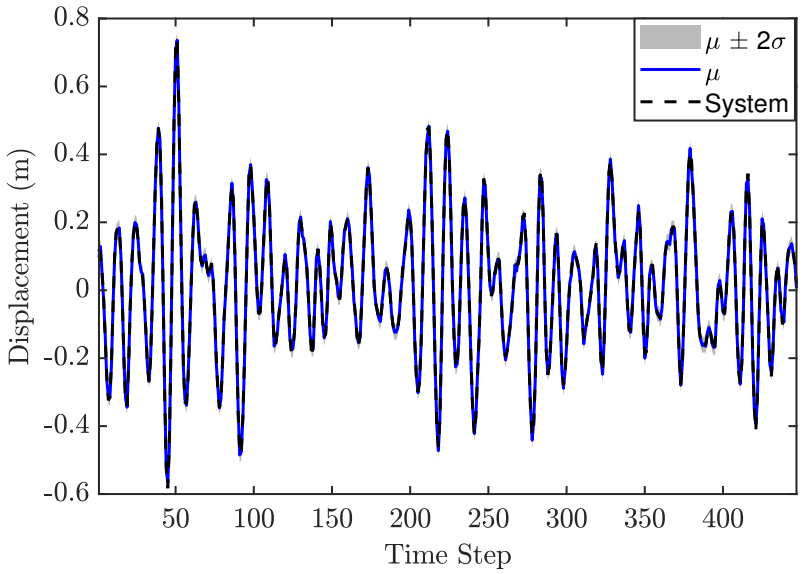

Figure 6.9: The plot shows the validation GP model of the displacement over time as predicted by the GP model (solid blue line) compared to the actual system (dashed black line). The GP model fits the system perfectly, as evidenced by the close alignment between the predicted and actual values.

Control performance

In NMPC control design, choosing a suitable sample time T_s is crucial, even if the validation metrics indicated that the trained GP model was suitable. For the reference trajectory design, T_s is set to 0.01 seconds in Equation (6.16), which is faster than obtaining in converting to discrete domain. Selecting the number of predictions ahead is the last stage of the GP-NMPC method. Figure (6.10) illustrates the closed loop performance of a linear oscillator based on one prediction ahead, or GP-NARX. That means the model was not able to capture the dynamic and requires dynamic simulation based on multiple steps ahead. In addition, the closed loop responses of unconstrained control in tracking tasks for a different prediction is given in Figure (6.11). It is clear that the GP model was able to predict the dynamics of the reference trajectory in which it leads the NMPC optimiser to provide the best control action. Furthermore, this outcome demonstrates that the GP-NOE with MPC not only gives an alternative control method for active vibration control but also provides more insights into the dynamics of structural systems.

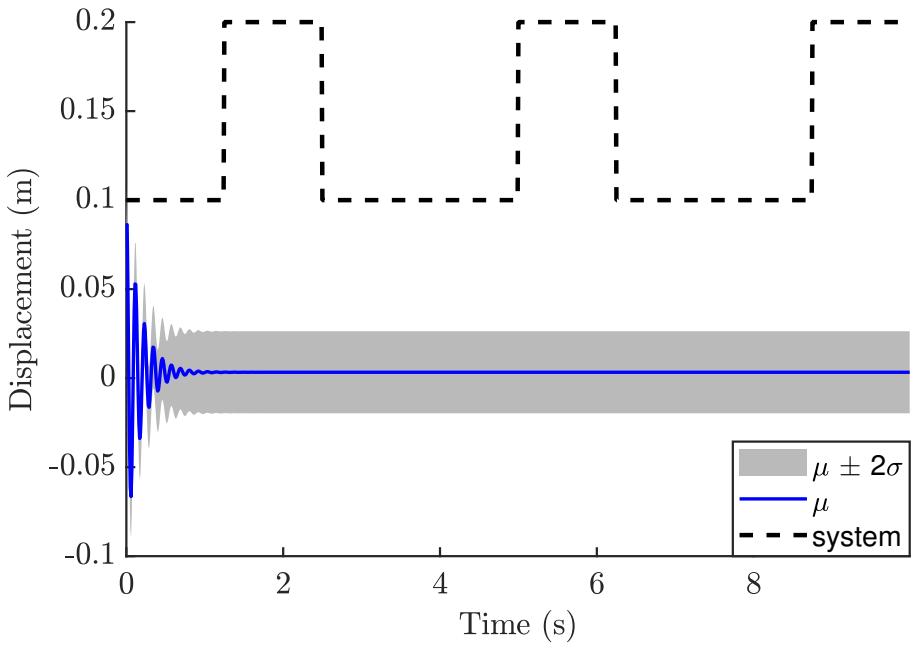

Figure 6.10: The plot shows the displacement response for a 1 step ahead prediction. The responses generally illustrate the system's ability not to follow the set point with GP-NARX model.

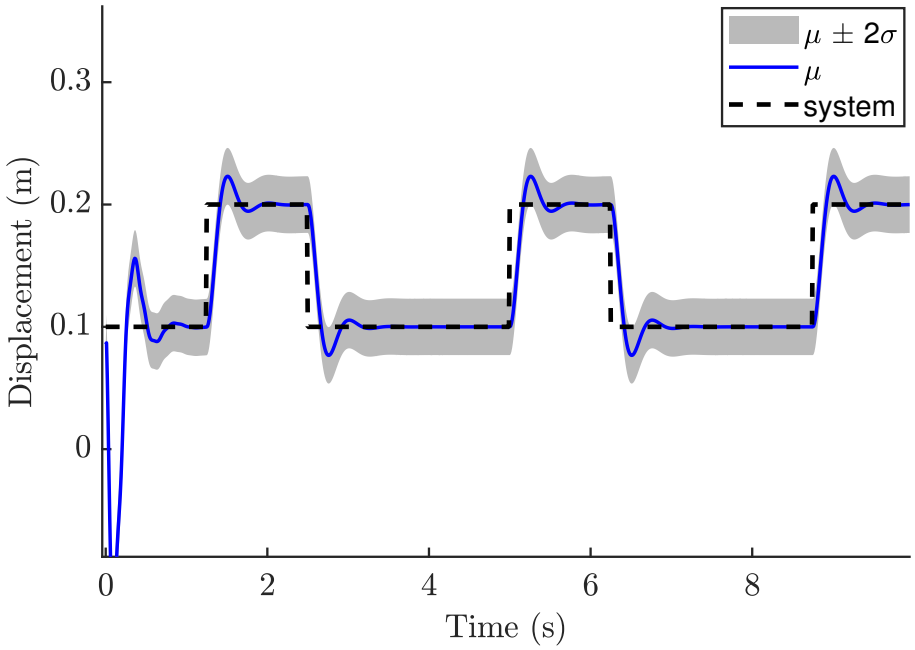

Figure 6.11: The plot shows the displacement response over time for a different prediction horizon.

6.5.2 Cantilever beam

Obtaining data

The procedure of obtaining data is still the same; however, cantilever beam poses a new challenge. In Chapter 4, the system included five modes, and the highest natural frequency is 871 rad/sec. With this value, the simulation of MPC is computationally expensive. To avoid this issue with having a more realistic case study, the dynamic system in this case study includes only two modes, where the highest natural frequency is 96 rad/sec. The sampling time is therefore 0.0218 seconds as a result of three times the natural frequency. In addition, two separate sets of dynamic data were obtained; as a result, the GP model was intended to be used in the control system. The first set was collected by exciting the cantilever beam using a random input generator that lasted 7 seconds. The input magnitude ranged from -7 to 7 N, with a total of 350 training points. The validation data was obtained using the same method but over extended periods of time. The input signals were 9 seconds long, with 450 points for validation. The white noise with a variance of 0.5 and a mean of zero was applied to both the identification and validation sets of data. Figure (6.12) displays the cantilever beam responses and input signals for both data sets. Figure (6.13) shows that there is a linear relationship between data.

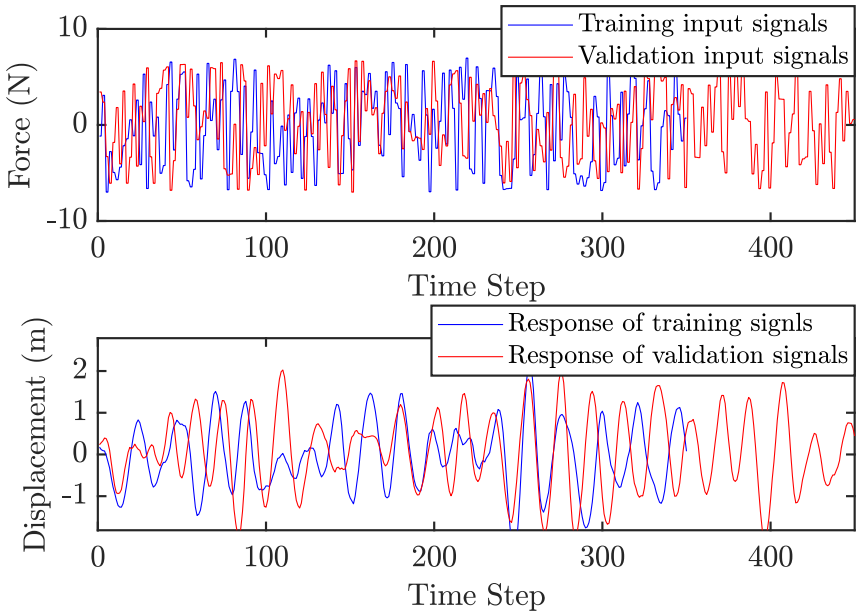

Figure 6.12: Comparison of training and validation input signals (top) and their corresponding displacement responses (bottom) over time.

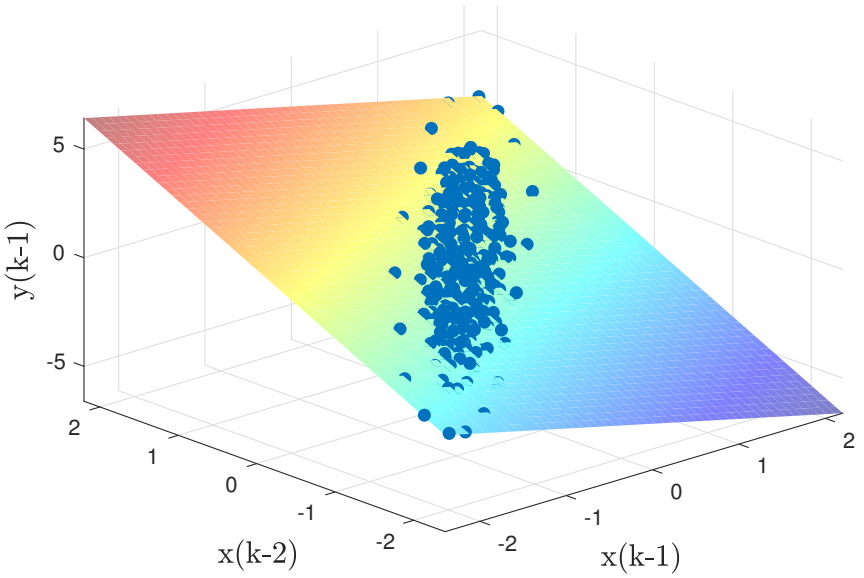

Figure 6.13: The 3D scatter plot shows the relationship between the input and target, illustrating that the data represents a linear system.

Model identification

Figure (6.14) presents the GP model predictions for several numbers of lags. Figure (6.14a) shows the model prediction of one lag where the performance indicates that one lag should be enough even though the variance is higher than the rest of the results. However, the result of one lag model has shown in previous cases study poor control performance. The GP model prediction is getting better when the number of lags increases, as shown in Figure (6.14d). Intuitively, the cantilever response will be dominated by its first mode of vibration, which would imply the use of a GP-NARX model with at least two lags. It is not clear, however, whether the GP is able to capture richer dynamics than just the first mode since it learns a nonlinear function of the lags rather than a linear one. In contrast, for an ARX model, there is a direct equivalence between the number of lags and the number of dynamic modes. The SE-ARD covariance function was also used, providing a specified scale for each lag. The selected set of hyperparameters of order 2 was $\theta = [0.0446, 0.0411, 0.0071, 0.0028, 180.806]$. These values suggest the GP model is strict in the dynamic system trained for; otherwise, this GP model can cause issues in the MPC controller by providing poor prediction. Figure (6.15) shows that the selected GP model was also suitable for validation data. Hence, the GP model is utilised as an offline and fixed within MPC.

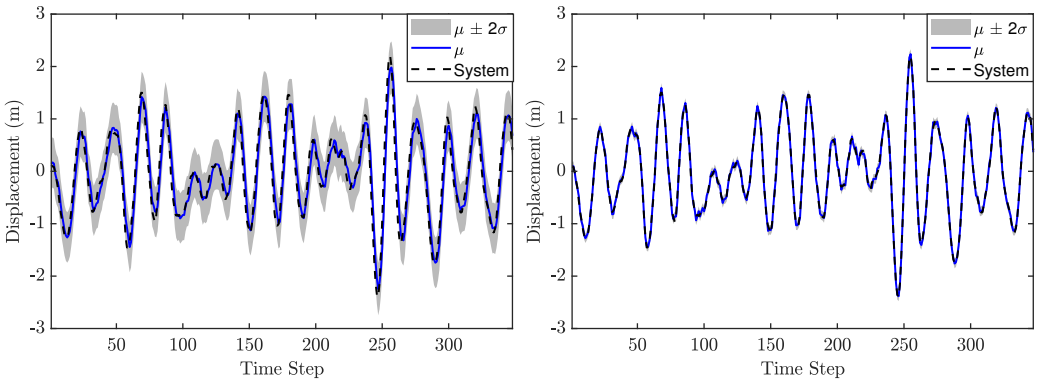

(a) GP Model Prediction with one lag. (b) GP Model Prediction with 2 lags.

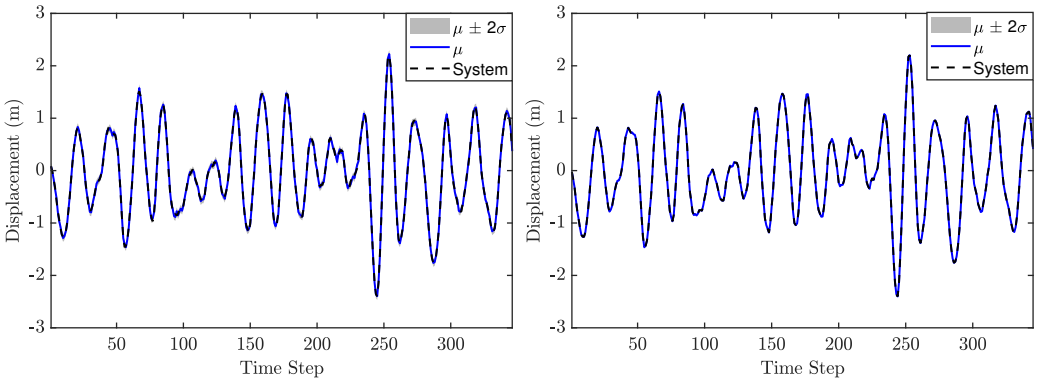

(c) GP Model Prediction with 3 lags. (d) GP Model Prediction with 4 lags.

Figure 6.14: GP model predictions for several numbers of lags, from one lag to four lags.

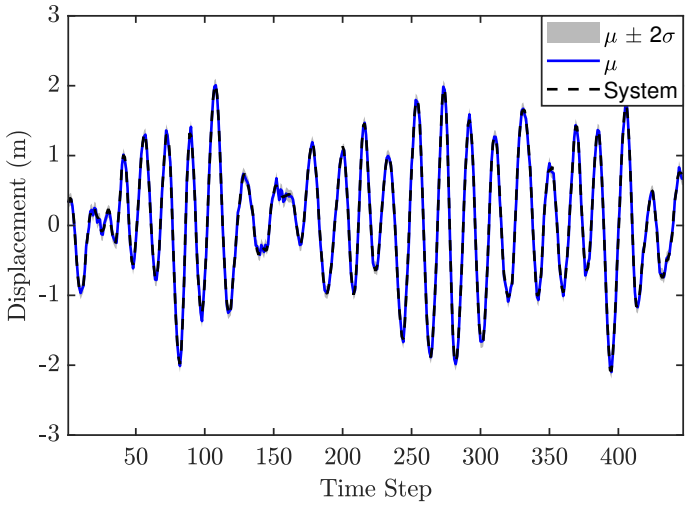

Figure 6.15: The GP validation model fits the system perfectly, as evidenced by the close alignment between the predicted and actual values.

Control performance

The last case study demonstrated GP-NOE within MPC provided a controlled response with 8 steps ahead. In MPC literature, the general rule is that a larger prediction horizon typically leads to better performances, although it makes the computation time longer. This might not be the case in GP-NMPC; however, this section presents the response of GP-NMPC with several numbers of predictions ahead. Before demonstrating the control performance of GP-NMPC applied to the cantilever beam, several control settings must be defined. First, Equation (6.16) sets T_s to be 0.01 second and T_{sim} is one second for the reference trajectory design. The cost function of Equation (6.14) used in this case. Figures (6.16) show the response of the cantilever beam with 5 steps ahead. Although the control system can track the step input, it is still slow. Figure (6.17) shows that the response 8 steps ahead is better. However, it is still too early to make this a general acceptance rule with GP-MPC because it requires additional stability and feasibility testing.

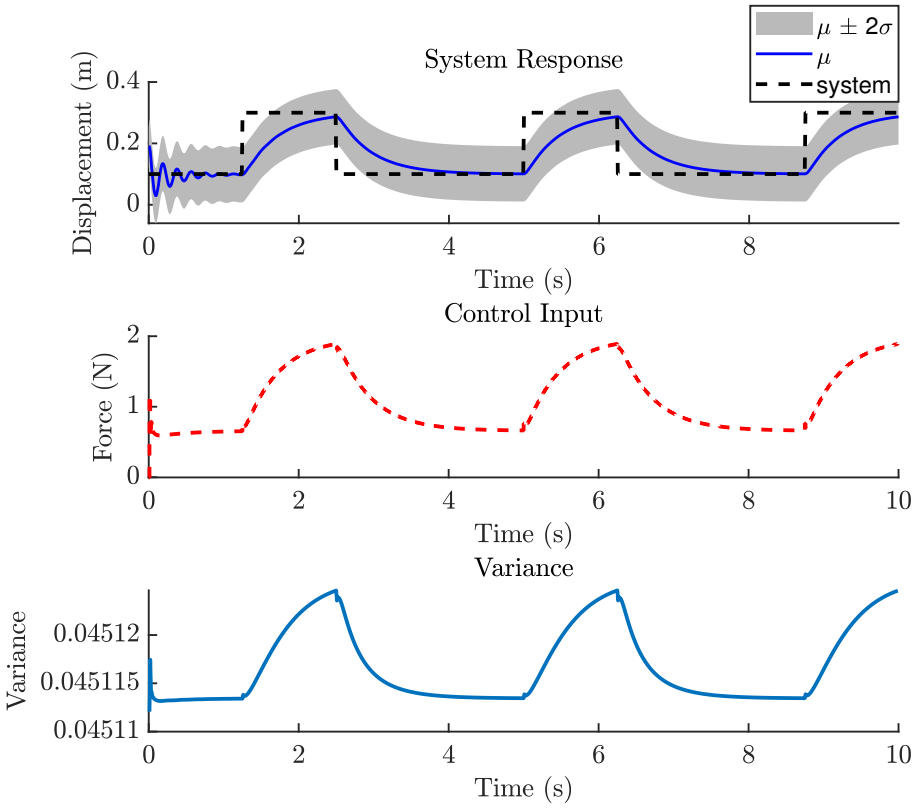

Figure 6.16: The top figure depicts the GP-NMPC response, with a highlight on the uncertainty region for five steps. The middle and bottom figures depict the required control inputs and variance to track the setting points.

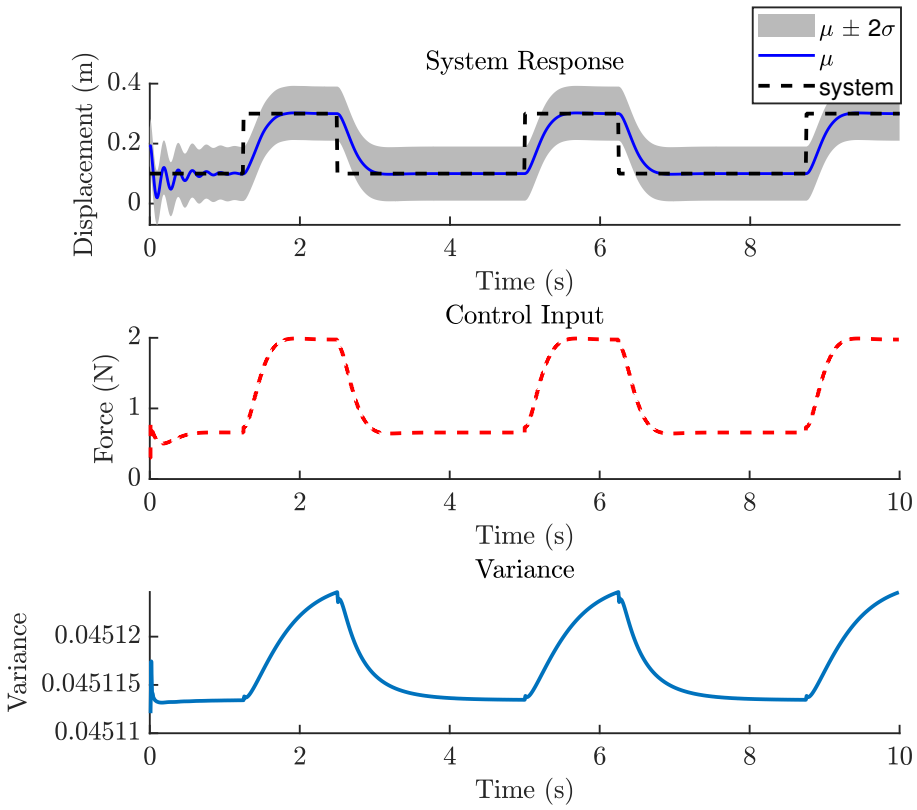

Figure 6.17: The top figure depicts the GP-NMPC response, with a highlight on the uncertainty region for the next eight steps. The middle and bottom figures depict the required control inputs and variance to track the setting points.

6.6 Discussion

The primary aim of this chapter was to answer whether DDC based on GP model for vibration control can be an alternative approach to the classical model methods, which is related to O2 of this thesis. In general, GP-NOE with NMPC can be a control method when the modelling of the system is complex or unknown.

For nonlinear system identification with GP, several important modelling points need to be considered. The sampling time is a critical factor as it affects not only the systems' discretisation but also the performance of the MPC controller. The selection of lags was obtained by model performance criteria. In SHM, the task of selecting lags becomes sometimes an optimisation problem, particularly when considering a higher number of lags. For control purposes, the optimisation tasks are not necessary since the real time control applications prefer reduced and sufficient

number of lags as a results of minimising the computational time. Lastly, there are several tuning parameters that can make the GP model performance better, such as the choices of covariance function, optimisation methods, and GP structures; however, the covariance function of SE-ARD with conjugate optimisation method and the structure of the GP-NOE model were suitable for discrete and continuous flexible systems.

The control design using GP faces several issues. The utmost burden is the computation cost. This issue can be overcome by adopting the predictive functional control concept. This MPC controller has shown its efficacy in both case studies, especially when the cost function includes the variance of GP prediction. The number of predictions is a critical factor, and it has been shown in linear cases that it is aligned with a general rule of increasing the number of steps to get better control performances. Finally, the unconstrained optimisation problem can provide sufficient control performance in terms of fast response, but more control realistic scenario of incorporating the trust region or uncertainty of prediction with MPC has to be constrained optimisation problem by the variance of GP-NOE model prediction.

6.7 Summary

This chapter presents a novel GP-NMPC controller that has been applied to the dynamics of flexible structures. The introduced model uses GP-NOE as an offline, fixed model within the NMPC controller. The GP predicts the output values and their uncertainty, allowing the control optimiser to avoid regions with high uncertainty. Numerical results demonstrate the effectiveness of this conceptual framework in both discrete and continuous flexible systems.

Three points can be used to summarise this work's value and contribution. It is, first and foremost, a first step towards defining some GP structure terms that are used in the structural dynamics and control systems fields by the GP community. Second, this framework uses the latest developments in data-driven modelling and control to achieve vibration control. Finally, this novel GP-NMPC model with a cantilever beam serving as a linear structural system has been presented in the XIVth International Conference on Recent Advances in Structural Dynamics (RASD2024), Southampton, UK. The next step with the GP-NMPC control system is to explore the efficacy of this method when the dynamics of the system are completely nonlin-

ear, as shown in the next chapter.

Chapter 7

Nonlinear model predictive control for nonlinear flexible structures: Gaussian process model

Highlights:

- A novel approach to controlling nonlinear structures using data-driven modelling and control methods is presented.
- The role of GP in nonlinear system identification and control design for dynamic systems is expanded to include Duffing oscillators.
- Designing GP-NARX within NMPC for nonlinear flexible systems presents additional challenges, particularly in determining the number of coincidence points in predictive control.

7.1 Towards GP-NMPC of nonlinear structural systems

In order to illustrate the efficacy of the GP-NMPC framework on a nonlinear system, data simulated from a Duffing oscillator system will be used. In the asymmetric case when a nonlinear stiffness is present, the relevant equation of motion is,

$$m\ddot{x} + c\dot{x} + kx + \beta x^3 = f(t) \tag{7.1}$$

Data were simulated here by integrating the equation of motion using a fourth-order fixed-step Runge–Kutta algorithm, as expressed in Appendix C. The parameters adopted were $m = 0.1\,\mathrm{kg}$, $c = 0.2\,\mathrm{N{\cdot}s{\cdot}m^{-1}}$, $k = 1\,\mathrm{N{\cdot}m^{-1}}$, and $\beta = 1 \times 10^3\,\mathrm{N{\cdot}m^{-3}}$. The time step used was $\Delta t = 0.001$ seconds corresponding to a sampling frequency of 1 kHz. The procedure for getting an adequate model is like that in Chapter 6, however it was difficult and time-consuming to reach a reliable GP model for control purposes.

7.2 Numerical results

To demonstrate the similarity and difficulty between linear and nonlinear cases, this section is divided into three subsections: obtaining data, model identification, and control performance.

7.2.1 Obtaining data

The training data were collected by exciting the Duffing oscillator by a random input and the force magnitude ranged from -20 to 20 N. The time span was from 0 to 10 seconds, which means the number of training points was 10,000. The validation data was obtained using the same method but over extended periods of time. The time span was from 0 to 13 seconds, which means the number of training points was 13000. To obtain a full experimental design, white noise with a variance of 0.005 and a mean of zero was applied to both the identification and validation data sets. Adding variance prevents the GP from becoming singular, ensuring better predictions and improved model performance. Figure (7.1) displays the Duffing

responses and input signals for both data sets. Figure (7.2) presents the 3D surface plot of the system responses, and it shows the training data presetting the nonlinear system. There is, however, a note that needs to be mentioned. The number of training and validation points is relatively high, which causes the identification and later control simulations to run slowly as a result of inverting the covariance matrix. This requires another design step, which is how to choose the training data that will represent the model.

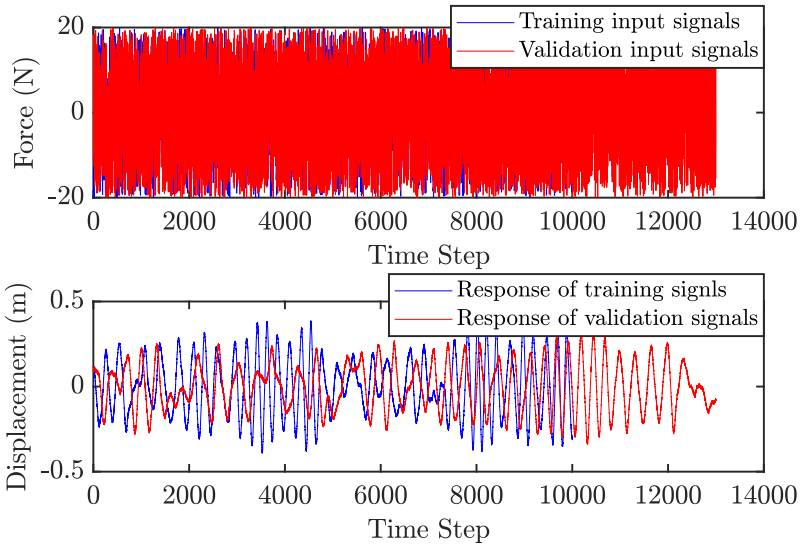

Figure 7.1: Comparison of training and validation input signals (top) and their corresponding displacement responses (bottom) over time.

7.2.2 Model identification

Before determining the system order, as in the linear case study, the model identification here requires starting by building a Hankel matrix. The Hankel matrix is a particular matrix structure formed by a system's input-output data, with identical elements along each ascending diagonal. This structure makes it possible to identify the system model based on observed data by using matrix factorization techniques to extract information about the system's internal state, such as its order. The number of training and validation points will be affected by the number of lags and the size of the sampling steps in the data. For example, when we say the order of the system is 2 and the sample size is 25 in the training and validation data, the number of training points was 350 and 450 for validation, as shown in Figures (7.3) and (7.4). Having said that, the rest of the procedures is similar to previous cases.

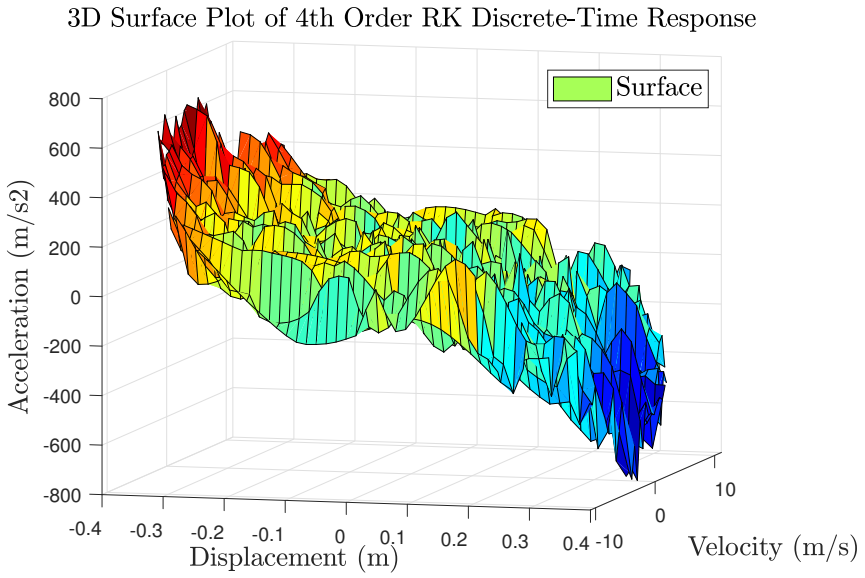

Figure 7.2: Visualization of the space between the input and target data. The 3D scatter plot shows the relationship between the input and target, illustrating that the data represents a nonlinear system.

The SE-ARD covariance function was then used, providing a specified scale for each lag. Conjugate gradient was chosen as the optimisation approach for this problem due to its convergence properties [14]. The hyperparameters were then trained using the maximum likelihood method. The selected set of hyperparameters is presented in Table (7.1).

Based on model performance criteria on Table (7.1), it can be said that the system order can be either two or three. The MSLL values in both orders are negative, indicating that both are possible choices; however, these values are nearly identical. SMSE reached the same conclusion regarding both orders. In that case, two lags or the system order two may be appropriate in terms of avoiding overfitting problems and providing a faster prediction in real time for control applications. Figure (7.4) depicts the GP model prediction based the validation data sets and it can be seen that the GP model prediction based on two or three lags are good.

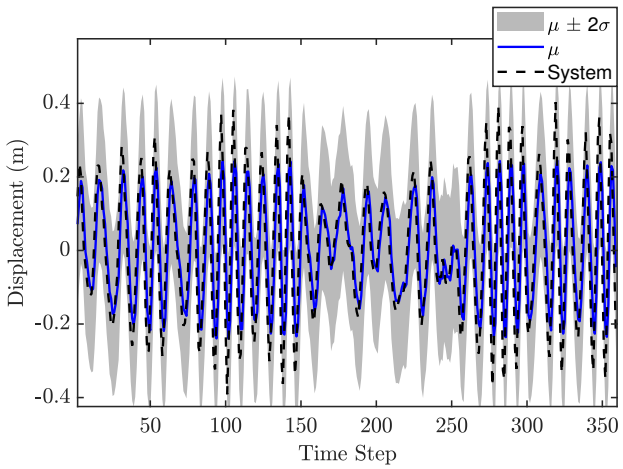

(a) GP Model Prediction based on training dataset with one lag.

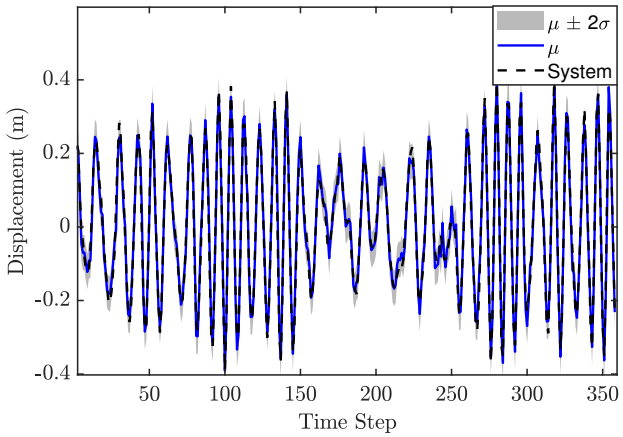

(b) GP Model Prediction based on training dataset with 2 lags.

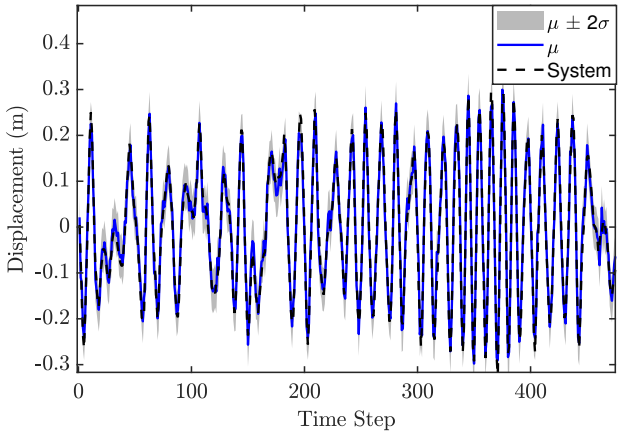

(c) GP Model Prediction based on training dataset with 3 lags.

Figure 7.3: The plot shows the trained GP model of the displacement over time as predicted by the GP model (solid blue line) compared to the actual system (dashed black line). GP model predictions for several numbers of lags, from one lag to three lags.

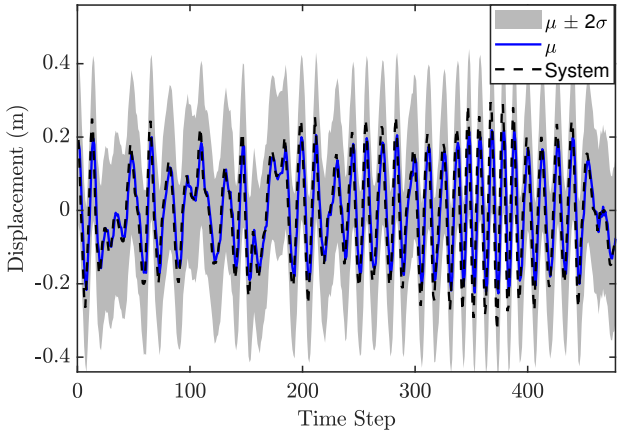

(a) GP Model Prediction based on validation dataset with one lag.

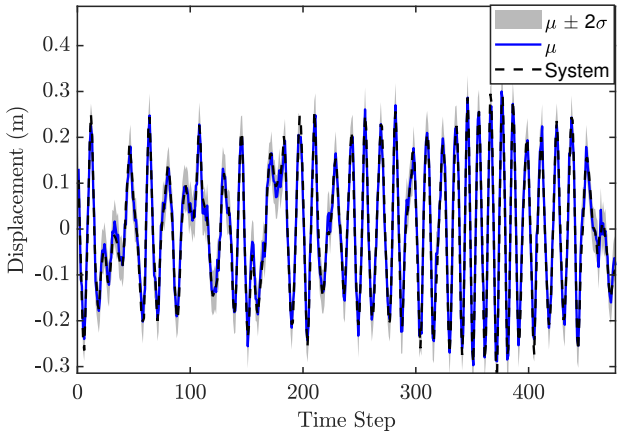

(b) GP Model Prediction based on validation dataset with 2 lags.

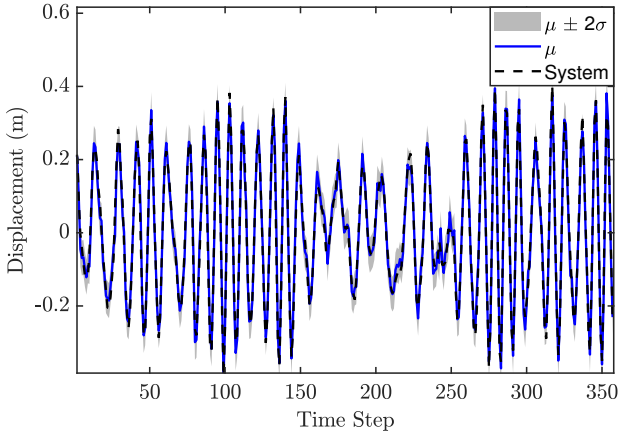

(c) GP Model Prediction based on validation dataset with 3 lags.

Figure 7.4: The plot shows the validation GP model of the displacement over time as predicted by the GP model (solid blue line) compared to the actual system (dashed black line).

Table 7.1: Model identification and validation results with hyperparameters and noise levels.

Model Order	**Ident. Data**		**Validation**		**Hyperparameters**							**Noise**
	SMSE	**MSLL**	**SMSE**	**MSLL**	**ly3**	**ly2**	**ly1**	**lu3**	**lu2**	**lu1**	$\sigma_{\mathbf{f}}$	$\sigma_{\mathbf{n}}$
3	0.0160	-2.06	0.021	-1.9	1.506	1.067	0.504	0.00093	0.0379	0.0009	0.517	0.005
2	0.01631	-2.054	0.021	-1.89	x	0.651	1.127	x	0.0013	0.0390	0.4727	0.005
1	0.37	-0.4921	0.229	-0.5466	x	x	1.521	x	x	0.0553	0.216	0.005

7.2.3 Control performance

The MPC's control design is still based on PFC, with a cost function similar to Equation (6.14). Equation (6.16) specifies a T_s of 0.016 seconds for the reference trajectory. It has previously been demonstrated that the number of predictions in the GP model is important, and that having more predictions leads to better performance; however, this is not always the case, especially when the GP model is not perfect. Figure (7.5) illustrates the closed loop performance of the Duffing oscillator based on one prediction ahead, which is similar to GP-NARX in structural dynamics. That means the model was not able to capture the dynamic and requires dynamic simulation based on multiple steps ahead. In addition, the closed loop responses of unconstrained control in tracking tasks for five and ten steps ahead are given in Figures (7.6) and (7.7). The GP model was able to predict the dynamics of the tracking trajectory in which it leads the NMPC optimiser to provide the best control action. Furthermore, the control force in Figure (7.7) indicates that there are ringing issues. The cause of this issue is either poor performance of the GP model prediction as shown in Figure (7.8a) or insufficient discretization in the MPC controller.

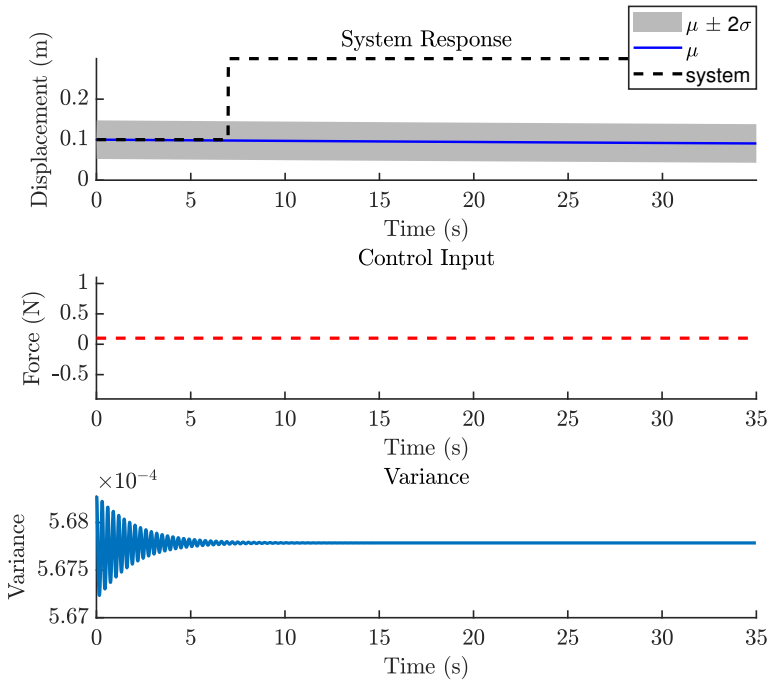

Figure 7.5: The upper figure depicts the GP-NMPC response, with a highlight on the uncertainty region for five steps. The middle and lower figures depict the required control inputs and variance to track the setting points.

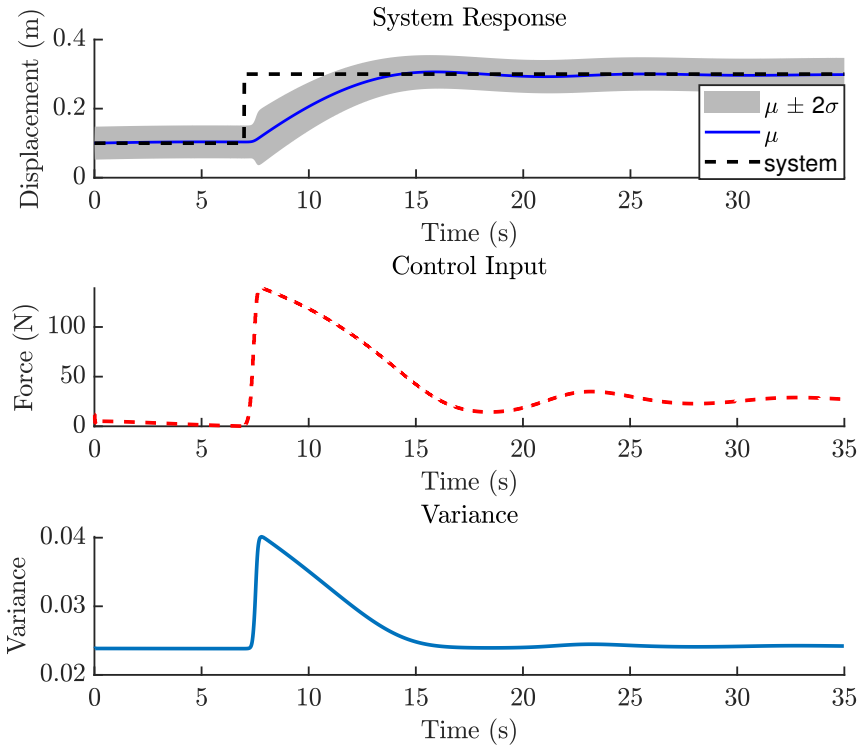

Figure 7.6: The control performance of MPC controller based on 5 steps ahead.

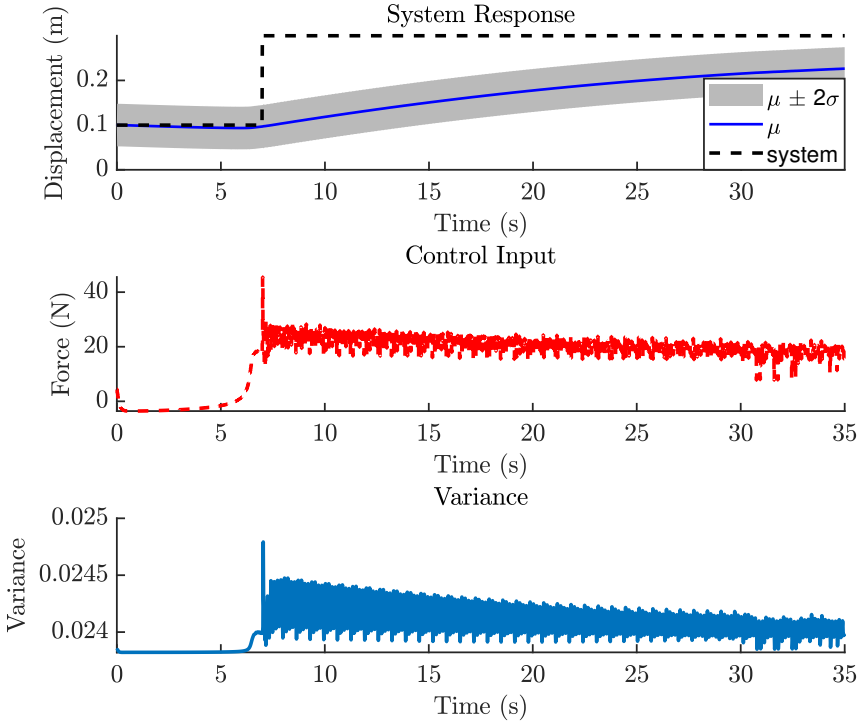

Figure 7.7: The control performance of MPC controller based on 10 steps ahead.

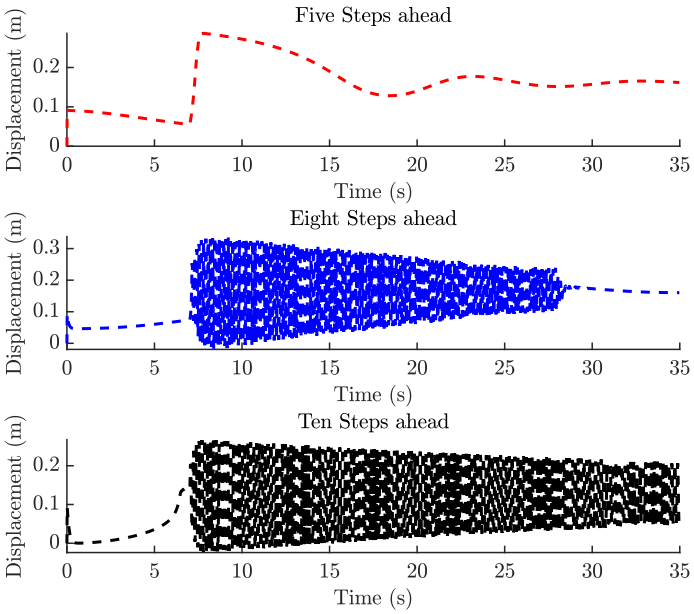

(a)

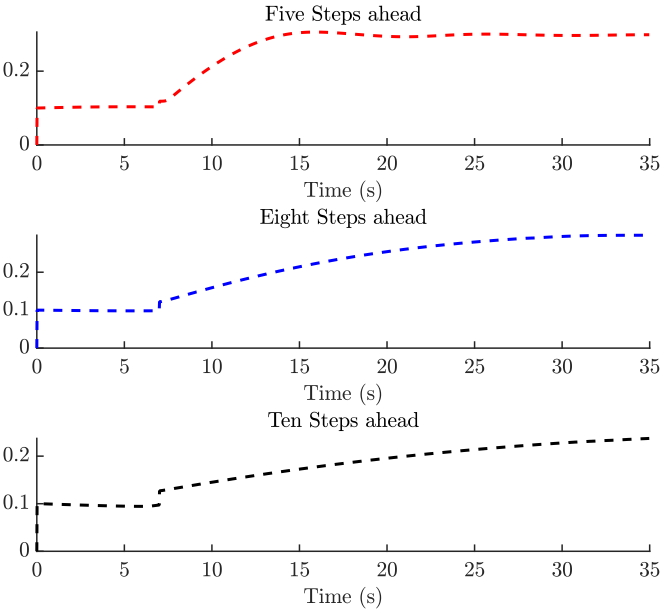

(b)

Figure 7.8: (a) Illustrating the GP model predictions for different steps. (b) Illustrating the reference trajectory of several steps ahead in which larger number of prediction might lead to slow response.

7.3 Discussion

The main objective of this chapter was not only to demonstrate the feasibility and effectiveness of GP-NOE within NMPC in nonlinear systems, but also to propose alternative vibration control methods, which are related to O2 in the thesis. The main discussion points have been elaborated in Chapter 6; however, some additional points in modelling and control need to be pointed out.

Although the model was designed for control, the system's nonlinearity required the collection of a large amount of data. Building a Hankel matrix was required at this stage, which is not always the case, especially in linear cases. Furthermore, the assessment of lag selection was not informative in this nonlinear case, but it did show that both models were suitable for MPC controllers. In terms of control design, the MPC algorithms and cost function were still appropriate for this nonlinear system, but the number of predictions for the GP-NOE was not as simple as in linear cases.

7.4 Summary

This chapter demonstrated the effectiveness of the GP-NMPC controller's novelty when applied to nonlinear system dynamics. The introduced framework incorporates GP-NOE as an offline, fixed model into the NMPC controller. The GP predicts the output values and their uncertainty, allowing the control optimiser to avoid regions of high uncertainty. The numerical results show that this novel framework works in both linear and nonlinear systems. The outcomes of this chapter and the linear oscillator of Chapter 6 have been published in the 31st International Conference on Noise and Vibration Engineering (ISMA2024), Leuven, Belgium. The primary results of the Duffing oscillator case study were presented as a poster in the 8th IEEE Conference on Control Technology and Applications (CCTA2024), Newcastle, UK. With these valuable results, the Bayesian approach in terms of modelling has proven its effectiveness in active vibration control. Consequently, designing an active vibration control system based on Bayesian filtering will be proposed in the next chapter.

Chapter 8

Feedback control of flexible structure with Bayesian filtering

Highlights:

- Bayesian filtering in a spillover problem is introduced.
- Optimal control with robust issues are presented and discussed.
- Identifying the system poles with machine learning algorithms, to avoid the spillover problem, is explored and presented
- A better control performance is shown with suggestion to adopt different algorithms.

8.1 Overview

Until now, the majority of the novel presented methods used Bayesian principles in modelling. The objective of this chapter is to address the identification of flexible structural dynamics subject to uncertainty by using Bayesian state space models,

with the intention of developing a vibration control system. This requires incorporating the identified uncertainty of the structure into the control strategy. The proposed method comprises a combination of two Bayesian identification techniques, Gaussian filters, namely the Kalman Filter (KF) and Expectation-Maximization (EM) algorithms, with a linear optimal controller (LQR). The key contribution of this work is to demonstrate how the methodology of Bayesian state estimation and LQR control algorithms might work in cases when there is spillover instability from unmodelled modes in the system. In what follows, Section 8.2 describes the problem mathematically and then restates the research questions that are addressed in the remainder of the chapter. Control tactics are then introduced, emphasizing the differences between designing a LQG controller based on separate principles, and the synthesis of control and observer gains. Section 8.4 introduces the stochastic state space models in either Bayesian recursive estimation or EM algorithms. Finally, a simply-supported beam is presented and discussed as an application along with its results.

8.2 Problem description

In structural dynamics, flexible structures are described as distributed parameter systems in which the systems are theoretically infinite dimensional. Those infinite dimensional must be captured to model the behaviour of the system. However, due to computer limitations and modelling errors, a reduced model is often used as a solution to that modelling issue, that is sufficiently accurate. From a control perspective, actively controlling flexible structures still needs to fundamentally control the large dimensional systems with a much smaller dimensional controller. To put it differently, the reduced model is based on selecting critical elastic modes that can capture the dynamics of the system. Those critical modes are chosen based on the system performance requirements, such as sensitivity, and mostly the first low-frequency modes of the system. Because of the inherent low damping of flexible structures, particularly in the space environment, there is a risk that state feedback based on a reduced model destabilizes residual modes that are not included in the structural model contained in the observer. This phenomenon is called spillover instability and Balas in [65] introduced this concept in 1978.

Bayesian frameworks have become an interesting research topic in structural dy-

namics, especially where quantifying the uncertainty is concerned. The early work concerning Bayesian active vibration control was done by Dertimanis et al. and Moradi et al. [72, 73], although they have not considered spillover problems in their cases. Various factors make Bayesian frameworks applicable in engineering applications [127]. First, they preserve information because they are based strictly on the probability axioms. Second, they provide the probability density function (PDF) of the model state conditional to the available data, which can then be applied to probability based system identification and control techniques. Bayesian system identification provides a wide range of algorithms that can be utilized in quantifying uncertainty, especially in the control of flexible structures. The expected maximum likelihood algorithm (EM algorithm) and Kalman filter are formulated based on Bayesian formalizations and are well known and heavily used in engineering. Recently, Bayesian recursive estimation has been proposed in structural health monitoring as a result of the estimation of latent force applied into the system, for example [178]. The possibilities of coupling advanced recursive Bayesian estimation with semi-active and active control have also been explored in [142, 143]. As a consequence, the remaining question is whether truncated and parameter errors will be captured and managed in an active vibration control framework by using these Bayesian techniques.

Mathematically, this unmeasurable influence is referred to as disturbance or noise. As a result, Equations (4.23) and (4.24) are used and repeated here for convenience:

$$\mathbf{x_s}(k+1) = A_d\mathbf{x_s}(k) + B_d\mathbf{u}(\mathbf{k}) + w_n(k) \tag{8.1}$$

$$y(k) = C_d\mathbf{x_s}(k) + D_d\mathbf{u}(\mathbf{k}) + v_n(k) \tag{8.2}$$

where $w_n(k)$ is the process noise due to disturbance or modelling inaccuracies; $v_n(k)$ is the measurement noise caused by sensor inaccuracy. The assumption here is that they are both independent and identically distributed as shown here:

$$w_n \sim N(0, Q_n) \qquad v_n \sim N(0, R_n) \tag{8.3}$$

where Q_n and R_n are the covariances of the process and measurement noises, respectively. Since this work is addressing the spillover issue, the complex model that has a close fidelity to the actual system is represented as $\begin{bmatrix}\dot{x}_c & \dot{x}_r\end{bmatrix}^T$. Here, the subscript c refers to the controlled modes, whereas r refers to residual modes, which

are ignored in the control design. With these extra subscripts, subscripts s and d are dropped from Equations (8.1) and (8.2).

$$\begin{bmatrix} \dot{x}_c \\ \dot{x}_r \end{bmatrix} = \begin{bmatrix} A_c & 0 \\ 0 & A_r \end{bmatrix} \begin{bmatrix} x_c \\ x_r \end{bmatrix} + \begin{bmatrix} B_c \\ B_r \end{bmatrix} u + \begin{bmatrix} w_c \\ w_r \end{bmatrix} \tag{8.4}$$

$$y = \begin{bmatrix} C_c & C_r \end{bmatrix} \begin{bmatrix} x_c \\ x_r \end{bmatrix} + \begin{bmatrix} v_c \\ v_r \end{bmatrix} \tag{8.5}$$

The strategy here is that the interaction between the control system and the residual mode can be expressed and analysed as $\begin{bmatrix} \dot{x}_c & \dot{e}_c & \dot{x}_r \end{bmatrix}^T$ where the state variable with error is defined as $e = x_c - \hat{x}_c$ and expressed in Equation (8.6). Also G_c and K_c are gains of the controller and observer, respectively. As a result of either observation spillover $K_c C_r$ or control spillover $B_r G_c$, the eigenvalues of the system move away when they are non-zero. These coupling terms determine how much they move. The poles of residual dynamics are usually barely stable, particularly in lightly damped systems, and become unstable even when a small change occurs. Figure (8.1) depicts the block diagram of the spillover mechanism.

$$\begin{bmatrix} \dot{x}_c \\ \dot{e}_c \\ \dot{x}_r \end{bmatrix} = \begin{bmatrix} A_c - B_c G_c & B_c G_c & 0 \\ 0 & A_c - K_c C_c & -K_c C_r \\ B_r G_c & B_r G_c & A_r \end{bmatrix} \begin{bmatrix} x_c \\ e_c \\ x_r \end{bmatrix} \tag{8.6}$$

The remaining question is whether we can first construct a system based on controlled modes despite the fact that the system experienced residual effects and the control method is based on coupling Bayesian filtering and optimal control. Therefore, the main questions addressed in this study are: (a) What is the primary difference between the formulation described above and Model Error Sensitivity Suppression (MESS)? (b) Would the control performance change when the system parameters are detected offline using the Expectation-Maximization (EM) algorithm?

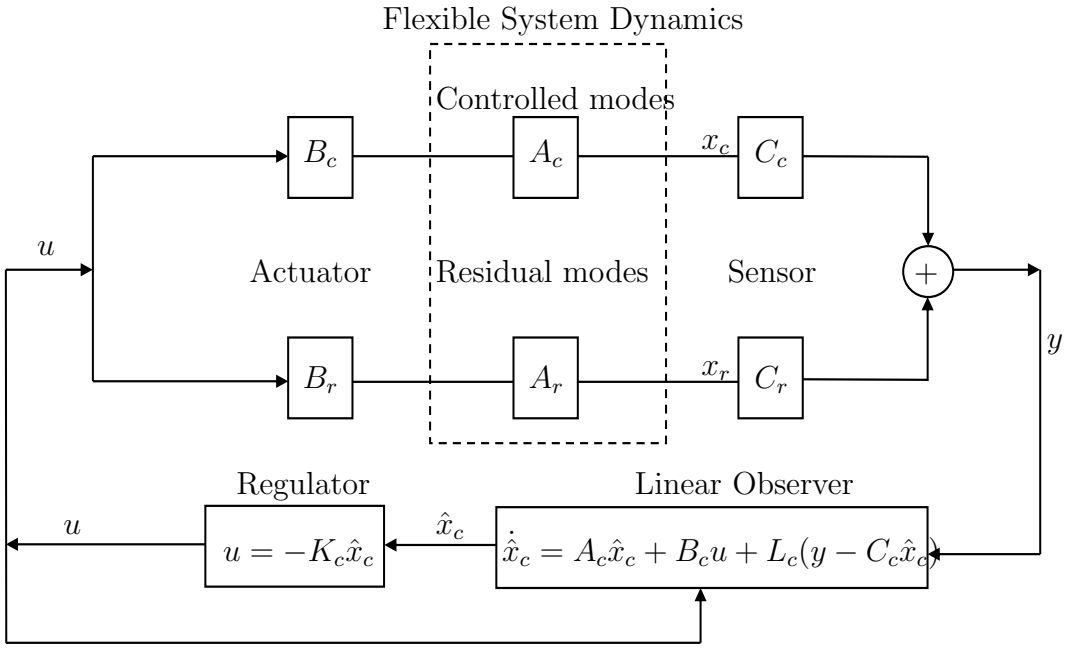

Figure 8.1: Spillover mechanism [3].

8.3 The control tactic

The key benefit of state feedback control is its capacity to synthesise a full state feedback in which controller gains are chosen to satisfy desired closed loop system characteristics. Due to two factors, the LQG controller is an appropriate optimal control strategy for this investigation since it addresses uncertainty. First, LQG is designed to take into account process and measurement noises, with the presumption that they are additive white noise. Second, it is possible to build the linear observer, often the KF, independently of the optimal controller. This approach is known as the separation principle. However, the LQG can also be built so that the regulator gain is produced by synthesising the controller and observer poles jointly. Figure (8.2) depicts the general block diagram of the LQG. The significant component of optimal control is the effectiveness of weighted matrices to restrict the influence of the system's states and inputs. This section includes a brief overview of optimal control for the sake of completeness and the interested reader is referred to [3, 16].

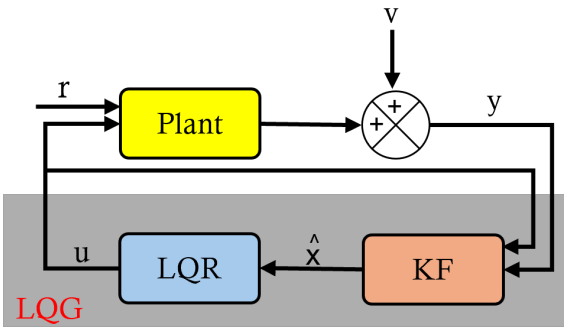

Figure 8.2: The general block diagram of LQG methods based on the separation principle and gain synthesis for controller and observer.

8.3.1 Linear Quadratic Regulator

One of the most popular control methods is the linear quadratic regulator (LQR). This is the most basic and widely used formulation; it can be modified to account for time-varying systems and cost functionals with finite horizons. Assuming that the pair (A, B) in Equation (8.1) is controllable in the scenario where the system matrix A is not necessarily stable, we are looking for a constant gain of linear state feedback,

$$u = -Gx \tag{8.7}$$

such that the following quadratic cost functional is minimized

$$J = \sum_{n=0}^{\infty} (x^T Q x + u^T R u) \tag{8.8}$$

which requires Q and R to be semi positive definite and strictly positive definite, respectively . Because R is strictly positive definite, it indicates that any control has a cost, whereas the positive definiteness of Q implies that some of the states may be irrelevant to the task at hand. The performance index has two contributions; the first one reflects the desire of bringing the controlled variable to zero (minimizing the error) while the second one that of keeping the control input as small as possible. In addition, states here are assumed to be available which it is not true. Coupling an observer with the LQR leads to a control design called the LQG based on separation

principle. It can be shown that the solution of this optimization problem is

$$G = R^{-1}B^T P \tag{8.9}$$

where P is the symmetric positive definite solution of the algebraic Riccati equation

$$PA + A^T P + Q - PBR^{-1}B^T P = 0 \tag{8.10}$$

The Riccati equation is nonlinear in P; if (A, B) is a controllable pair (stabilizable is actually sufficient), and (A, Q) is observable, then the existence and uniqueness of the solution are guaranteed. Once these conditions exist, the closed-loop system

$$x[k+1] = (A - BG)x[k] \tag{8.11}$$

is asymptotically stable.

8.4 State and parameter estimation for stochastic dynamic systems

8.4.1 Bayesian state estimation

State feedback implicitly assumes that full knowledge of the state variables is available for feedback. This assumption cannot be held in practice, however, either because of the failure of a direct connection to the state variable or because sensor devices are not available or too costly [117]. In either case, designing an estimator is necessary. Recursive Bayesian estimating is the most general form of state estimation in which it is the task of estimating the probability density function (PDF) for the state of a process that is not directly observable. In general, recursive Bayesian estimation works by modelling the process and updating it to account for new measurements acquired from the real process. The computations are performed recursively in two steps. First, the next state is projected by extending the current state over the next time step using the nonlinear transition function of state propagation belief. Second, taking new measurements into account, this prediction is modified using the measurement likelihood given by the nonlinear measurement

equation. However, this works with certain assumptions [119]. First, the states follow a first order Markov process. Second, the measurements are conditionally independent given the states. Also, the basis of the update stage is given by the Bayesian rule. Mathematically, the first and third assumptions are described as follows:

$$p(x_k|y_{k-1}) = \int p(x_k|x_{k-1})p(x_{k-1}|y_{k-1})dx_{k-1} \tag{8.12}$$

$$p(x_k|y_k) = \frac{p(y_k|x_k)}{p(y_k|y_{k-1})}p(x_k|y_{k-1}) \tag{8.13}$$

Unfortunately, these equations cannot be solved analytically in practice as it requires a multidimensional integral, which becomes intractable as the size of the state space grows. The Kalman filter is then the closed form solution to the Bayesian filtering equations for the filtering model, where the dynamic and measurement models are linear and Gaussian as in Equations (8.1) and (8.2). It is an optimal recursive Bayesian filter restricted to the class of linear Gaussian estimation problems. The KF requires a dynamic model of the system, known control inputs, and measurements containing white noise. Under these strict assumptions, it provides optimal state estimates by recursively predicting the states, estimating the uncertainty of the predicted states, computing a weighted average of the predicted and measured values, and refining the predicted states. In probabilistic terms the state space model becomes:

$$p(x_k|x_{k-1}) = \mathcal{N}(x_k|A_{k-1}x_{k-1}, Q_{k-1}) \tag{8.14}$$

$$p(y_k|x_k) = \mathcal{N}(y_k|C_k x_k, R_k) \tag{8.15}$$

The process of estimating the state of the system by using the KF with the above equations can be summarized as:

- The prediction step is:

$$\begin{aligned} \bar{\mathbf{m}}_k &= \mathbf{A}_{k-1}\mathbf{m}_{k-1}, \\ \bar{\mathbf{P}}_k &= \mathbf{A}_{k-1}\mathbf{P}_{k-1}\mathbf{A}_{k-1}^\top + \mathbf{Q}_{k-1}. \end{aligned} \tag{8.16}$$

  Where $\bar{\mathbf{m}}_k$ and $\bar{\mathbf{P}}_k$ are the mean and covariance.

- The update step is:

$$\begin{aligned}
\mathbf{v}_k &= \mathbf{y}_k - \mathbf{H}_k \bar{\mathbf{m}}_k, \\
\mathbf{S}_k &= \mathbf{H}_k \bar{\mathbf{P}}_k \mathbf{H}_k^\top + \mathbf{R}_k, \\
\mathbf{K}_k &= \bar{\mathbf{P}}_k \mathbf{H}_k^\top \mathbf{S}_k^{-1}, \\
\mathbf{m}_k &= \bar{\mathbf{m}}_k + \mathbf{K}_k \mathbf{v}_k, \\
\mathbf{P}_k &= \bar{\mathbf{P}}_k - \mathbf{K}_k \mathbf{S}_k \mathbf{K}_k^\top.
\end{aligned} \tag{8.17}$$

Where the innovation $\mathbf{v}_k$ captures the new information in $\mathbf{y}_k$, $\mathbf{S}_k$ is the predicted covariance of $\mathbf{y}_k$, and the Kalman gain $\mathbf{K}_k$ determines how much we should trust the new information. The recursion is started from the prior mean $\mathbf{m}_0$ and covariance $\mathbf{P}_0$. For more background on the Bayesian filter, the basics of the idea are covered in these resources [119, 130, 185].

8.4.2 EM algorithm for maximum likelihood estimation

The expectation maximum (EM) algorithm is used to find the maximum likelihood of the parameters iteratively when direct optimization of the posterior distribution is not possible [130]. There are numerous numerical search techniques available for maximising the log likelihood, but Shumway and Stoffer in [186] demonstrate a conceptually simpler estimating approach based on the Expectation Maximization algorithm. The interested reader can have a comprehensive background to this algorithm in these resources [187–189]. Conceptually, the EM algorithm finds a set of parameters which maximises the total expected log likelihood by iteratively estimating the latent states in the model (the "expectation" step) and updating the parameters of the model to best fit these expected latent states (the "maximisation" step). One advantage of this approach is that it is guaranteed to improve, at every step, the expected total log likelihood of the model, such that it is guaranteed to converge to a (local) maximum likelihood solution.

8.5 Identifying noise dynamics

It is frequently necessary in control design and estimation or prediction to identify not just the dynamics from input to output signals, but also the noise dynamics; how noise and disturbance disrupt the system; where noise enters; and if the noise is

colored and associated. Various strategies for recognising both input-output dynamics and noise dynamics are available in system identification. The Equations (8.1) and (8.2) contain both process and measurement noise. Process noise is classified into two types. First, the noise is caused by discrepancies between the expected and present states, and the source of this problem is an inaccurate transition matrix A. Making the covariance matrix Q big enough to cause the system to self-correct might be the answer to this problem. Second, process noises may be considered as random disturbances in a dynamic system. When two problems are combined, the situation becomes challenging. In this case, the dynamic of the process was utilised to replicate the white noises. This approach is termed differential equations with driving white noise and has a broad review in [130]. The continuous time noise process can be inferred over the model by the following:

$$Q = \int_0^{\triangle t} \Phi(\triangle t - \tau) L q L^T \Phi(\triangle t - \tau) d\tau \tag{8.18}$$

where, $\Phi(\tau) = e^{F(\Delta t - \tau)}$. Once discretised, the filtering and smoothing distributions for a time point t in a data record and the T time points may now be recovered using the Kalman filtering equations and the Rauch-Tung-Striebel (RTS) smoother.

8.6 Numerical application

In order to explore the efficacy of both proposed methods, the case study of Balas' work in [65] is now extended to cover advanced algorithms of optimal control and Bayesian recursive estimation. Despite being a fairly basic problem in terms of active vibration control, it is particularly illustrative of the idea of spillover instability, which frequently occurs when the high frequency dynamics of a structure are neglected. This issue consists of a uniformly and simply supported beam with a point force actuator at $x = l/6$ and a displacement sensor at $x = 5l/6$. The only difference from the properties in Balas' work is that there is damping in the system and it is set to 1 %. The general idea of this simulation is that while two extra residual modes are taken into consideration, the active controller only controls the lowest three natural frequencies of the beam. Then, the beam will be excited through process noise as described in Equation (8.18). This gives unit amplitude to the plant which contains controlled and uncontrolled modes. Finally, the form of the dynamic parameters of

the plant before discretization is displayed below:

$$A = \begin{bmatrix} O & I \\ -{\omega_i}^2 & -2\omega_i\xi_i \end{bmatrix} \quad B = \begin{bmatrix} 0 \\ B_i \end{bmatrix} \quad C = \begin{bmatrix} C_i & 0 \end{bmatrix} \tag{8.19}$$

where,

$$\begin{aligned} \omega_n &= [9.8696, 39.4784, 88.8264, 157.9137, 246.7401] \qquad \text{rad/sec} \\ B &= [0, 0, 0, 0, 0, 0.9724, 1.6995, 1.9977, 1.7920, 1.1341]^T \\ C &= [0.5137, -0.8815, 0.9989, -0.8326, 0.4298, 0, 0, 0, 0, 0] \end{aligned} \tag{8.20}$$

This section has provided the general description of the main simulation of both proposed methods. After this point, any extra steps of the simulation will be described in subsequent sections. The first case study is what the structural control community is familiar with which is the standard LQG approach; after that identifying the parameters offline approach will be discussed second.

8.6.1 The standard LQG approach

As previously stated, the LQR design is completely independent of the KF. To begin, Figure (8.3) illustrates a plant's pole placement, and it is obvious that the system is marginally stable. The difficulty with this type of system is that it is not advisable to design an aggressive controller, which is another source of spillover, as shown by the blue response in Figure (8.4). The concept here is that, even if the system is not decoupled into controlled and suppressed modes as MESS techniques do, the weight matrices of the optimal control still restrict the states of the system by employing just one actuator and one sensor. The question remains as to which states should be restricted. The approach utilised in this study restricts the first mode because it contains most of the system's energy. Second, the system's uncertainty, as emphasised by Bayesian KF, provides an overview of what may go wrong in each predicted state. The mean squared error (MSE) is used to evaluate uncertainty. Figure (8.5) and (8.6) depict the estimation of three modes' displacements and velocities, with the MSE indicating that the error increases as the dynamic of the actuator involved in the loop increases.

The key result of this suggested strategy is that the beam response was suppressed by

weighted matrices, as demonstrated in Figure (8.4) by the orange response. That response was obtained with avoiding certain system constraints, such as the prescribed degree of stability and low pass filter. Table (8.1) displays the values of the Q and R matrices in optimal control, as well as the observer and controller gains.

Table 8.1: The optimal control properties of each proposed method.

	The standard LQG control parameters
Q	diag [0.001, 1 , 1 , 100, 100, 100]
R	10
Control gain	$G_{con.}$ = [-1.7531, -5.4278, -26.2253, 2.8662, 2.2862, 2.2862]
	The LQG Regulator
Q	diag [0.001, 0.001,0.001,100,100,100]
R	10000
Control gain	$G_{regulator}$ = [0.2148, 0.1410, -0.0485, 0.0659, 0.0153, 0.0118]
KF gain	$L_{regulator}$ = $[0.0104, 0.0014, 0.0122, -0.0035, 0.0239, 1.1606]^T$

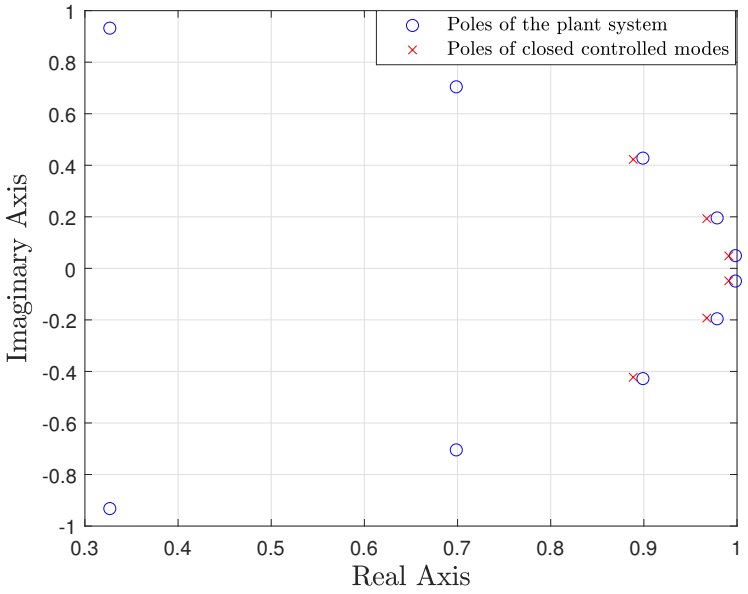

Figure 8.3: Locations of the poles in the open-loop and closed loop systems.

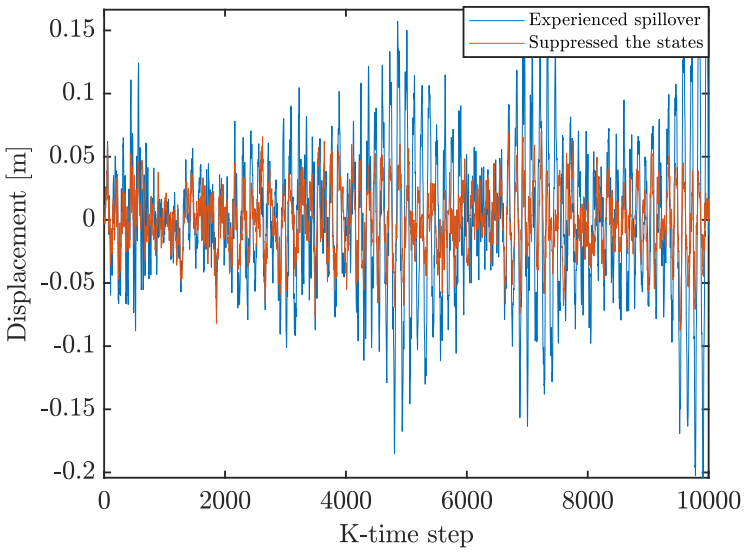

Figure 8.4: Response of the simply-supported beam driven by LQG regulator.

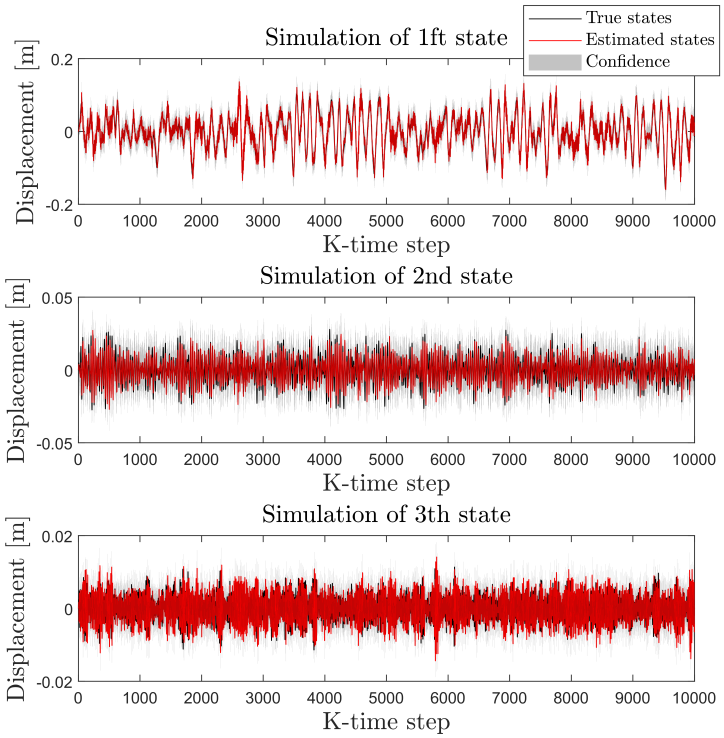

Figure 8.5: Estimated displacement of three modes combined with true states. The figure shows that the estimation of the first state was more accurate, along with higher confidence in the estimation. Other displacement states were disturbed by white noise, making it difficult to obtain a reliable estimation.

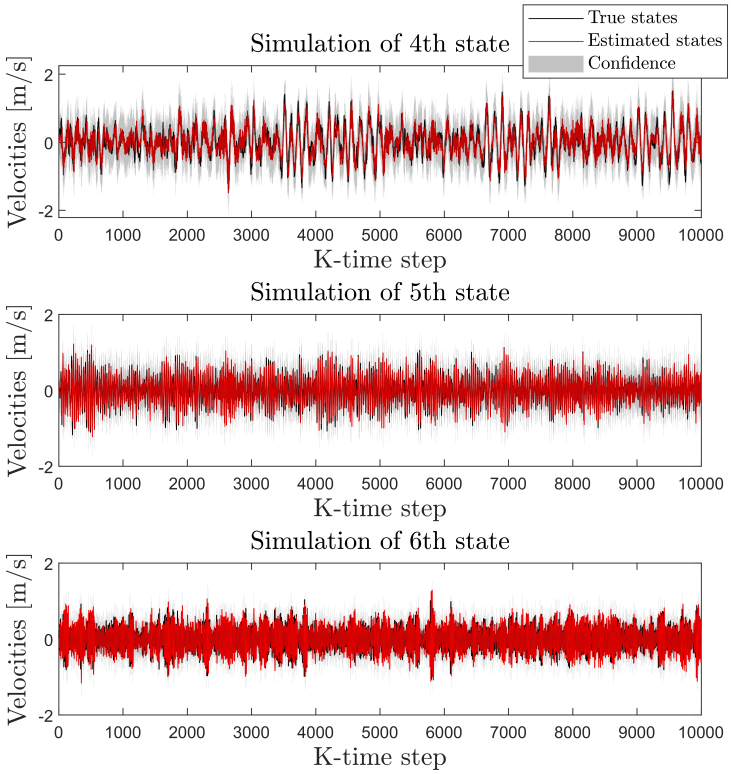

Figure 8.6: Estimated velocity of three modes combining with true states.

8.6.2 LQG regulator based on parameters estimated from EM algorithms

The main benefit of this technique is that it investigates the efficacy of controller and observer gain synthesis while providing a comprehensive overview of the dynamic characteristics of the beam, particularly the process noise. This method consists of two steps: generating data and constructing a LQG regulator. Mathworks Matlab was used to create the data based on the simulation from the previous stage. The data is subsequently given to the EM algorithm, which estimates the dynamic parameters. The parameters estimated in this work are $\theta = [A, C, Q_n, R_n, \mathbf{m}, \mathbf{P}]$. Some observations concerning EM should be mentioned before presenting the LQG regulator findings. First, the initial condition of these parameters has an influence, since these values force the algorithms to approach the lower bound's local minimum. This suggests that finding the best estimated parameters is an iterative process that requires prior assumptions and understanding of these values. Second, it is possible

that the EM algorithms provide infinity as values for these parameters, resulting in an invertible initial value for the A matrix. Third, as a validation method, the true values of the parameters were fed into EM algorithms as initial conditions, and the estimated parameters were almost identical owing to noise effects.

Now, Figure (8.7) depicts the poles of the estimated A matrix compared to the true poles of first three modes of the simply-supported beam. The initial conditions of these parameters θ were given based on understanding the dynamics of the beams. Figure (8.8) shows the response of the simply-supported beam and the pole locations of the open loop compared to the closed loop systems; also, the control parameters of this method is displayed in Table (8.1). Based on these observations, three comments need to be made. First, even though the estimated parameters gave acceptable and reasonable values, the estimated covariance matrix of the process noise is remarkably big. This causes the second point. The main feature of the LQG regulator is addressing the process and measurement noise while synthesising the gains of the controller and observer. That cannot be achieved in this case while considering this huge and colored process noise. It is also noticeable that the closed loop poles barely moved toward the stable region as shown in Figure (8.9). Finally, although the optimal controller failed to alter the dynamical behaviour of the beam, this proposed method gave a scientific way of addressing the closed and real dynamics of noises either in process or in measurements.

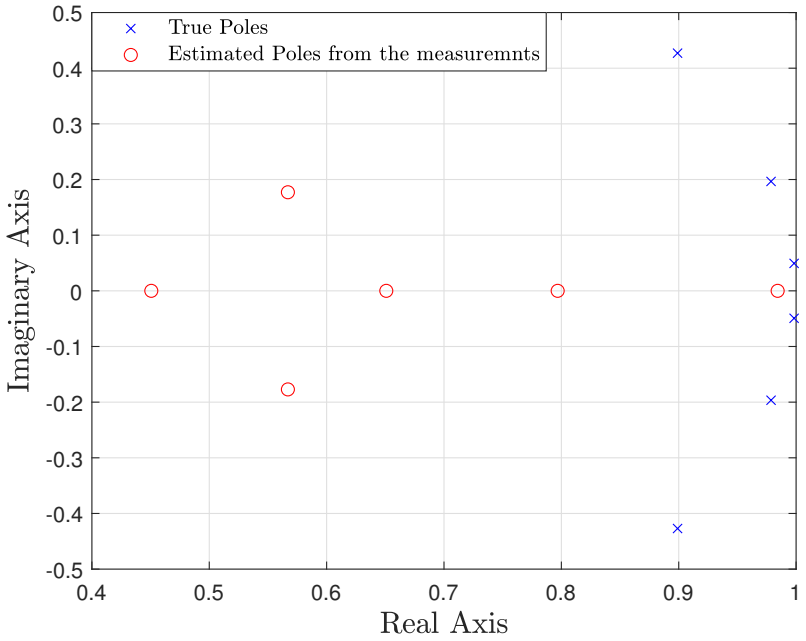

Figure 8.7: Poles of the true system based on first principles (blue crosses) and poles estimated on the basis of the expected maximum likelihood algorithm (red circles).

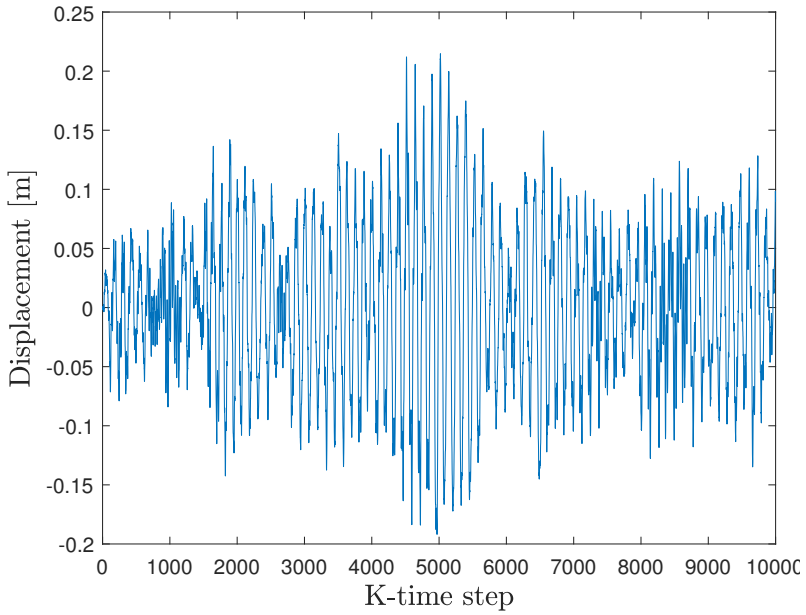

Figure 8.8: Response of the simply-supported beam driven by the LQG regulator.

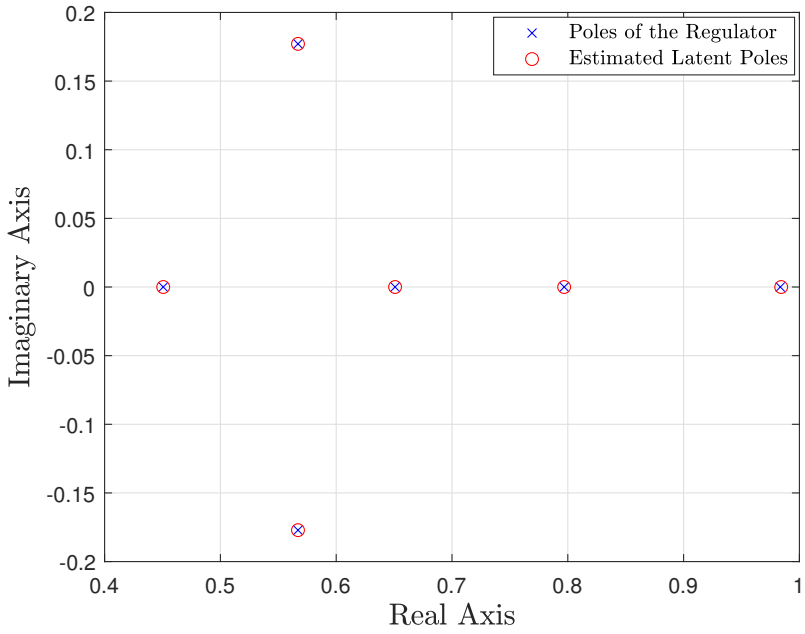

Figure 8.9: Locations of the poles in the open loop and closed loop systems.

8.7 Summary

The spillover problem has been extensively studied for decades, and this chapter demonstrated how data-driven methods provided new insights into the problem. More importantly, the objective O4 has been met, resulting in the development of a Bayesian state estimator for structural control systems. This chapter offered two distinct feedback control techniques to deal with uncertainty in flexible structural dynamics. The first technique is the traditional LQG, which is based on a separate principle in which a recursive Bayesian estimation serves as the foundation for the KF coupled with the LQR. With fewer constraints, vibration effects can be suppressed. The primary benefit of using Bayesian state estimation in feedback control is that it allows control engineers to identify which states should be restricted without separating the system into controlled and suppressed states. In addition, designing weight matrices prior to computing the Ricatti equation to reduce the consequences of exciting the suppressed states may be less relevant due to the uncertainty of state estimation, particularly as MSE provides the effects of high uncertainty. However, the noise of the system was still designed based on the dynamic of the process system.

The second feedback control method offers a distinct perspective. The new aspect of this concept is that the EM algorithm produced more realistic values for dynamic parameters. Based on the first principle, this method produces values that are similar to the real dynamics; however, the values of process noise cannot be classified as Gaussian noise. As a result, optimal control was unable to offer control gains capable of altering dynamical behaviour. Furthermore, the results of this chapter was presented in the 30th International Conference on Noise and Vibration engineering (ISMA2022), Leuven, Belgium.

Chapter 9

Conclusions and future work

9.1 Summary of thesis

Starting with the broadest possible context, Chapter 1 provided an overview of the motivations and challenges of vibration control. Having considered the data-driven revolution in several fields of engineering, the objectives and contributions of this thesis were given before concluding Chapter 1 with the thesis outline.

Chapter 2 gave an overview of data-driven modelling and control methods, demonstrating the potential of probabilistic machine learning models. The regression problem was discussed, and the GP was introduced as an alternative method for regression problems and a Bayesian tool for engineering applications. Then, MPC was introduced in a general way before being presented based on MBC method in Chapter 5 and based on DDC in Chapter 6.

Chapter 3 provided a literature review on data-driven methods in three research fields: structural control, modelling, and estimation. In structural control, the vibration suppression of passive, semi-active, and active control approaches was discussed in terms of addressing nonlinearity and unhidden dynamics issues from a data-driven perspective. The modelling approaches were explored and developed in the field of SHM. The modelling section emphasised the Bayesian approach's effectiveness in engineering applications. This led to the estimation area where Bayesian filtering is used in recent engineering applications. In the end, this summary of the literature review was given with a highlight of the possibilities of employing data-driven

approaches in either modelling or control in active vibration control applications.

In Chapter 4, the dynamics of a cantilever beam were presented. The content of this chapter was the basis of the case studies in Chapters 5, 6, and 8. This chapter presented the modal analysis methods and the subsequent state space representation of the cantilever beam. Since GP works in discrete time domain, all state space models were transferred into discrete systems. Then, the numerical values of the system parameters were evaluated.

In response to the knowledge gap revealed by the literature review, Chapter 5 introduced the novel approach of data driven identification, in the active vibration setting. This work addressed the difficulties imposed by the limitations of the actuator in the range of active vibration control, where it requires incorporating an inverse GP of static nonlinearity within the Wiener and Hammerstein models. The model starts with designing regulator MPC for the cantilever beam, in which the aim is to identify the optimal control force. Utilizing the GP is the second step towards quantifying the uncertainty and limitation of the proof mass actuator by designing an inverse GP for the static nonlinearity. This quantification leads to an MPC controller using a steady-state target optimization tracking approach, in which the controller provides the optimal voltage required to eliminate vibration within the controller's limitations. The numerical outcome indicated that the proposed scheme was capable of supplying the necessary voltage, which eliminated the structure's vibration within an actuator's limits.

Chapter 6 investigated the possibility of applying Nonlinear Model Predictive Control (NMPC) to flexible structures by utilising recent developments in models that have been learnt from example data. The GP was used as a black-box model in NMPC; it provides both the prediction of the system output and the associated confidence. In a control context, a GP can be utilised as a discrepancy model for linear or nonlinear flexible dynamic structures within MPC or even as the nonlinear model of the system itself. The Nonlinear Output Error model (GP-NOE) is a popular GP structure for dynamic systems that is utilised in predictive control strategies and requires predictions to be propagated to the control horizon. This novel framework was evaluated on the linear oscillator and the cantilever beam with light damping, and the results demonstrated robust control performance in both tracking and regulator tasks. The positive results inspired additional investigation into the proposed technique, particularly in the setting of a fully nonlinear system, as demonstrated in Chapter 7 where the Duffing oscillator served as a case study.

However, in the nonlinear case, some difficulties were experienced. First, identifying the model was more difficult than with linear case studies. Second, the rule that increasing the number of predictions leads to better performance was not valid.

Until this point of the thesis, the data-driven approaches were based on Bayesian modelling method even though Bayesian principles can be used in modelling and filtering. In light of this approach, Chapter 8 addressed the identification of flexible structural dynamics subject to uncertainty by using Bayesian state space models, with the intention of developing a vibration control system for a problem with Spillover. This requires incorporating the identified uncertainty of the structure into the control strategy. The proposed method comprised a combination of two Bayesian identification techniques, Gaussian filters, namely the Kalman Filter (KF) and EM algorithms, with a linear quadratic regulator (LQR). The key contribution of this work is to demonstrate how the methodology of Bayesian state estimation and LQR control algorithms might work in cases when there is spillover instability from unmodeled modes in the system. A simulated simply supported beam subjected to spillover instability served as a case study for validation of the proposed method. It was shown that Bayesian state space model of Kalman filter coupled with LQR controller were able to suppress the effects of Spillover. While the EM algorithm was able to estimate the dynamic parameters, it was still difficult to assume the process noise as Gaussian.

The following section will cover conclusions and main contributions to knowledge.

9.2 Conclusions and original contributions

The primary conclusions of this research can be drawn as follows:

1. Machine learning techniques, particularly Bayesian modelling and filtering methods, can be suitable alternatives to traditional vibration control approaches. This integration not only improves control, but it also provides novel perspectives into dynamic systems using probabilistic models.

2. Nonlinear system identification using Gaussian Processes and their application in control design for flexible systems represent a new data-driven approach for addressing complex and unknown dynamics in the field of vibration control.

Furthermore, the additional contributions can be summarised as follows;

- Bayesian system identification, employed in modelling and filtering, provided a new perspective for addressing vibration control problems using traditional models such as orientated box models.
- Several novel approaches to data-driven identification of discrete and continuous systems were presented, ranging from Wiener-Hammerstein models to Gaussian process nonlinear output error models.
- Several model predictive controllers were proposed, based on both model based control and data driven control. In general, the complexity of traditional approaches increased trust in the model's reliability, whereas new models provided new insights and control tools in the system.
- The conceptual design of employing the Wiener-Hammerstein model within model predictive control while accounting for mechanical saturation was proposed. This novel framework incorporated two model predictive controllers, which provided control force.
- The Gaussian process nonlinear output error model within model predictive control was an effective model for both linear and nonlinear structural systems, though determining the number of predictions required some trial and error. This contribution also clarified terminology used in a variety of engineering fields.
- The predictive functional control method reduced computational costs through the use of the cost function from Equation (6.14).
- Bayesian state estimators have been offered numerous advantages in structural dynamics, and this can be extended to active vibration control. Two distinct methods based on Bayesian estimators, the Kalman filter and EM algorithms, offered a different angle of solving the spillover problem.

9.3 Discussion and future works

The research carried out in this thesis has shown the feasibility and effectiveness of incorporating Bayesian methods into control systems; however, there is still a

large scope for interesting future avenues in the arena of active vibration control under uncertainty within the context of a Bayesian approach of either modelling or estimation. It is worth bearing in mind that using a GP modelling approach combined with a Bayesian state estimation approach as an observer within the context of vibration control has not yet been proposed in the literature. Consequently, this future work would need to be divided into separate general avenues: vibration control with Bayesian state estimation and vibration control with a GP model.

A Bayesian filter is employed in the literature to address structural health monitoring problems such as input estimation or joint estimation; however, the control aspects or effects require further investigation. In Chapter 8, the implementation of Bayesian approaches to form an adaptive control in active vibration settings has demonstrated potential and raised interesting research paths to be explored. First, the noise in filtering design was assumed to be Gaussian, whereas it would be more practical to assume or account for coloured noise in the design of active vibration control. Furthermore, the Bayesian filter did not take into account certain aspects of structural vibration, such as collocated and noncollocated systems, or, more importantly, actuator dynamics.

Considering machine learning tools, the Gaussian process is a promising technology for the control community. In general, incorporating GP with control systems is in its early stages of research and engineering applications, yet validation and experimentation work, whether from this work or the literature, is still rare due to computational costs in real time. The thesis's expected future work in this area can be summarized as follows.

In Chapter 5, it was demonstrated that incorporating the GP model within the Wiener-Hammerstein model for vibration control contributes to accurately representing various complex dynamic systems, including nonlinear systems; nevertheless, more in-depth future research is needed to investigate simpler MPC strategies, different block-oriented models, and real-world applications. In terms of implementation, the proposed model can be used as a novel data-driven identification approach to investigate the actuator's limitations when using active vibration control. Furthermore, incorporating the Wiener-Hammerstein model into a complete feedback control system remains challenging because the overall control algorithm requires additional simplifications of the MPC-Wiener-Hammerstein model.

Regarding control principles with GP, the first interesting challenge among control

concepts is the lack of analytical tools of a closed-loop system, such as stability and convergence. In terms of control algorithms, optimal control, particularly nonlinear model predictive control, has demonstrated its effectiveness in active vibration control in Chapters 6 and 7, but continued efforts are needed to make the control system more applicable. First, nonlinear programming optimisation is essential for effective numerical implementation. This work proposed predictive functional control as a step forward in this direction, but an extensive investigation of the number of predictions ahead in either linear or nonlinear systems is still required. Second, the control problem for the GP-NMPC was unconstrained, whereas ensuring a reliable NMPC control action requires a constrained optimisation control problem subject to the GP-NOE model confidence level. This leads to another recommendation: approximation simulation in system identification using the GP model could be more appropriate and realistic in capturing the dynamic behaviour of a closed-loop system.

Model identification adaptive control is one of the adaptive control methods coupled with a GP model. Figure (3.13) illustrates a block design for model identification adaptive control. According to the author of [14], this method can be used to quantify system uncertainty and design an appropriate control strategy. Even though the spillover problem was addressed using the Bayesian filtering approach in this thesis, the advantage of adaptive control strategies is that residual modes can be included in the system, and the GP will help in determining the uncertainty region in which the controller can eliminate the effects of spillover. Control with feedback for cancelling nonlinearities is also a possibility for implementing this type of control algorithm.

A final broad recommendation in this subject is that the research on operational digital twins has gained significant attention in both academia and industry. One of the applications in this area could include incorporating the digital twin model into the GP-NMPC strategy to form an adaptive controller. Using a digital twin can improve both predictive and control performance.

Appendix A

Validation of the dynamic of the beam

A.1 System matrices for state-space representation in discrete time

The state-space matrices are as follows:

$$A_d = \begin{bmatrix} 0.9999 & 0 & 0 & 0.0009998 & 0 & 0 \\ 0 & 0.9954 & 0 & 0 & 0.0009975 & 0 \\ 0 & 0 & 0.9641 & 0 & 0 & 0.0009853 \\ -0.2353 & 0 & 0 & 0.9996 & 0 & 0 \\ 0 & -9.219 & 0 & 0 & 0.9935 & 0 \\ 0 & 0 & -71.39 & 0 & 0 & 0.9588 \end{bmatrix}$$

$$B_d = \begin{bmatrix} 8.709 \times 10^{-6} \\ -8.698 \times 10^{-6} \\ 8.642 \times 10^{-6} \\ 0.01742 \\ -0.01738 \\ 0.01716 \end{bmatrix}$$

$$C_d = \begin{bmatrix} 2 & -2 & 2 & 0 & 0 & 0 \end{bmatrix}$$

$$D_d = \begin{bmatrix} 0 \end{bmatrix}$$

A.2 Calculating the deflection of the beam

There are several validation methods for establishing the validity of the dynamic data acquired in this thesis. Calculating deflection is one of these methods. The deflection at the end of a cantilever beam under a force F is given by:

$$\text{Deflection}_{\text{end}} = \frac{F \cdot L^3}{3 \cdot E \cdot I}$$

Using the geometry of the cantilever beam in Table (4.2) and an assumed force of $10N$, the analytical value of the deflection at the end of the beam is 1.5253 m. Figure A.1 depicts simulation cases based on data from the cantilever beam used in this thesis, displaying the expected output.

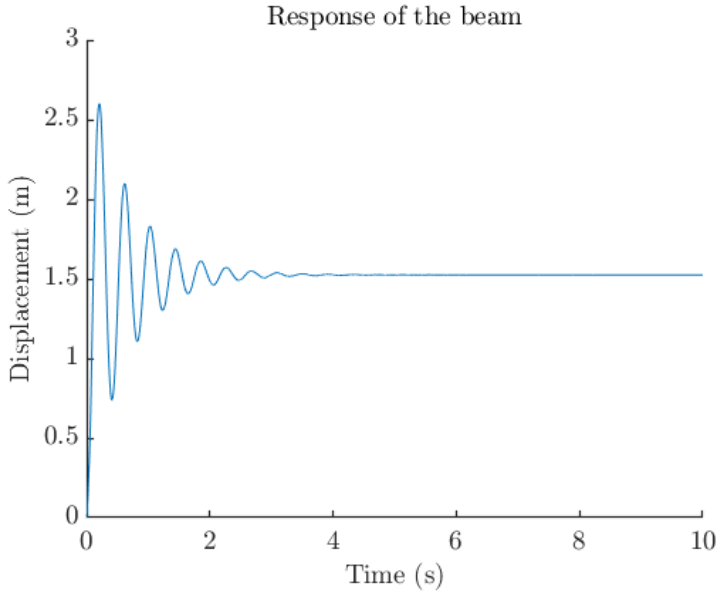

Figure A.1: The validation response is to obtain the same result as the analytical method

Appendix B

Derivation of stack inequality equations

B.1 Formulating a unified stacked inequality constraint for multiple system constraints

This section aims to vectorise input, state, and terminal state constraints into a single equation, as shown in Equation B.1. It is important to note that this step is described in several references with different letters; however, the MPC lecture notes from the University of Sheffield explained this step in a better and more concise letter [165], which this thesis adapted.

$$\left.\begin{aligned} P_x x(k+i|k) &\leq q_x \\ P_u u(k+i|k) &\leq q_u \\ P_{x_N} x(k+N|k) &\leq q_{x_N} \end{aligned}\right\} \quad i = 1, \ldots, N-1 \quad \longrightarrow \quad P_c u(k) \leq q_c + S_c x(k) \tag{B.1}$$

We start with the input constraints:

$$P_u u(k+i|k) \leq q_u, \quad i = 0, 1, \ldots, N-1 \tag{B.2}$$

For multiple steps ahead, this constraint can be collected and stacked as follows:

$$\underbrace{\begin{bmatrix} P_u & 0 & \dots & 0 \\ 0 & P_u & \dots & 0 \\ \vdots & \vdots & \ddots & \vdots \\ 0 & 0 & \dots & P_u \end{bmatrix}}_{\tilde{P}_u} \underbrace{\begin{bmatrix} u(k|k) \\ u(k+1|k) \\ \vdots \\ u(k+N-1|k) \end{bmatrix}}_{u(k)} \leq \underbrace{\begin{bmatrix} q_u \\ q_u \\ \vdots \\ q_u \end{bmatrix}}_{\tilde{q}_u}$$

Therefore, the input constraint can be written as compact forms:

$$\tilde{P}_u \mathbf{u}(k) \leq \tilde{q}_u \tag{B.3}$$

Now, the state constraints are similar and can be recall from Equations (3.22) and (3.24) as:

$$\begin{aligned} P_x x(k+i|k) &\leq q_x, \quad i = 1, 2, \dots, N \\ P_{x_N} x(k+i|k) &\leq q_{x_N}, \quad i = 0, 1, \dots, N-1 \end{aligned} \tag{B.4}$$

Then, after stacking and including the initial state, the compact form of state constraint is obtained as:

$$\underbrace{\begin{bmatrix} P_x \\ 0 \\ 0 \\ \vdots \\ 0 \end{bmatrix}}_{\tilde{P}_{x_0}} x(k|k) + \underbrace{\begin{bmatrix} 0 & 0 & \dots & 0 \\ P_x & 0 & \dots & 0 \\ 0 & P_x & \dots & 0 \\ \vdots & \vdots & \ddots & \vdots \\ 0 & 0 & \dots & P_{x_N} \end{bmatrix}}_{\tilde{P}_x} \underbrace{\begin{bmatrix} x(k+1|k) \\ x(k+2|k) \\ \vdots \\ x(k+N|k) \end{bmatrix}}_{x(k)} \leq \underbrace{\begin{bmatrix} q_x \\ q_x \\ q_x \\ \vdots \\ q_{x_N} \end{bmatrix}}_{\tilde{q}_x} \tag{B.5}$$

Therefore, the state constraint equation becomes one of the following equations:

$$P_{x_0} x(k) + \tilde{P}_x x(k) \leq \tilde{q}_x \tag{B.6}$$

$$\tilde{P}_x x(k) \leq \tilde{q}_x - P_{x_0} x(k) \tag{B.7}$$

Utilising the prediction model of Equation (3.16) in order to come up with constraint equations without initial conditions, the input and state constraints become:

$$\tilde{P}_x(Fx(k) + Gu(k)) \leq \tilde{q}_x - \tilde{P}_{x_0}x(k) \tag{B.8}$$

$$\tilde{P}_x Gu(k) \leq \tilde{q}_x + (-\tilde{P}_{x_0} - \tilde{P}_x F)x(k) \tag{B.9}$$

Then, it can be in a matrix form as:

$$\underbrace{\begin{bmatrix} \tilde{P}_u \\ \tilde{P}_x G \end{bmatrix}}_{P_c} \mathbf{u}(k) \leq \underbrace{\begin{bmatrix} \tilde{q}_u \\ \tilde{q}_x \end{bmatrix}}_{q_c} + \underbrace{\begin{bmatrix} 0 \\ -\tilde{P}_{x_0} - \tilde{P}_x F \end{bmatrix}}_{S_c} x(k) \tag{B.10}$$

Therefore, we have:

$$P_c \mathbf{u}(k) \leq q_c + S_c x(k) \tag{B.11}$$

The terminal cost constraints need some extra attention. Since it is related to the stability of the system, the constraints contains the control gain in order to make a closed model within the constraints. In regulator, the terminal constraints are described as follows:

$$\underbrace{\begin{bmatrix} P_x & 0 & \dots & 0 \\ P_u K_\infty & 0 & \dots & 0 \\ 0 & P_x & \dots & 0 \\ 0 & P_u K_\infty & \dots & 0 \\ \vdots & \vdots & \ddots & \vdots \end{bmatrix}}_{\mathcal{M}} \underbrace{\begin{bmatrix} (A + BK_\infty)^0 \\ (A + BK_\infty)^1 \\ \vdots \\ (A + BK_\infty)^{n-1} \end{bmatrix}}_{P_{x_N}} x(k+N|k) \leq \underbrace{\begin{bmatrix} q_x \\ q_u \\ q_x \\ q_u \\ \vdots \end{bmatrix}}_{q_{x_N}} \tag{B.12}$$

Note that:

$$\mathcal{M} = I_{n\times n} \otimes \begin{bmatrix} P_x \\ P_u K_\infty \end{bmatrix}, \quad q_{x_N} = \mathbf{1}_{n\times 1} \otimes \begin{bmatrix} q_x \\ q_u \end{bmatrix} \tag{B.13}$$

In tracking:

$$\tilde{q}_{x_N} = \mathbf{1}_n \otimes \begin{bmatrix} q_x - P_x x_{\text{ss}} \\ q_u - P_u u_{\text{ss}} \end{bmatrix} \tag{B.14}$$

B.2 Algorithm of LQ-MPC regulator control problem

Algorithm 1 FH-LQR Design for Cantilever Beam

1: **Initialize:** Number of modes N_{mode}, sampling time T, system matrices (A, B, C, D)
2: **Discretize:** Convert system to discrete time using zero-order hold (ZOH)
3: **Set Control Parameters:**
4: Define cost matrices Q, R
5: Compute control gains K using LQR
6: Calculate terminal cost matrix P
7: **Build MPC Matrices:**
8: Generate prediction matrices F, G
9: Construct cost matrices H, L, M
10: Define input and state constraints (P_u, q_u, P_x, q_x)
11: **Simulate MPC:**
12: **for** each time step k **do**
13: Update state $x(k)$ using the system dynamics
14: Solve the quadratic program to obtain optimal control $u(k)$
15: Apply $u(k)$ to the system and store results
16: **end for**

B.3 Algorithm of LQ-MPC tracking control problem

Algorithm 2 FH-LQR Design for Proof Mass Actuator with SSTO

Initialize: Define system matrices $A_{cp}, B_{cp}, C_{cp}, D_{cp}$ for the proof mass actuator
Discretize: Convert continuous system to discrete using zero-order hold (ZOH)
Set Control Parameters:
    Define cost matrices Q_p, R_p
    Compute control gains K_p using LQR
    Calculate terminal cost matrix P_p
Build MPC Matrices:
    Generate prediction matrices F_p, G_p
    Construct cost matrices H_p, L_p, M_p
    Define input and state constraints (P_u, q_u, P_x, q_x)
    Determine terminal constraints (P_{xN}, q_{xN}) for deadbeat control
First Optimization (SSTO):
    Define target equilibrium pair (x_{ss}, u_{ss})
    Solve for (x_{ss}, u_{ss}) using equality constraints $A_{eq}x_{ss} = b_{eq}$ under input and state constraints
    Adjust constraints $P_{u,\text{ssto}}, q_{u,\text{ssto}}, P_{x,\text{ssto}}, q_{x,\text{ssto}}$ for SSTO
Simulation:
for each time step k **do**
        Update state $x(k)$ using system dynamics
        Solve the optimization problem to obtain optimal control $u(k)$ with SSTO constraints
        Apply $u(k)$ to the system and store results
        Calculate and store the cost $J(k)$
end for

Appendix C

Details of 4th order Runge-Kutta scheme

The numerical integration scheme is a 4th-order Runge-Kutta method [190], detailed below for completeness.

$$x_{t+1} = x_t + \frac{\Delta t}{6}\left(k_1 + 2k_2 + 2k_3 + k_4\right) \tag{C.1}$$

$$k_1 = f(t, x_t) \tag{C.2}$$

$$k_2 = f\left(t + \frac{\Delta t}{2}, x_t + \frac{\Delta t}{2} \cdot k_1\right) \tag{C.3}$$

$$k_3 = f\left(t + \frac{\Delta t}{2}, x_t + \frac{\Delta t}{2} \cdot k_2\right) \tag{C.4}$$

$$k_4 = f(t + \Delta t, x_t + \Delta t \cdot k_3) \tag{C.5}$$

Where Δt is the time step.

Bibliography

[1] D. J Inman. *Vibration with Control*. Wiley, 2006.

[2] D Geir E and F Paganini. *A Course in Robust Control Theory : A Convex Approach*. Springer New York, 2002.

[3] A Preumont. *Vibration Control of Active Structures: An Introdcution*. Solid Mechanics and its Application, Springer, 1999.

[4] S Thenozhi and W Yu. Advances in modeling and vibration control of building structures. *Annual Reviews in Control*, 2013.

[5] D Frangopol and Y Tsompanakis. *Maintenance and Safety of Aging Infrastructure: Structures and Infrastructures*. CRC Press, 2014.

[6] D Wagg and S Neild. *Nonlinear Vibration with Control for Flexible and Adaptive Structures*. Springer, 2010.

[7] D. J Wagg and S. A Neild. A review of non-linear structural control techniques. *Proceedings of the Institution of Mechanical Engineers, Part C: Journal of Mechanical Engineering Science*, 2011.

[8] J. P Noël and G Kerschen. Nonlinear system identification in structural dynamics: 10 more years of progress. *Mechanical Systems and Signal Processing*, 2017.

[9] W Gawronski. *Advanced Structural Dynamics and Active Control of Structures*. Mechanical Engineering Series. Springer New York, 2004.

[10] J Hauth. *Grey-Box Modelling for Nonlinear Systems*. PhD thesis, Fraunhofer Institute for Industrial Mathematics, Germany, 2008.

[11] Z Yang, D Eddy, S Krishnamurty, I Grosse, P Denno, Y Lu, and P Witherell. Investigating Grey-Box Modeling for Predictive Analytics in Smart Manufacturing. In *International Design Engineering Technical Conferences and Computers and Information in Engineering Conference*, 2017.

[12] J Schoukens and L Ljung. Nonlinear system identification: A user-oriented road map. *IEEE Control Systems Magazine*, 2019.

[13] W Liu. *Introduction to Hybrid Vehicle System Modeling and Control*. John Wiley and Sons, 2013.

[14] J Kocijan. *Modelling and Control of Dynamic Systems Using Gaussian Process Models*. Springer series, Advances in Industrial Control, 2016.

[15] V Dertimanis, E Chatzi, and F Weber. LQR – UKF Semi–Active Control of Uncertain Structures. In *EACS 2016 – 6th European Conference on Structural Control*, 2016.

[16] L Fortuna and M Frasca. Optimal and robust control: Advanced topics with MATLAB®. *Optimal and Robust Control: Advanced Topics with MATLAB*, 2012.

[17] R Kalman. Contributions to the theory of optimal control. *Boletin de la Sociedad Matematica Mexicana*, 1960.

[18] R. E Kalman. A new approach to linear filtering and prediction problems. *Journal of Fluids Engineering, Transactions of the ASME*, 1960.

[19] Z.-S Hou and Z Wang. From model-based control to data-driven control: Survey, classification and perspective. *Information Sciences*, 2013.

[20] H. J van Waarde, J Eising, H. L Trentelman, and M. K Camlibel. Data informativity: A new perspective on data-driven analysis and control. *IEEE Transactions on Automatic Control*, 2019.

[21] S. L Brunton and J. N Kuts. *Data Driven Science and Engineering - Machine Learning, Dynamical Systems, and Control*. Cambridge Press, 2017.

[22] A McHutchon. *Nonlinear Modelling and Control using Gaussian Processes*. PhD thesis, Department of Engineering, University of Cambridge, 2014.

[23] C. E Rasmussen and C. K. I Williams. *Gaussian Processes for Machine Learning*. The MIT Press, 2005.

[24] C. E García, D. M Prett, and M Morari. Model predictive control: Theory and practice—a survey. *Automatica*, 1989.

[25] E Camacho and C Bordons. *Model Predictive Control in the Process Industry*. Advances in Industrial Control. Springer London, 2012.

[26] J. L Garriga and M Soroush. Model predictive control tuning methods: A review. *Industrial & Engineering Chemistry Research*, 2010.

[27] Z Li and R Evans. Minimum-variance control of linear time-varying systems. *Automatica*, 1997.

[28] S Qin and T. A Badgwell. A survey of industrial model predictive control technology. *Control Engineering Practice*, 2003.

[29] J Richalet, A Rault, J Testud, and J Papon. Model predictive heuristic control: Applications to industrial processes. *Automatica*, 1978.

[30] D Mayne, J Rawlings, C Rao, and P Scokaert. Constrained model predictive control: Stability and optimality. *Automatica*, 2000.

[31] S. S Dughman. *Improving Tracking in Optimal Model Predictive Control*. PhD thesis, University of Sheffield, 2018.

[32] G. W Housner, L. A Bergman, T. K Caughey, A. G Chassiakos, R. O Claus, S. F Masri, R. E Skelton, T. T Soong, B. F Spencer, and J. T. P Yao. Structural Control: Past, Present, and Future. *Journal of Engineering Mechanics*, 1997.

[33] T Soong and B. F. S Jr. Supplemental energy dissipation: state-of-the-art and state-of-the-practice. *Engineering Structures*, 2002.

[34] F Casciati, J Rodellar, and U Yildirim. Active and semi-active control of structures-theory and applications: A review of recent advances. *Journal of Intelligent Material Systems and Structures*, 2012.

[35] H. H Saaed T. E. Nikolakopoulos G. Jonasson J-E. A state-of-the-art review of structural control systems. *Journal of Vibration and Control*, 2015.

[36] N. R Fisco and H Adeli. Smart structures: Part i - active and semi-active control. *Scientia Iranica*, 2011.

[37] S Korkmaz. A review of active structural control: Challenges for engineering informatics. *Computers and Structures*, 2011.

[38] H Frahm. Device for damping vibration of bodies. Technical report, U.S. Patent No. 989,958., 18 Apr. 1911.

[39] P. A Irwin and B Breukelman. Recent applications of damping systems for wind response. In *Proceedings of the Sixth World Congress of the Council on Tall Buildings and Urban Habitat, Melbourne, Australia*, 2001.

[40] S G. Tructural mechanics and dynamics branch 2002 annual report. Technical report, NASA, 2002.

[41] K Liu and K Rouch. Optimal passive vibration control of cutting process stability in milling. *Journal of Materials Processing Technology*, 1991.

[42] F Yang, R Sedaghati, and E Esmailzadeh. Vibration suppression of structures using tuned mass damper technology: A state-of-the-art review. *Journal of Vibration and Control*, 2022.

[43] M Smith. Synthesis of mechanical networks: the inerter. *IEEE Transactions on Automatic Control*, 2002.

[44] I Ullah, K. D Wagg, and N. D Sims. *Vibration Suppression in Flexible Structures using Hybrid Active and Semi-active Control*. PhD thesis, The University of Sheffield, 2017.

[45] B. F. S Jr. and S Nagarajaiah. State of the art of structural control. *Journal of Structural Engineering*, 2003.

[46] F Saka, S Takaeda, and T Tamaki. Tuned liquid column damper-new type device for suppression of building vibrations. In *Proceedings of International Conference on High-rise Buildings*, 1989.

[47] A Teramura and O Yoshida. Development of vibration control system using u-shaped water tank. In *11th World Conference on Earthquake Engineering.*, 1996.

[48] S Colwell and B Basu. Tuned liquid column dampers in offshore wind turbines for structural control. *Engineering Structures*, 2009.

[49] W WM. Method and means for translating electrical impulses into mechanical force, 1947. US Patent No. 2,417,850.

[50] J Rabinow. The magnetic fluid clutch. *Electrical Engineering*, 1948.

[51] B. F Spencer, S. J Dyke, M. K Sain, and J. D Carlson. Phenomenological model for magnetorheological dampers. *Journal of Engineering Mechanics*, 1997.

[52] S. J Dyke, B. F. S Jr, M. K Sain, and J. D Carlson. Modeling and control of magnetorheological dampers for seismic response reduction. *Smart Materials and Structures*, 1996.

[53] W. H Liao and D. H Wang. Semiactive vibration control of train suspension systems via magnetorheological dampers. *Journal of Intelligent Material Systems and Structures*, 2003.

[54] G Yao, F Yap, G Chen, W Li, and S Yeo. Mr damper and its application for semi-active control of vehicle suspension system. *Mechatronics*, 2002.

[55] Y. M Delijani, S Cheng, and F Gherib. Sequential neural network model for the identification of magnetorheological damper parameters. *Smart Materials and Structures*, 2024.

[56] K. K Ahn, D. Q Truong, and M. A Islam. Modeling of a magneto-rheological (mr) fluid damper using a self tuning fuzzy mechanism. *Journal of Mechanical Science and Technology*, 2009.

[57] J Wang, K Xu, C Shao, L Peng, and Y Cui. Data-driven probabilistic model of magneto-rheological damper for intelligent vehicles using gaussian processes. In *The IEEE 25th International Conference on Intelligent Transportation Systems (ITSC)*, 2022.

[58] N. R Fisco and H Adeli. Smart structures: Part ii - hybrid control systems and control strategies, 2011.

[59] P Guo. *Damping System Designs using Nonlinear Frequency Analysis Approach*. PhD thesis, The University of Sheffield, 2012.

[60] T. T Soong and G. D Manolis. Active structures. *Journal of Structural Engineering*, 1987.

[61] J. P Lynch. Active structural control research at kajima corporation. *The National Science Foundation's Summer Institute in Japan Program, Research Project*, 1998.

[62] H Okubo, N Komatsu, and T Tsumura. Tendon control system for active shape control of flexible space structures. *Journal of Intelligent Material Systems and Structures*, 1996.

[63] B. R Davis and A. G Thompson. Optimal linear active suspensions with integral constraint. *Vehicle System Dynamics*, 1988.

[64] I Chopra. Status of application of smart structures technology to rotorcraft systems. *American Helicopter Society*, 2000.

[65] M. J Balas. Active control of flexible systems. *Journal of Optimization Theory and Applications*, 1978.

[66] K Xue, A Igarashi, and T Kachi. Optimal sensor placement for active control of floor vibration considering spillover effect associated with modal filtering. *Engineering Structures*, 2018.

[67] C Chantalakhana. Stability improvement of modal controllers for suppressing beam vibrations using a hybrid control scheme. *Proceedings of the IEEE International Conference on Industrial Technology*, 2002.

[68] A Montazeri, J Poshtan, and A Yousefi-Koma. Design and analysis of robust minimax lqg controller for an experimental beam considering spill-over effect. *IEEE Transactions on Control Systems Technology*, 2011.

[69] K. H Rew, J. H Han, and I Lee. Multi-modal vibration control using adaptive positive position feedback. *Journal of Intelligent Material Systems and Structures*, 2002.

[70] J. R Sesak and P. W Likins. Model error sensitivity suppression: Quasi-static optimal control for flexible structures. In *The 18th IEEE Conference on Decision and Control including the Symposium on Adaptive Processes*, 1979.

[71] B. D. O Anserson and J. B Moore. *Optimal Control: Linear Quadratic Methods*. Prentice Hall, 1989.

[72] B Shafai, S Beale, H Niemann, and J Stoustrup. Ltr design of discrete-time proportional-integral observers. *IEEE Transactions on Automatic Control*, 1996.

[73] M. S Miah, E. N Chatzi, and F Weber. Semi-active control for vibration mitigation of structural systems incorporating uncertainties. *Smart Materials and Structures*, 2015.

[74] L. I Wilmshurst. *Analysis and control of nonlinear vibration in inertial actuators*. PhD thesis, University of Southampton, 2015.

[75] O. N Baumann and S. J Elliott. Destabilization of velocity feedback controllers with stroke limited inertial actuators. *The Journal of the Acoustical Society of America*, 2007.

[76] L Wilmshurst, M. G Tehrani, and S Elliott. Nonlinear vibrations of a stroke-saturated inertial actuator. In *11th International Conference on Recent Advances in Structural Dynamics (RASD2013)*, 2013.

[77] J Chase, M Yim, and A. A Berlin. Integrated centering control of inertially actuated systems. *Control Engineering Practice*, 1999.

[78] D. K Lindner, G. A Zvonar, and D Borojevic. Performance and control of proof mass actuators accounting for stroke saturation. *J. Guid. Control Dyn.*, 1994.

[79] D. K Lindner, G. A Zvonar, and D Borojevic. Nonlinear control of proof mass actuator. *J. Guid. Control Dyn.*, 1997.

[80] J. G Chase, S. E Breneman, and H. A Smith. Robust h_∞ static output feedback control with actuator saturation. *Journal of Engineering Mechanics*, 1999.

[81] L Wilmshurst, M. G Tehrani, and S Elliott. Active control and stability analysis of flexible structures using nonlinear proof-mass actuators. In *Ninth International Conference on Structural Dynamics (EURODYN 2014)*, 2014.

[82] M. D Borgo, M. G Tehrani, and S. J Elliott. Dynamic analysis of two nonlinear inertial actuators in active vibration control. In *27th International Conference on Noise and Vibration Engineering (ISMA2016)*, 2016.

[83] M. D Borgo, M. G Tehrani, and S. J Elliott. Identification and analysis of nonlinear dynamics of inertial actuators. *Mechanical Systems and Signal Processing*, 2019.

[84] M. D Borgo, M. G Tehrani, and S. J Elliott. Active nonlinear control of a stroke limited inertial actuator: Theory and experiment. *Journal of Sound and Vibration*, 2020.

[85] K LI and S THOMPSON. FUNDAMENTAL GREY-BOX MODELLING. In *Proceedings of the European Control Conference 2001*, 2001.

[86] M Haywood-Alexander, R. S Mills, M. D Champneys, M. R Jones, M. S Bonney, D Wagg, and T. J Rogers. Full-scale modal testing of a hawk t1a aircraft for benchmarking vibration-based methods. *Journal of Sound and Vibration*, 2024.

[87] M. A Eroglu. *Observer based control of an magnetorheological damper*. PhD thesis, The University of Sheffield, 2013.

[88] P. C Young. Time Variable Parameter Estimation. In *15th IFAC Symposium on System Identification, IFAC Proceedings Volumes*, 2009.

[89] A Jain, T. X Nghiem, M Morari, and R Mangharam. Learning and control using gaussian processes: towards bridging machine learning and controls for physical systems. In *2018 ACM/IEEE 9th International Conference on Cyber-Physical Systems (ICCPS), Porto, Portugal*, 2018.

[90] K Worden, R. J Barthorpe, E. J Cross, N Dervilis, G. R Holmes, G Manson, and T. J Rogers. On evolutionary system identification with applications to nonlinear benchmarks. *Mechanical Systems and Signal Processing*, 2018.

[91] K Worden, C. X Wong, U Parlitz, A Hornstein, D Engster, T Tjahjowidodo, F Al-Bender, D. D Rizos, and S. D Fassois. Identification of pre-sliding and sliding friction dynamics: Grey box and black-box models. *Mechanical Systems and Signal Processing*, 2007.

[92] J. P Amezquita-Sanchez and H Adeli. Feature extraction and classification techniques for health monitoring of structures. *Scientia Iranica*, 2015.

[93] M Jamil, M. N Khan, S. J Rind, Q Awais, and M Uzair. Neural network predictive control of vibrations in tall structure: An experimental controlled vision. *Computers and Electrical Engineering*, 2021.

[94] C Song, C Yu, Y Xiao, and J Zhang. Fuzzy logic control based on genetic algorithm for a multi-source excitations floating raft active vibration isolation system. *Advances in Mechanical Engineering*, 2017.

[95] B Chen, Y Wang, R Wang, Z Zhu, L Ma, X Qiu, and W Dai. The gray-box based modeling approach integrating both mechanism-model and data-model: The case of atmospheric contaminant dispersion. *Symmetry*, 2020.

[96] G Kerschen, K Worden, A. F Vakakis, and J. C Golinval. Past, present and future of nonlinear system identification in structural dynamics. *Mechanical Systems and Signal Processing*, 2006.

[97] C. M Bishop. *Pattern Recognition and Machine Learning (Information Science and Statistics)*. Springer-Verlag, 2006.

[98] G Kerschen, J. C Golinval, and F. M Hemez. Bayesian model screening for the identification of nonlinear mechanical structures. *Journal of Vibration and Acoustics, Transactions of the ASME*, 2003.

[99] P. L Green and K Worden. Bayesian and Markov chain Monte Carlo methods for identifying nonlinear systems in the presence of uncertainty. *Philosophical Transactions of the Royal Society A: Mathematical, Physical and Engineering Sciences*, 2015.

[100] T Al-Hababi, M Cao, B Saleh, N. F Alkayem, and H Xu. A critical review of nonlinear damping identification in structural dynamics: Methods, applications, and challenges. *Sensors (Switzerland)*, 2020.

[101] I. J Leontaritis and S. A Billings. Input-output parametric models for non-linear systems part i: deterministic non-linear systems. *International Journal of Control*, 1985.

[102] S Billings. *Nonlinear System Identification: NARMAX Methods in the Time, Frequency, and Spatio-Temporal Domains*. Wiley, 2013.

[103] L Piroddi, M Farina, and M Lovera. Polynomial narx model identification: A wiener-hammerstein benchmark. In *IFAC Proceedings Volumes*, 2009.

[104] M Farina and L Piroddi. Simulation error minimization-based identification of polynomial input-output recursive models. In *IFAC Proceedings Volumes*, 2009.

[105] H. B. J S. A. Billings and S Chen. Properties of neural networks with applications to modelling non-linear dynamical systems. *International Journal of Control*, 1992.

[106] C. F. N. C S. Chen, S. A. Billings and P. M Grant. Practical identification of narmax models using radial basis functions. *International Journal of Control*, 1990.

[107] K Worden, W. E Becker, T. J Rogers, and E. J Cross. On the confidence bounds of gaussian process narx models and their higher-order frequency response functions. *Mechanical Systems and Signal Processing*, 2018.

[108] D. J Pitchforth, T. J Rogers, U. T Tygesen, and E. J Cross. Grey-box models for wave loading prediction. *Mechanical Systems and Signal Processing*, 2021.

[109] S. D Silva, L. G Villani, M Rébillat, and N Mechbal. Gaussian process narx model for damage detection in composite aircraft structures. *Journal of Nondestructive Evaluation, Diagnostics and Prognostics of Engineering Systems*, 2022.

[110] F Lindsten, T. B Schön, and M. I Jordan. A semiparametric bayesian approach to wiener system identification. In *IFAC Proceedings Volumes*, 2012.

[111] W. E Leithead, E Solak, and D. J Leith. Direct identification of nonlinear structure using gaussian process prior models. In *2003 European Control Conference (ECC)*, 2003.

[112] M Schoukens and K Tiels. Identification of block-oriented nonlinear systems starting from linear approximations: A survey. *Automatica*, 2017.

[113] H. J Tulleken. Grey-box modelling and identification using physical knowledge and bayesian techniques. *Automatica*, 1993.

[114] T Bohlin and S Graebe. Issues in Nonlinear Stochastic Grey-Box Identification. *IFAC Proceedings Volumes*, 1994.

[115] R Venkataraman and P Seiler. System identification for a small, rudderless, fixed-wing unmanned aircraft. *Journal of Aircraft*, 2019.

[116] L. A Bull, I Abdallah, C Mylonas, L. D Avendaño-Valencia, K Tatsis, P Gardner, T. J Rogers, D. S Brennan, E. J Cross, K Worden, A. B Duncan,

N Dervilis, M Girolami, and E Chatzi. *Data-Centric Monitoring of Wind Farms: Combining Sources of Information*. CRC Press, 2023.

[117] C. T Chen. *Linear system theory and design*. The Oxford Series in Electrical and Computer Engineering, 1999.

[118] J Hong, S Laflamme, J Dodson, and B Joyce. Introduction to state estimation of high-rate system dynamics. *Sensors (Switzerland)*, 2018.

[119] H. H Afshari, S. A Gadsden, and S Habibi. Gaussian filters for parameter and state estimation: A general review of theory and recent trends. *Signal Processing*, 2017.

[120] M. S Grewal and A. P Andrews. *Kalman Filtering: Theory and Practice with MATLAB*. John Wiley and Sons, 2015.

[121] V Awasthi and K Raj. A survey on the algorithms of kalman filter and its variants in state estimation. *Current Approaches in Science and Technology Research*, 2011.

[122] B Anderson and J Moore. *Optimal filtering*. Dover Publications Inc, 2012.

[123] S Eftekhar Azam, E Chatzi, and C Papadimitriou. A dual Kalman filter approach for state estimation via output-only acceleration measurements. *Mechanical Systems and Signal Processing*, 2015.

[124] Eleni N. Chatzi and Andrew W. Smyth. The unscented Kalman filter and particle filter methods for nonlinear structural system identification with non-collocated heterogeneous sensingy. *Structural Control and Health Monitoring*, 2009.

[125] C Montella. The Kalman Filter and Related Algorithms A Literature Review. *Research Gate*, 2011.

[126] J Ko and D Fox. GP-BayesFilters: Bayesian filtering using Gaussian process prediction and observation models. *Autonomous Robots*, 2009.

[127] J Ching, J. L Beck, and K. A Porter. Bayesian state and parameter estimation of uncertain dynamical systems. *Probabilistic Engineering Mechanics*, 2006.

[128] Z CHEN. Bayesian Filtering: From Kalman Filters to Particle Filters, and Beyond. *A Journal of Theoretical and Applied Statistics*, 2003.

[129] F Naets, J Croes, and W Desmet. An online coupled state/input/parameter estimation approach for structural dynamics. *Computer Methods in Applied Mechanics and Engineering*, 2015.

[130] S Särkkä. *Bayesian filtering and smoothing*. Cambridge University Press, 2013.

[131] F Naets, R Pastorino, J Cuadrado, and W Desmet. Online state and input force estimation for multibody models employing extended Kalman filtering. *Multibody System Dynamics*, 2014.

[132] A Parus, B Powałka, K Marchelek, S Domek, and M Hoffmann. Active vibration control in milling flexible workpieces. *JVC/Journal of Vibration and Control*, 2013.

[133] J Remacle, J Lambrechts, and B Seny. Precise integration strategy for aseismic LQG control of structures. *International Journal for Numerical Methods in Engineering*, 2012.

[134] J Sanchez and H Benaroya. Review of force reconstruction techniques. *Journal of Sound and Vibration*, 2014.

[135] C. K Ma and D. C Lin. Input forces estimation of a cantilever beam. *Inverse Problems in Engineering*, 2000.

[136] C. K Ma, P. C Tuan, D. C Lin, and C. S Liu. A study of an inverse method for the estimation of impulsive loads. *International Journal of Systems Science*, 1998.

[137] C. C Ho and C. K Ma. Active vibration control of structural systems by a combination of the linear quadratic Gaussian and input estimation approaches. *Journal of Sound and Vibration*, 2007.

[138] S Moradi, S Eftekhar Azam, and M Mofid. On Bayesian active vibration control of structures subjected to moving inertial loads. *Engineering Structures*, 2021.

[139] L. R Ray. Nonlinear Tire Force Estimation and Road Friction Identification: Simulation and Experiments. *Automatica*, 1997.

[140] L. R Ray. Nonlinear State and Tire Force Estimation for Advanced Vehicle Control. *IEEE Transactions on Control Systems Technology*, 1995.

[141] M. S Miah, E. N Chatzi, V. K Dertimanis, and F Weber. Real-time experimental validation of a novel semi-active control scheme for vibration mitigation. *Structural Control and Health Monitoring*, 2017.

[142] V. K Dertimanis and E. N Chatzi. Lqr-ukf active comfort control of passenger vehicles with uncertain dynamics. In *18th IFAC Symposium on System Identification SYSID 2018*, 2018.

[143] V Dertimanis, E Chatzi, and S Masri. On the active vibration control of nonlinear uncertain structures. *Journal of Applied and Computational Mechanics*, 2020.

[144] G Chowdhary and S Lorenz. Control of a VTOL UAV via online parameter estimation. *Collection of Technical Papers - AIAA Guidance, Navigation, and Control Conference*, 2005.

[145] L. X Chen and G. P Cai. Design method of multiple time-delay controller for active structural vibration control. *Appl. Math. Mech.Engl*, 2009.

[146] B. J Emran and H Najjaran. A review of quadrotor: An underactuated mechanical system. *Annual Reviews in Control*, 2018.

[147] F Berkenkamp and A. P Schoellig. Safe and robust learning control with Gaussian processes. In *2015 European Control Conference, ECC 2015*, 2015.

[148] R Alkhatib and M. F Golnaraghi. Active structural vibration control: A review. *The Shock and Vibration Digest*, 2003.

[149] D.-W Gu, P. H Petkov, and M. M Konstantinov. *Robust Control Design with MATLAB®*. Advanced Textbooks in Control and Signal Processing. Springer London, 2013.

[150] N Tsokanas, D Wagg, and B Stojadinović. Robust Model Predictive Control for Dynamics Compensation in Real-Time Hybrid Simulation. *Frontiers in Built Environment*, 2020.

[151] K. J Åström. Adaptive Control. *Mathematical System Theory*, 1991.

[152] R Murray-Smith, T. A Johansen, and R. N Shorten. On transient dynamics, off-equilibrium behaviour and identification in blended multiple model structures. *1999 European Control Conference (ECC)*, 1999.

[153] R Murray-Smith and D Sbarbaro. Nonlinear adaptive control using non-parametric gaussian process prior models. In *The 15th Triennial World Congress of the International Federation of Automatic Control*, 2002.

[154] M Liu, G Chowdhary, B Castra da Silva, S.-Y Liu, and J. P How. Gaussian processes for learning and control: A tutorial with examples. *IEEE Control Systems Magazine*, 2018.

[155] J. M Umlauft. *Safe Learning Control for Gaussian Process Models*. PhD thesis, Technische Universität München, 2020.

[156] M Deisenroth, C Rasmussen, J Peters, and M Verleysen. Model-based reinforcement learning with continuous states and actions. *Advances in Computational Intelligence and Learning: Proceedings of the European Symposium on Artificial Neural Networks (ESANN 2008)*, 2008.

[157] M. P Deisenroth, R Calandra, A Seyfarth, and J Peters. Toward fast policy search for learning legged locomotion. In *2012 IEEE/RSJ International Conference on Intelligent Robots and Systems*, 2012.

[158] M. P Deisenroth and C. E Rasmussen. Pilco: a model-based and data-efficient approach to policy search, 2011.

[159] P Gardner, M Dal Borgo, V Ruffini, A. J Hughes, Y Zhu, and D. J Wagg. Towards the Development of an Operational Digital Twin. *Vibration*, 2020.

[160] K Worden. *Nonlinearity in Structural Dynamics: Detection, Identification and Modelling*. CRC Press, 2001.

[161] S. S Rao. *Mechanical Vibrations*. Pearson Prentice Hall, 2010.

[162] R Blevins. *Formulas for Natural Frequency and Mode Shape*. Krieger Publishing Company, 2001.

[163] J Rossiter. *A First Course in Predictive Control*. CRC Press, 2018.

[164] J Rawlings, D Mayne, and M Diehl. *Model Predictive Control: Theory, Computation, and Design*. Nob Hill Publishing, 2017.

[165] P Trodden. Lecture notes of model predictive control course at the university of sheffield (acs616). 2022.

[166] M Morari and J H. Lee. Model predictive control: past present and future. *Computers and Chemical Engineering*, 1999.

[167] A Bemporad, A Bemporad, M Morari, V Dua, and E. N Pistikopoulos. The explicit linear quadratic regulator for constrained systems, 2002.

[168] S. S Dughman and J. A Rossiter. A survey of guaranteeing feasibility and stability in mpc during target changes. In *IFAC-PapersOnLine*, 2015.

[169] M Ozsoy, N. D Sims, and E Ozturk. Actuator saturation during active vibration control of milling. *Mechanical Systems and Signal Processing*, 2025.

[170] B. L Zhang, Q. L Han, and X. M Zhang. Recent advances in vibration control of offshore platforms. *Nonlinear Dynamics*, 2017.

[171] L Hewing, J Kabzan, and M. N Zeilinger. Cautious model predictive control using gaussian process regression. *IEEE Transactions on Control Systems Technology*, 2020.

[172] S Särkkä. Use of gaussian processes in system identification. *Encyclopedia of Systems and Control*, 2021.

[173] J Kocijan, R Murray-Smith, C Rasmussen, and B Likar. Predictive control with gaussian process models. In *The IEEE Region 8 EUROCON 2003. Computer as a Tool.*, 2003.

[174] J Kocijan, R Murray-Smith, C. E Rasmussen, and A Girard. Gaussian process model based predictive control. In *Proceedings of the American Control Conference*, 2004.

[175] G Cao, E. M.-K Lai, and F Alam. Gaussian process model predictive control of unmanned quadrotors. In *2016 2nd International Conference on Control, Automation and Robotics (ICCAR)*, 2016.

[176] J Kocijan, J. S Institute, and J Kocijan. Gaussian process models for systems identification. In *The 9th International PhD Workshop on Systems and Control: Young Generation Viewpoint*, 2008.

[177] L. D Avendaño-Valencia, E. N Chatzi, and D Tcherniak. Gaussian process models for mitigation of operational variability in the structural health monitoring of wind turbines. *Mechanical Systems and Signal Processing*, 2020.

[178] T. J Rogers. *Towards Bayesian System Identification: With Application to SHM of Offshore Structures*. PhD thesis, The University of Sheffield, 2018.

[179] I Lind. *Regressor Selection in System Identification using ANOVA*. PhD thesis, Licentiate dissertation, Linköping University, 2001.

[180] F Allgöwer, R Findeisen, and Z. K Nagy. Nonlinear model predictive control: From theory to application. *Journal of The Chinese Institute of Chemical Engineers*, 2004.

[181] J Kocijan and D Leigth. Derivative observations used in predictive control. In *Proceedings of the 12th IEEE Mediterranean Electrotechnical Conference (IEEE Cat. No.04CH37521)*, 2004.

[182] J Richalet, S Abu El Ata-Doss, C Arber, H Kuntze, A Jacubasch, and W Schill. Predictive functional control - application to fast and accurate robots. *IFAC Proceedings Volumes*, 1987. 10th Triennial IFAC Congress on Automatic Control - 1987 Volume IV, Munich, Germany, 27-31 July.

[183] M. S Aftab, J. A Rossiter, and Z Zhang. Predictive functional control for unstable first-order dynamic systems. In *Lecture Notes in Electrical Engineering*. Springer Science and Business Media Deutschland GmbH, 2021.

[184] B Likar and J Kocijan. Predictive control of a gas–liquid separation plant based on a gaussian process model. *Computers and Chemical Engineering*, 2007.

[185] Z Chen. Bayesian filtering: From kalman filters to particle filters, and beyond. *Statistics*, 2003.

[186] R Shumway and D. S Stoffer. An approach to time series smoothing and forecasting using the em algorithm. *Journal of Time Series Analysis*, 1982.

[187] R Shumway and D Stoffer. *Time Series Analysis and Its Applications: With R Examples*. Springer, 2006.

[188] K Murphy. *Machine Learning: A Probabilistic Perspective*. MIT Press, 2021.

[189] C. M Bishop. *Pattern Recognition and Machine Learning (Information Science and Statistics)*. Springer, 2007.

[190] K Ogata. *Discrete-time Control Systems*. Prentice Hall, 1995.